CRUSTAL STRUCTURE

AND

REFLECTIONS FROM THE MOHOROVIČIĆ DISCONTINUITY

IN SOUTHERN CALIFORNIA

Thesis by

George G. Shor, Jr.

In Partial Fulfillment of the Requirements

For the Degree of

Doctor of Philosophy

California Institute of Technology

Pasadena, California

1954

ACKNOWLEDGMENTS

Because of the nature of observational seismology, the aid of many people was essential to the completion of this work. Dr. Charles Richter suggested the original problem from which the work has grown, supplied advice and encouragement throughout, and allowed me to make extensive use of his own work as a basis on which to build mine. Practically all the earthquake data used are based on past work by Dr. Richter; the precise locations of the Kern County aftershocks are all his work.

Dr. Beno Gutenberg provided information and helpful discussion and the privilege of making extensive use of Seismological Laboratory equipment and of the time of laboratory personnel.

Thanks are due to Ralph Gilman, John Nordquist, Gertrude Killeen, Violet Taylor, Francis Lehner, and to all the other members of the laboratory staff for aid, to Dr. Robert P. Sharp for the use of the exploration seismograph equipment in his custody, and to Dr. Hugo Benioff, Mr. Harry O. Wood, Dr. Pierre St. Amand and Dr. James A. Noble for much interesting discussion.

Officials and employees of the following companies gave permission to record blasts on their premises and aided in the blast recording program:

Morrison-Knudsen Company
Monolith Portland Cement Company
Livingston Rock and Gravel Company
California Portland Cement Company
Minnesota Mining and Manufacturing Company

Mr. A. L. Hansen of the Monolith Portland Cement Company deserves special thanks for his cooperation and patience.

Mr. David J. Leeds, Mr. Frank H. Werner, and Mr. Robert W. Knox of the U. S. Coast and Geodetic Survey provided valuable data from the stations at Nelson and Boulder City, Nevada; members of the staff of the University of California at Berkeley did the same by lending records from the Fresno and Mount Hamilton stations; Dr. Russell Raitt permitted the use of the Point Loma record of the 1949 Corona blast.

My wife not only performed the customary tasks of editing and typing this manuscript and urging me to get it done, but also the less usual tasks of tabulating data, plotting graphs, drafting, and making some computations, and the highly unusual services of setting out reflection equipment both in the broiling desert sun and in total darkness, acting as rodman for survey work, and sitting 75 to 250 feet from seven large explosions of 2 to 25 tons of dynamite, while I hid a mile down the road with recording equipment.

ABSTRACT

The thickness and structure of the crust of the earth have been studied in a limited area of southern California by means of reflected and refracted seismic waves. Two usable records of reflections from the Mohorovičić discontinuity at nearly vertical incidence were obtained from large quarry blasts. Each record shows a strong reflection with travel time near 10.6 sec. Strong reflections from the Mohorovičić discontinuity were also obtained at distances slightly beyond critical from blasts at one quarry. Many other records of blasts and of earthquakes show phases that may be interpreted as reflections from the Mohorovičić discontinuity.

Studies of refracted waves from blasts and earthquakes have given additional information about crustal velocities. When combined with the reflection data, they indicate that there is at least a slight decrease of velocity with depth somewhere in the crust and that there are significant variations in the arrival time of P_n at distant stations, indicating lateral variation either in crustal velocities or in the thickness of the crust.

Computations of the thickness of the crust near Monolith and Corona, California have been made from various assumptions of velocity structure. The results obtained by using any model that agrees with the refraction data or by assuming a single-layer crust agree closely. In this area the Mohorovičić discontinuity is 32 km below sea level and the mean velocity in the crust is 6.2 km/sec.

TABLE OF CONTENTS

I. INTRODUCTION

A. Background

When a compressional elastic wave strikes a velocity discontinuity within the earth, it may be reflected back into the material above, refracted into the material below, or both reflected and refracted. Reflected and refracted waves have each been used successfully in studying discontinuities in the sediments and the discontinuity bounding the core of the earth. The one other major discontinuity -- the Mohorovičić discontinuity -- has been studied almost entirely by refracted waves.

A. Mohorovičić first detected the existence of this discontinuity by the study of refracted waves from an earthquake in Croatia in 1909. It has since been found in every part of the world where studies of earthquakes and artificial explosions have been made; in practically every case these studies have used refracted waves. When Mohorovičić presented his results he postulated the existence of reflected waves from the discontinuity and computed theoretical travel time curves for them, but use of these curves did not add greatly to the knowledge of the discontinuity. Over most of the range of epicentral distances at which earthquakes are normally observed, the travel time curves of the reflected waves are close to those of many other phases. Reflections are not distinguishable from other phases in the type of recording normally used for earthquake studies and are ordinarily identified by their close agreement with travel time curves obtained from refraction

measurements. Because of the complexity of most seismograms and the variation in arrival times of reflected waves, caused by variation in depths of earthquakes, little use has been made of reflected phases in earthquake studies. The most extensive analysis of reflections in earthquake records has been by Gutenberg (1944b).

In recent years many studies of deep crustal structure have been made by means of artificial explosions. The most important studies have been those by Tuve and his co-workers at the Carnegie Institution of Washington, who have detected waves reflected at critical incidence from the Mohorovičić discontinuity in many areas of the United States and have used them as an important adjunct of the refraction method (Adams, Tuve, and Tatel, 1952; Rooney, Tatel, and Tuve, 1950; Tuve, 1948 - 1952; Vestine and Forbush, 1953). Katz (1953) recorded similar arrivals in New York. Reich (1953a; 1953b) reported the recording of deep reflections at vertical incidence from two quarry blasts in Germany; using velocities derived from refraction studies of large blasts, he definitely established the deeper reflection as one from the Mohorovičić discontinuity. Junger (1951) obtained deep vertical reflections in Montana from small shots. Hodgson (1953) reported the recording of critical incidence reflections in his studies of rockbursts in the Canadian Shield, and the same has been reported in rockburst studies in South Africa by Willmore, Hales, and Gane (1952).

In general, however, little use has been made of reflections in crustal studies, because of the difficulty in most cases of getting usable reflection data with the equipment normally used for

refraction studies.

There are some who have questioned the possibility of waves being reflected from the Mohorovičić discontinuity. One argument to this effect goes as follows:

(1) The change of velocity at the Mohorovičić "discontinuity" is a continuous one and therefore provides no interface to produce a reflected wave.

(2) The strong events at "critical distance" are refracted waves; their high amplitudes are produced by a very rapid increase of velocity with depth.

(3) Other "reflected events" found at shorter distances are merely unexplained phases that happen to arrive near the assumed travel time curves for the reflection from the Mohorovičić discontinuity.

The first point of this argument is an unproved assertion. If a reflection can be shown to exist, it will be evidence that the discontinuity is abrupt; there is no evidence to the contrary.

The second two arguments seem to have been answered by Reich's record of a reflection at almost vertical incidence; no deep refracted waves can exist at such short recording distance (500 m). To demonstrate that his record was not fortuitous, repetition of the experiment in another area was advisable for verification.

The success of the reflection method in commercial prospecting of the sedimentary layers leads one to believe that if reflections from the Mohorovičić discontinuity can be obtained, they will afford a powerful new tool for the study of crustal structure.

B. Purpose

The purpose of this investigation, then, was to determine whether reflections could be obtained from the Mohorovičić discontinuity in southern California and, if they could, to use the reflection data in combination with data from other sources to study velocities in and thickness of the earth's crust in this region.

To obtain these data required the following steps:

(1) Finding techniques for recording reflections from great depths in such a way as to identify them as reflections.

(2) Obtaining records of reflections from the Mohorovičić discontinuity from many epicentral distances, including both vertical and near-critical incidence.

(3) Determining the velocity structure of the crust by the study of direct and refracted waves traveling wholly within the crustal layers.

(4) Studying the travel times of waves refracted below the Mohorovičić discontinuity and thereby obtaining an independent source of data on crustal thickness.

For the first two steps blasts were more usable than earthquakes; for the remaining steps, data from blasts and earthquakes could be combined.

The problem originally considered was a study of the variation of reflection travel times in local earthquake records; it was found that the study of reflections in blasts was essential before the earthquake data could be used.

C. Nomenclature

A practice long in effect, that of assigning common rock names to crustal materials known only by their seismic velocities, has created considerable confusion. Throughout this paper the use of the terms "granitic layer", "basaltic layer", and "peridotitic layer" has been avoided. The nature of material at great depths is not known with any accuracy; use of these names in referring to velocity layerings merely perpetuates an old error. The only names used here, other than velocity designations, are:

Mohorovičić discontinuity -- the dividing surface between rocks having a P-wave velocity approximately eight kilometers per second and those with velocities mostly less than eight.

Sedimentary layers.

Crustal rock -- all material above the Mohorovičić discontinuity.

Mantle rock -- material below the Mohorovičić discontinuity and above the surface of the earth's core.

Rock names are used only to refer to materials actually seen at the surface of the earth.

The naming of phases observed in seismic records follows the notation in current use at the Pasadena Seismological Laboratory (Benioff, Gutenberg and Richter, 1953), except for reflected phases. These have in the past been named P28P, P35P, S35S, etc., the numbers referring to the depth of the reflecting horizon. In the present study, in which the depth of the reflecting horizon was to be determined, such names are inapplicable. This work deals primarily with the phase called P35P in Gutenberg's notation,

the untransformed compressional wave reflected from the Mohorovičić discontinuity (Gutenberg, 1951b). When the three other possible reflections from the Mohorovičić discontinuity -- in Gutenberg's notation P35S, S35P, and S35S -- are mentioned, they are suitably identified.

The following symbols are used throughout this paper; other symbols used only once are defined when used:

d -- focal depth of earthquake

h_j -- thickness of layer j

H -- depth of the Mohorovičić discontinuity

k -- constant term ("intercept time") in the travel time equation for P_n $t = k + \Delta / V_n$

t -- travel time

t_o -- vertical reflection time for a surface source

t' -- intercept on the time axis of any tangent to a reflection travel time curve

t^* -- travel time of reflection at critical incidence

V -- velocity of compressional waves

V_n -- velocity of compressional waves below the Mohorovičić discontinuity

V_j -- velocity of compressional waves in any crustal layer j

V_{max} -- maximum velocity of compressional waves above the Mohorovičić discontinuity

Z -- depth (positive downward)

$\alpha_{jn} = \left[\frac{1}{V_j^2} - \frac{1}{V_n^2}\right]^{1/2}$ in which V_j is velocity in layer j

Δ -- epicentral distance

Δ^* -- distance for critical reflection

D. Material Available

Reflection records used in this study consisted of three groups: blast records from very short distances, essentially vertical incidence; blast records from greater distances, including critical; and earthquake records from distances greater than vertical incidence.

The fourth possible classification, earthquake records at essentially vertical incidence, are in practice almost an impossibility since earthquakes rarely occur at such short distances from a station. Furthermore, an earthquake small enough to record clearly at a near-by station cannot be located accurately because it fails to record at more distant stations; if it is large enough to locate accurately, it produces records of such high amplitude at the near-by station that no events later than the first arrival can be recognized. This is a result of the unpredictable nature of earthquakes; the amplification of a given instrument cannot be reduced in expectation of a near-by earthquake.

One usable record in the first category, blast records at vertical incidence, was taken by laboratory personnel at Corona in 1951 on a single-channel seismometer. Two records on multiple-channel equipment were taken at Monolith and Mojave by the writer.

In the second category, blast records at greater distance, a large number of records were available from past work or were obtained during the study. Blasts at Colton have been recorded at 14 stations, blasts at Corona at 29 stations of which records of 21 were available for study, and blasts at Monolith at 19 stations.

Many of these records show events that can be interpreted as reflections.

A very large number of earthquake recordings were studied, many showing apparent reflections. The presence of large amplitudes in the S-wave group meant, however, that in general no records could be used from stations at distances between 10 and 35 km and there were very few records at shorter distances. Variations in focal depths of shocks and the difficulty of determining depth to the accuracy needed prevented the use of these records for computational purposes, because the travel times of reflected waves depend heavily on focal depth. In single-channel recording, reflections can be identified only by fitting to an assumed travel time curve.

As a result, apparent reflected phases in earthquake records can be used only to check travel time curves derived from other data and as a possible method of determining the focal depths of earthquakes, if the depth to the Mohorovičić discontinuity is known from other sources.

Refraction data came from many of the same blasts used for reflection study. Some of these data were from records timed by the writer; others were available in the laboratory files and in published material.

Much material usable in studying crustal velocities and travel times of P_n came from studies of the Kern County earthquakes of 1952 and 1953 and from publications on travel times of earthquake waves at short distances (Richter, 1950; Gutenberg, 1951b).

Blasts used in this study are listed in Table I; previously unpublished readings from blasts and earthquakes are tabulated in the Appendix. Locations of stations and blast sites are shown on the base map included as an insert.

Table I

Date	Tons	Type of Explosive	Timed at Origin	Studied by
Corona. Coordinates: 33° 50.8' N, 117° 30.4' W; elevation: 350 m; company: Minn. Mining and Mfg. Co.; nature of rock: quartz latite porphyry.				
Aug. 6, 1949	78	Nitramon = 60% dynamite	Yes	Gutenberg; Rooney, Tuve, and Tatel
Mar. 31, 1951	60	Nitramon	Yes	Gutenberg
July 26, 1952	185	Nitramon	Yes	Shor
Monolith. Coordinates: 35° 08.7' N, 118° 23.7' W; elevation: 1500 m; company: Monolith Portland Cement Co.; nature of rock: recrystallized limestone within granitic area.				
Sept. 6, 1952	33	60% dynamite	No	Shor
Jan. 23, 1953	12	60% dynamite	No	Shor
June 5, 1953	10	60% dynamite	Yes	Shor
Aug. 1, 1953	25	60% dynamite	Yes	Shor
Victorville. Coordinates: 34° 37.88' N, 117° 16.35' W; company: Southwestern Portland Cement Co.; nature of rock: recrystallized limestone within granitic area.				
Sept. 12, 1931	20	Ammonium nitrate = 70% dynamite	Yes	Wood and Richter
Mojave. Coordinates: 35° 00' N, 117° 58' W; elevation: 770m; company: Morrison-Knudsen Co., for Santa Fe Railroad right-of-way; nature of rock: granitic. (Reflection recording only).				
June 19, 1953	4.4	40% dynamite	Yes	Shor
July 2, 1953	9¼	40% dynamite	No	Shor

Table I (cont'd)

Date	Tons	Type of Explosive	Timed at Origin	Studied by
Colton. Coordinates: 34° 03.8' N, 117° 20.4' W; elevation: 350-450 m; company: California Portland Cement Co.; nature of rock: recrystallized limestone within granitic area.				
Apr. 17, 1937	65	5% dynamite	Yes	Richter
June 8, 1937	11		No	Richter
Jan. 29, 1938 (2 blasts)	22 59	10% dynamite (some higher)	Yes	Richter
Dec. 23, 1939	67		No	Richter
Sept. 6, 1941			No	Richter
Oct. 4, 1941			No	Richter
Jan. 10, 1942			No	Richter
May 2, 1942	37		Yes	Richter
Sept. 10, 1949 (2 blasts)			No	Shor
Nov. 3, 1949 (2 blasts)			No	Richter
Dec. 19, 1951			No	Shor
Dec. 21, 1951			No	Shor
Feb. 13, 1952 (2 blasts?)			No	Shor
May 22, 1952			No	Shor

E. Recording Methods

Recording methods included those of both earthquake seismology and exploration seismology. Most of the records used were obtained from the permanent and portable stations established by the Seismological Laboratory to study local earthquakes. Two of the most important records in the study were obtained by a modification of exploration methods. The difficulties encountered and techniques used in obtaining these latter records deserve some mention.

Considerations discussed in Sec. II C and the experiences of Tuve and of Reich indicate that positive identification of reflections requires the use of multiple-channel equipment. A small portable six-channel set became available in the summer of 1953 and was used to record seven quarry blasts. Of these, only two produced records of possible reflections and only one can be considered definite. The failure of the others must be charged to the difficulties of learning a technique of operation, not necessarily to the absence of reflected waves. Of the five failures, two records at Colton and one at Palos Verdes had excessive background noise; there was instrument failure at one Monolith blast; at one Mojave blast the record was started late because of poor communications. In all cases the multiple-channel equipment was used for recording near the shotpoint; recording of reflections near critical incidence was done with standard single-channel equipment.

High local noise levels were a serious problem. Recording

within five hundred meters of the blast site was generally inadvisable, for disturbance from sliding rock, from machinery, and movement of quarry personnel masked any possible reflections. At distances beyond five hundred meters from the blast, away from public highways, railroad, and surf, recording was satisfactory if quarry milling operations were stopped during the blast.

The instruments used were not specifically designed for this type of work and gave some trouble. Most exploration instruments have extremely high recording speeds and inability to handle very long record strips without jamming. To record all possible crustal reflections and sufficient radio time signals, the record had to run for at least twenty seconds and preferably a minute. At a minimum record speed of 190 mm/sec this created an unmanageably long record. Better results would have been obtained if camera speed could have been reduced to about 40 mm/sec.

The automatic volume control and suppressor on the instruments could never be put into satisfactory adjustment and were therefore left off for all blasts. While this gave some information about relative amplitudes, it eliminated all information in the early part of the record.

The problem of recording firing time of quarry blasts properly has in the past proved extremely difficult to solve. The system of timing used in commercial exploration seismology involves recording either the firing impulse from the blaster or the time of breaking of the cap. Each of these systems requires a connection from the blaster to the recording equipment or an inductive pickup from a

wire wrapped around the cap leads. Quarry operators are justifiably concerned over the possibility of stray current from the recording equipment detonating the charge prematurely. Quarry safety regulations, therefore, now generally prohibit the connection of any extraneous wires to either the blaster, the cap leads, or the explosive. The use of any wires carrying current in the vicinity of the explosive is discouraged for similar reasons. This eliminates not only systems using the firing impulse but also those involving a broken wire within the charge. Even if it were not prohibited, use of the firing impulse is not advisable because the caps and fuse used in quarry work may have an appreciable delay.

The best solution involves the use of a seismometer (or geophone) at a distance from the blast sufficiently short that the travel time of the seismic wave from the blast to the geophone is small compared with the quantities to be measured. For most long-distance refraction measurements this distance can be one or two hundred meters; for short-distance reflection work, in which velocities at shallow depth must be evaluated from the first arrivals on the record for use in elevation and weathering corrections, the allowable distance from the explosive is reduced to a few meters. At these distances from blasts of several tons of dynamite, geophones must be considered expendable. In the present program, the geophone was replaced with a cheap permanent magnet loudspeaker and audio output transformer combination placed face down over the loaded hole. Because of the high amplitude of motion and sonic

frequencies present in quarry blasts, this device produced a signal readable even when run through two miles of high-resistance combat telephone wire to the recorder. Loudspeakers were never recovered in working condition.

Obtaining absolute time for determining travel times to distant stations was more difficult. At the Monolith blast of June 5, 1953 and at many previous blasts used for refraction studies by the Seismological Laboratory, a portable Benioff vertical seismometer with standard 60 mm/min continuous recording was used. Timing was obtained from chronometer minute marks; signals from radio station NPG were used to establish the chronometer rate. Time signals from NPG are not continuous and on this type of recording can be read only to the nearest 0.1 sec. Chronometers may develop rate changes during transportation to the blast site and are not usually kept there long enough to determine the new rate accurately. This method of timing is accurate to 0.1 sec under very favorable conditions and is more likely to be in error by 0.2 or 0.3 sec.

An alternative method, that of transmitting a tone signal through the telephone lines to Pasadena where better time-keeping facilities are available, was usable but often failed in operation. Impressing the continuous time signals from radio station WWV directly onto the timing trace of the equipment was successful on one blast. A good watch with a sweep second hand was checked against the WWV signal beforehand, and the blast was delayed until the beginning of the one minute of every five during which WWV stops its audio tone and sends only time ticks at one-second intervals.

A few seconds before the beginning of the quiet minute the recording equipment was started and the signal given to fire. The end of the audio tone gave the minute and second, and the succeeding WWV second ticks, when compared with the timing marks in the recording equipment, gave the time to 0.001 sec and checked the accuracy of the internal timing system of the recorder.

Establishing communication with the shooter, who in every case was unfamiliar with recording work, proved to be essential and difficult. It was necessary to find out well in advance where he would be stationed to fire the shot, to have him indicate when he was ready and then have him wait to fire until a signal was given by the instrument operator. The only effective method was to have one crew member at the shotpoint to give the shooter his instructions and to relay messages by telephone to the instrument operator.

Instrument adjustments were comparatively simple. In all cases the amplification was set so that background noise gave barely visible galvanometer motion, and filtering was set to the lowest possible frequency band. At this setting, "R - 35" on the Century instruments, the amplifier pass band was nearly flat from 8 to 30 cps. The response characteristic of the geophones probably cut off the low-frequency side of this band. The observed frequency of the reflection on the Monolith record was 14 cps, indicating that a somewhat lower frequency response might have been desirable.

Most of the other blast records and all the earthquake records were taken on continuously recording instruments operating at relatively slow speeds. The records from the stations of the Seismo-

logical Laboratory, the University of California, and the U. S. Coast and Geodetic Survey are almost all from short period seismometers intended for the study of local earthquakes. Most of the readings used in this paper from these stations are from Benioff vertical moving-coil or variable-reluctance seismometers with a period of 1.0 sec, recording with 0.25-sec galvanometers. In some cases readings are taken from Benioff horizontal variable-reluctance seismometers with similar characteristics, from short-period Benioff horizontal variable-capacity seismometers using electronic amplification and hot-stylus recording, and from Wood-Anderson horizontal torsion seismometers. All of the instruments of these three groups of stations that were used in this study record either at 60 mm/min (on photographic paper or heat-sensitive paper) or at 15 mm/min on photographic film which is enlarged to 120 mm/min for reading.

Blast records using higher speed recording were those of the Carnegie Institution of Washington operated by Tuve and the Point Loma station operated by Raitt for the 1949 Corona blast. The Point Loma record was taken with a hydrophone, electronic amplification, and a Brush ink recorder.

Times on the records from the regular stations are determined to 0.1 sec. The chronometer readings and time corrections are often this accurate. Determination of the beginning of a particular phase is not so accurate and may introduce errors of a few tenths of a second.

II. THEORY

A. Travel Times of Reflections

The general nature of the travel time curve of an untransformed reflected wave is well known. For a single layer of constant velocity overlying a sharp discontinuity, it is the hyperbola:

$$V_1^2 t^2 = \Delta^2 + (2H - d)^2$$

in which V_1 = velocity in upper layer
t = travel time
Δ = epicentral distance
H = depth to reflector
d = depth of source in layer

For a multiple-layer case with the source at the base of layer r, the travel time curve is defined by the equations:

$$t = 2\sum_1^n \frac{h_j}{V_j} \sec i_j - \sum_1^r \frac{h_j}{V_j} \sec i_j$$

$$\Delta = 2\sum_1^n h_j \tan i_j - \sum_1^r h_j \tan i_j$$

in which i is defined by:

$$\sin i_1 : \sin i_2 : \sin i_3 \ldots\ldots = V_1 : V_2 : V_3 \ldots\ldots$$

for all layers. If the velocity varies continuously with depth, the summations can be replaced with integral signs.

A reflection travel time curve may be defined by the inverse slope $d\Delta/dt$ (the "apparent velocity") and the time intercept t' of its tangent as functions of distance; at three distances these bear a simple relation to the velocities and thicknesses of the layers above the reflector. For a single-layer case:

$$\text{at } \Delta = 0, \quad \frac{d\Delta}{dt} = \infty; t' = t_o = \frac{2H - d}{V_1}$$

$$\text{at } \Delta = \Delta^*, \quad \frac{d\Delta}{dt} = V_n = V_1^2 \frac{t^*}{\Delta^*}; \quad t' = (2H - d)\sqrt{\frac{1}{V_1^2} - \frac{1}{V_n^2}}$$

$$\text{as } \Delta \to \infty, \quad \frac{d\Delta}{dt} \to V_1; \quad t' \to 0$$

in which V_1 = velocity in upper layer
V_n = velocity in lower layer
t' = time intercept of the tangent
Δ^* = distance for critical reflection
t^* = travel time for critical reflection
t_o = travel time of vertical reflection

For a multiple-layer case, or a case of continuous arbitrary variation of velocity above a reflector at layer n:

$$\text{at } \Delta = 0, \quad \frac{d\Delta}{dt} = \infty; \; t' = t_o = 2\int_0^H \frac{dz}{V} - \int_0^d \frac{dz}{V}$$

$$\text{at } \Delta = \Delta^*, \quad \frac{d\Delta}{dt} = V_n; \; t' = 2\int_0^H \sqrt{\frac{1}{V^2} - \frac{1}{V_n^2}}\, dz - \int_0^d \sqrt{\frac{1}{V^2} - \frac{1}{V_n^2}}\, dz$$

$$\text{as } \Delta \to \infty, \quad \frac{d\Delta}{dt} \to V_{max}; t' \to 2\int_0^H \sqrt{\frac{1}{V^2} - \frac{1}{V_{max}^2}}\, dz - \int_0^d \sqrt{\frac{1}{V^2} - \frac{1}{V_{max}^2}}\, dz$$

in which V = velocity at any depth less than H
V_{max} = highest velocity above layer n

The curve starts with an infinite apparent velocity; with distance the apparent velocity decreases continuously. At $\Delta = \Delta^*$ the horizontally refracted wave begins, represented by a straight line tangent to the reflection curve. The two lines separate, the apparent velocity of the reflected wave continuously decreasing until it finally approaches asymptotically the highest velocity above the reflecting layer. In a single-layer case the intercept of the asymptote is zero and the reflected wave merges with the direct

wave. In the more general case it does not. If the velocity structure is approximated by a series of layers of finite thickness and constant velocity, each having higher velocity than the layer above it, the reflection curve approaches a straight line with the apparent velocity and intercept representing the wave refracted at the upper surface of the layer immediately above the reflector and merges with it indistinguishably.

If no such finite layers exist and if velocity increases continuously with depth, the reflection travel time still approximates the travel time plot of a nonexistent refracted wave traveling in an infinitely thin layer just above the reflector with the highest velocity reached in the section.

If the more general case is taken, in which velocity increases or decreases either continuously or by steps (never equaling or exceeding the velocity below the reflector), the apparent velocity of the reflection travel time curve still approaches the highest velocity above the reflector. The intercept time is such that the reflection asymptote is the travel time curve that would be observed if this layer of maximum velocity were located directly above the reflector.

In summary, the reflection travel time curve approaches, at distances not far beyond critical, a straight line. Only in the case of constant velocity above the reflector is this asymptote the travel time curve of the direct wave. In other cases, the reflection travel time curve approaches that of some real or imaginary refracted wave. If the region of highest velocity in

the section is separated from the reflector by a region of lower velocity, the asymptotic reflection travel time plot parallels that of the refracted wave through this layer, following it by a constant time interval.

Adequately recorded reflection data can, then, provide three different items of information about the material above the reflector, namely, the quantities:

(1) $\int_0^H \frac{dz}{V}$

(2) $\int_0^H \sqrt{\frac{1}{V^2} - \frac{1}{V_n^2}}\, dz$

(3) V_{max}

The first of these is provided by the reflection method alone; the second and third are provided also by the refraction method.

B. Amplitudes

Calculations of the relative amplitudes to be expected from reflected waves have been made by Knott, Zoeppritz, and many others; a summary of material on this subject has been published by Gutenberg (1944a).

The vertical component of the surface displacement due to a body wave from a surface source is defined by the equation:

$$D = CT\, w(i_o)\, \Pi f \sqrt{\frac{\left| d \cos i_o / d\Delta \right|}{\Delta \cos i_o}}$$

in which
- D = vertical component of surface displacement
- Δ = epicentral distance
- C = a constant depending on energy of shock and units used
- T = period of waves
- $w(i_o)$ = ratio of vertical displacement to incident wave amplitude at surface
- Πf = product of all factors f which are square roots of the ratio of the reflected or refracted waves to the incident energy at each discontinuity encountered by the wave
- i_o = angle of incidence at the surface

Modified from Gutenberg (1944b)

Values of $w(i_o)$ and f are given by Gutenberg (1944a) for several ratios of velocity and density above and below the discontinuity. The function:

$$\sqrt{\frac{\left| d \cos i_o / d\Delta \right|}{\Delta \cos i_o}}$$

depends only on the velocity-depth profile of the material above the reflector and has been calculated for the simple case of a layer 32 km thick with velocity 6.2 km/sec overlying material with velocity 8.2 km/sec. The relative amplitude of the reflected wave to

be expected, the function D/CT, has been plotted as Figure 1. Too many simplifying assumptions have been made for this to be anything more than an indication of distances at which the best records may be expected; only the shape of the curve is important.

It is apparent that there are two peak areas at which high amplitude reflections can be expected: near the source and at distances near critical.

Interference from shear waves makes part of the distance range unsuitable for reflection recording. With the velocities found in southern California, the direct S-phase may be expected to interfere strongly with a reflection from the Mohorovičić discontinuity between 20 and 45 km from a surface source. For earthquake sources at normal depth, the range of interference is between 10 and 35 km.

Some information about the velocity contrast at the Mohorovičić discontinuity could be obtained from accurately calibrated instruments, by determining the variation of amplitude with distance and comparing it with the theoretical value derived from various velocity assumptions. In the present program calibration of the instruments used was not sufficiently well determined for such study.

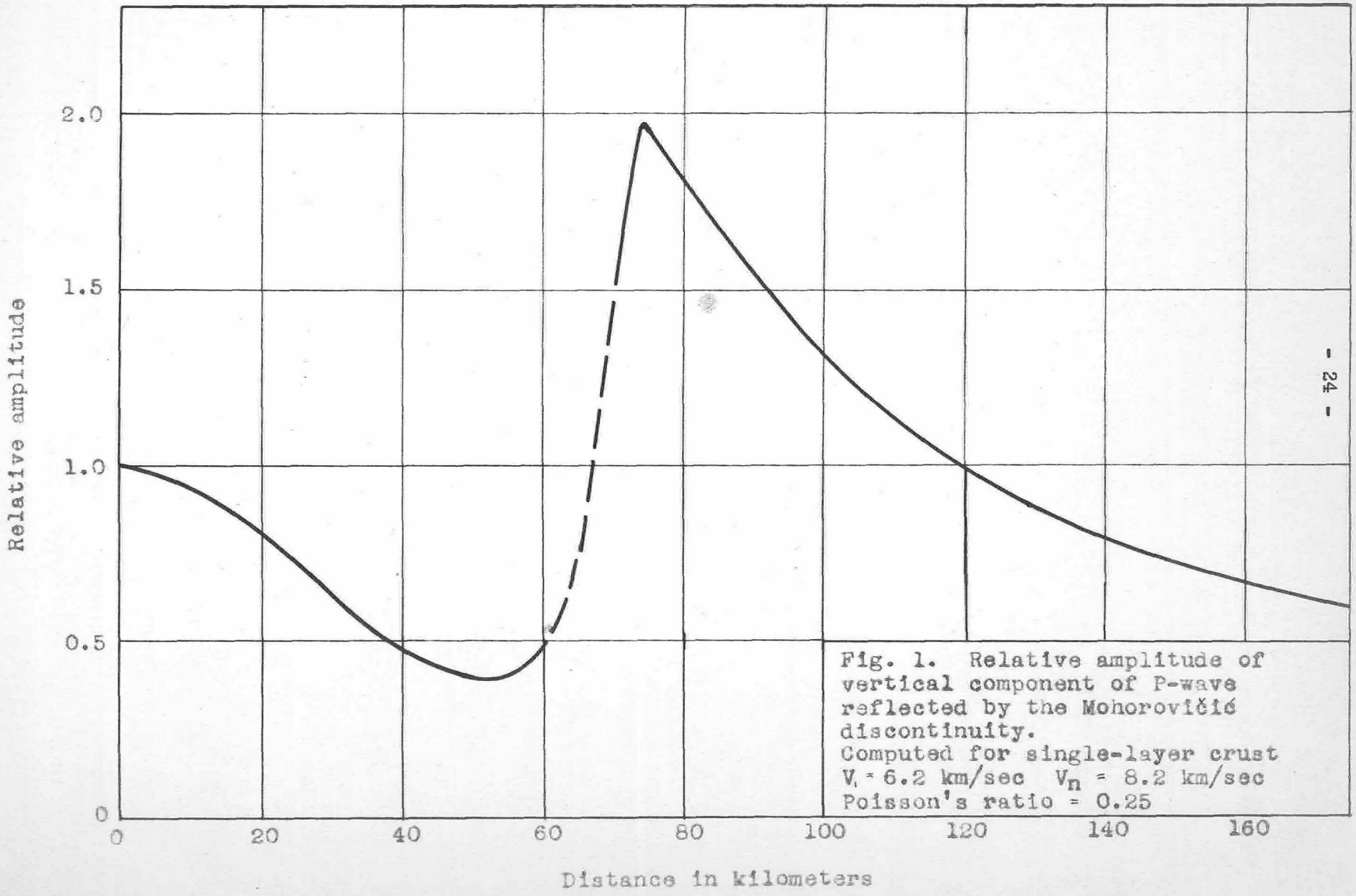

Fig. 1. Relative amplitude of vertical component of P-wave reflected by the Mohorovičić discontinuity.
Computed for single-layer crust
V_1 = 6.2 km/sec V_n = 8.2 km/sec
Poisson's ratio = 0.25

C. Criteria for Recognition of Reflections

The three most distinctive features of reflected waves have been discussed in the previous sections. They are: the very high apparent velocity at short distances; decrease in apparent velocity with distance (upward curvature of the time-distance plot); and the increase of amplitude near critical distance. These give the only usable criteria for identification of reflections.

The first criterion is used in reflection prospecting. If sufficient geophones are used to ensure that the same event is followed over an appreciable interval of ground surface near the source, the time delay between the nearest and the farthest geophones (the "stepout", in exploration terminology) is a function both of the dip of the reflecting horizon and of the "apparent velocity". In most commercial work the two effects are separated by shooting dynamite charges at opposite ends of the spread of geophones. However, if low dip is assumed for the reflecting horizon, the difference between a direct and a reflected wave is easily ascertained. A sample calculation will show the order of magnitude of the effects to be expected.

If a spread of geophones extends over a range from one to two kilometers from a surface source, and if a limit for the velocity of any possible nonreflected wave is set at 10 km/sec, the time delay for a wave traveling horizontally from the first to the last geophone will be more than 0.100 sec. However, if a reflection from a depth of 30 km having an average vertical velocity of 6

km/sec is recorded, the time delay from the first to the last geophone will be 0.004 sec. Therefore, in most cases a deep reflection can be readily identified by its small "stepout" across a multiple-trace record near the source. Recognition of a reflection in this way requires recording at short distances from the source.

The second criterion, decreasing apparent velocity, is more difficult to observe. An event must be followed for sufficient distance for curvature of the travel time plot to become observable. For a single-layer case with a surface source, the curvature

$$\frac{d^2t}{d\Delta^2} = \frac{d^2}{d\Delta^2}\left(\frac{\sqrt{\Delta^2 + 4H^2}}{V}\right) = \frac{4H^2}{V}\ (\Delta^2 + 4H^2)^{-3/2}$$

so that the curvature is greatest at $\Delta = 0$, where

$$\left[\frac{d^2t}{d\Delta^2}\right]_{\Delta=0} = \frac{1}{2HV}$$

in this case about 0.003 sec/km/km. To observe effects of curvature apart from effects of weathering and topography requires numerous stations with very accurate timing ranging from the source to five or ten kilometers away, a difficult requirement.

The third criterion, amplitude variation, has been used by Tuve and Tatel in the identification of critical reflections (Tuve, 1949). It requires the use of calibrated instruments over a wide range of distances including the critical one. The greatest drawback to this criterion by itself is the present insufficient knowledge of the amplitude variations of refracted waves near the critical distance.

III. PRESENTATION OF DATA

A. Vertical Reflections from Blasts

Two usable vertical incidence records were obtained during this study, plus one so weak that it served only as confirmation of the first two and was not the basis for any computation.

Recording of a 25-ton blast at Monolith, California produced the multiple-trace record duplicated and enclosed as an insert. Instrumental information is marked on the record.

The quarry is located near the top of a hill of recrystallized limestone, surrounded by granitic rocks of the Sierra complex (Fig. 2). The depth of the limestone is unknown. According to Dr. J. P. Buwalda (oral communication), the depth of the body is probably large compared with its lateral dimensions, which gives it a depth measurable in kilometers. Officials of the Monolith quarry report only that the base of the limestone is at least 1000 ft below the top of the hill, but that no deep drilling has been done to explore beyond. This gives information only to the level of the lowest recording point.

The first arrivals on the multiple-trace record indicate a velocity of 3.9 km/sec, both from the shotpoint to the nearest geophone 1.115 km away and from that to the farthest geophone at 1.792 km. The three points lie on a straight line with an error of only 0.001 sec, less than the accuracy of measurement. This indicates that the weathered layer is negligible and that the limestone extends at least one hundred meters below the lowest

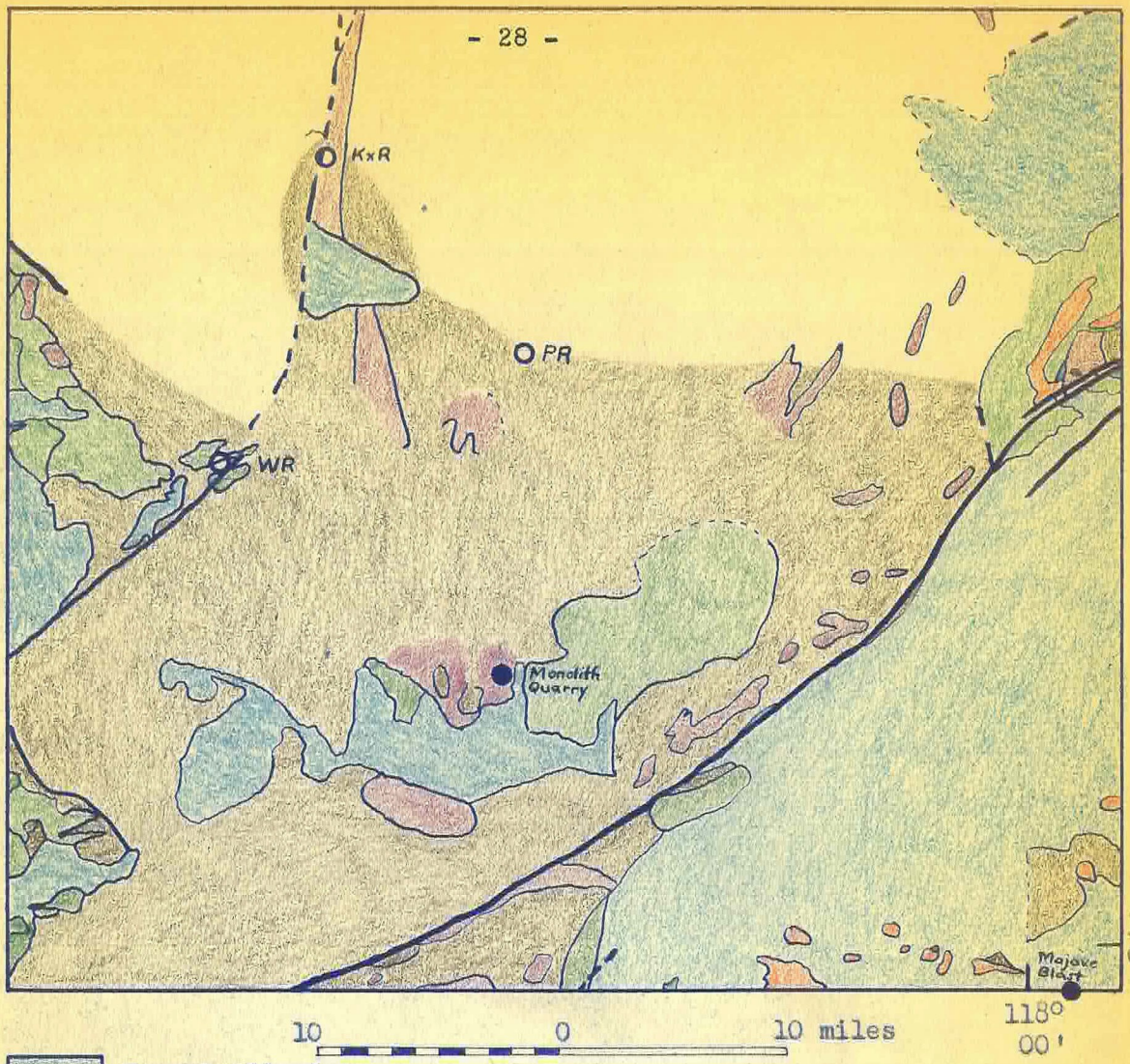

Fig. 2. Geologic map of Monolith area.
Modified from Geologic Map of California
Jenkins (1938) Scale 1:500,000

○ Seismograph stations
● Blast sites

geophone. Velocities from this level down are unknown. Because of the small lateral dimensions of the body, however, it can be assumed that the wave traveling downward enters granitic rock at a shallow depth unless the walls of the limestone body are perfectly vertical.

The one definite reflection occurs on the record 10.8 sec after the firing time. Timing on the trough of the reflected event gives the following:

Trace	1	2	3	4	5	6
Geophone elevation (km)	1.234	1.236	---	---	---	1.257
Direct time (sec)	10.823	---	10.823	10.824	10.829	10.834
Time corrected to elev. of No. 1 (sec)	10.823	---	10.821	10.821	10.825	10.828

Shotpoint elev. 1.500 km.

The elevation corrections are based on an apparent velocity of 3.9 km/sec and on elevations interpolated between the surveyed elevations of the end geophones and the recording point. Elevations of geophones 3, 4, and 5 could not be recovered when the surveying was done.

The stepout is essentially flat, indicating reflection from a very deep horizon of low dip. Using the stepout value of 0.005 sec for a spread length of 0.67 km indicates a 10 percent dip north into the Sierra Nevada, which is not unreasonable. The true beginning of the event is at the point where the line on the

record begins to turn down (downward line motion equals upward ground motion), which is about 0.04 sec before the trough on all traces. Correcting this beginning to the shot and recording points at an elevation of 1000 m, because the hill from geophone 1 to the shotpoint is known to be limestone with velocity 3.9 km/sec, and assuming that the limestone extends at least 234 m more in depth, gives a reflection time of 10.59 sec.

Because of the lack of automatic volume control or suppression on this record, the interval between the first arrivals and 6 sec is unreadable. Between 6 and 9 sec there are a few events, the erratic stepout of which brands them probably as random coincidences. There is a possible reflection at 9.2 sec; stepout is excessive but can be interpreted as being caused by interference from other energy. The mean travel time, corrected to datum at 1000 m, is 9.02 sec. Jamming began on the record after 34 sec. No events after the phase at 10.8 sec occurred which showed any consistency from trace to trace.

The event at 10.8 sec satisfies the principal criterion for identification as a reflection: nearly simultaneous arrival on a long line of seismometers near the source. It also shows some increase over the amplitude level before and after it.

Identifying this event as a reflection from the Mohorovičić discontinuity is less certain. Late reflections are often explainable as multiples of previous reflections. If this is a first multiple, the primary reflection should be near 5½ sec; at this time the record is of such high amplitude that the pos-

sibility cannot be checked. In this case, the reflection would come from an interface at a depth of $10\frac{1}{2}$ km, using the velocity of limestone, or 15 km, using the velocity of granite. It seems improbable that the base of the limestone could be this deep, but 15 km could be the base of the Sierra batholith; further work is needed to check this alternative.

The possibility that the reflection at 10.8 sec is a higher order multiple is eliminated by the absence of any strong reflections between 6 and 9 sec.

The best evidence seems to indicate that this event is a true reflection with a travel time of 10.59 sec corrected to 1000 m datum. If the average velocity to the reflecting horizon is between 6 and $6\frac{1}{2}$ km/sec, the depth of the horizon is between 32 and 35 km.

The second record, obtained by similar methods, was from a 4-ton construction blast east of Mojave, California. The essential part, showing a possible weak arrival at 10.9 sec, is shown in Figure 3. It is not very convincing and serves only as corroboration of the Monolith record.

A record from the Corona quarry was obtained on a Benioff vertical variable reluctance seismometer with continuous direct photographic recording at 60 mm/min. It is shown much enlarged in Figure 4 with the original faint lines reinforced. A strong single-cycle event is visible 10.49 sec after the first motion, with motion down on the record. A less outstanding half-cycle event at 8.80 sec has motion up on the record. Direction of

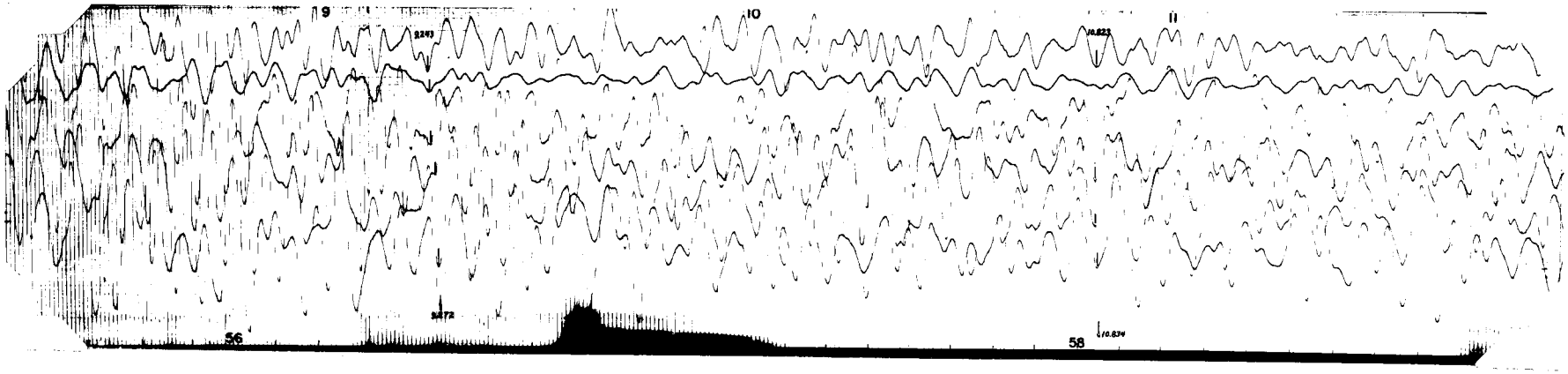

Portion of reflection record from Monolith, August 1, 1953

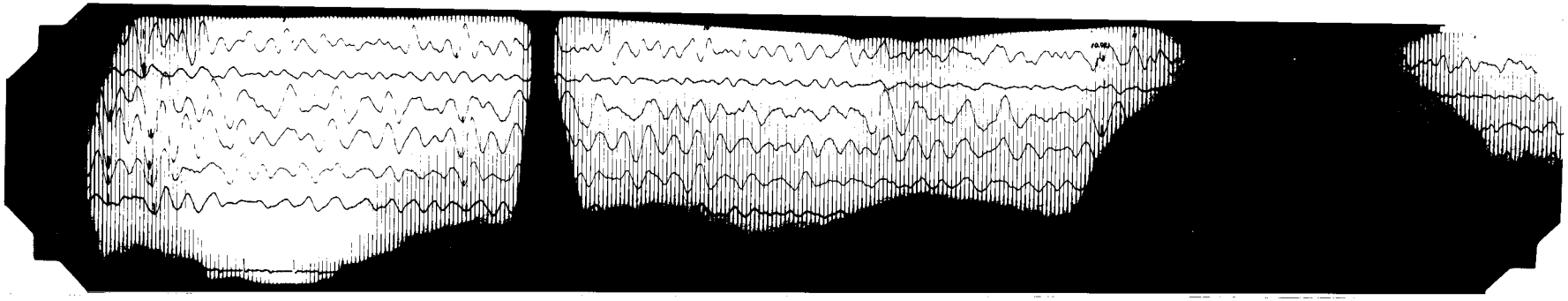

Portion of reflection record from Mojave, June 19, 1953

Fig. 3

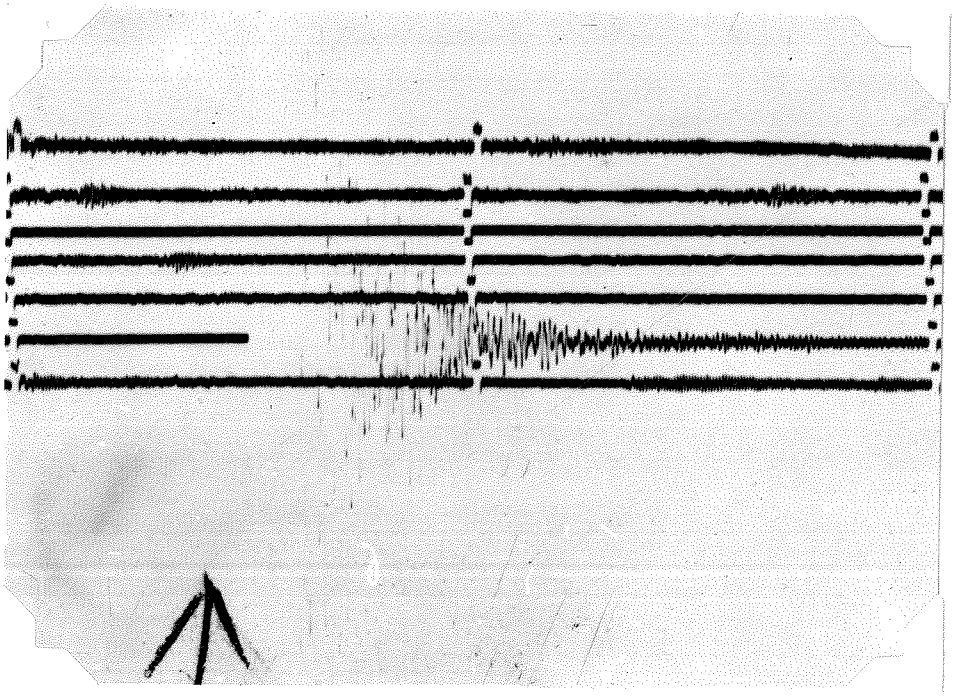

Reflection record from Corona, March 31, 1951.

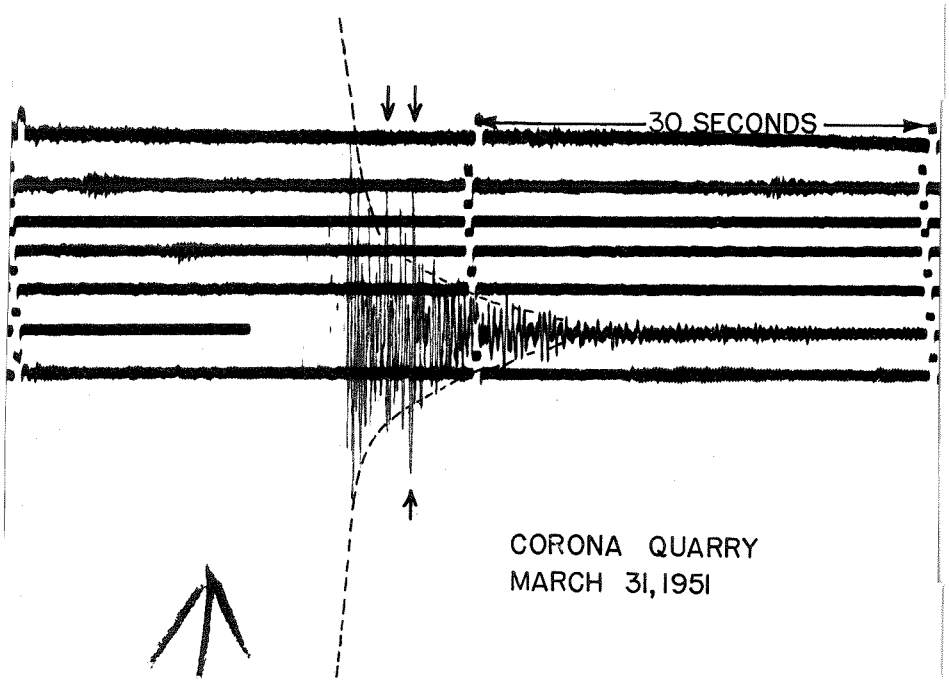

Same record with lines reinforced.

Fig. 4

initial motion is unreadable. The seismometer was approximately 150 m from the explosive source. To correct back to origin time, it may be assumed that the velocity in the competent latite porphyry in the quarry is between 3 and 6 km/sec. This gives a travel time for the 150 m of 0.025 to 0.050 sec. Arbitrarily assuming the latter for the shallow weathered material gives travel times of 8.85 and 10.54 sec for the two events. The Corona quarry is at an elevation of 350 m above sea level; correcting to the 1000 m datum of the Monolith record, using a velocity for the intervening material between 4 and 7 km/sec, gives corrected reflection times of 9.04 to 9.17 and 10.73 to 10.86 sec compared with the corrected times for Monolith of 9.02 and 10.59 sec.

Effectively, the two blasts show arrivals at identical times and no apparent arrivals later. This alone is not sufficient proof that both records show reflections from the Mohorovičić discontinuity; it does imply that the two records represent the same event, and the Monolith record shows it to be a reflection from a depth corresponding to that of the Mohorovičić discontinuity. The weaker and less definite earlier arrivals on both records, preceding the strong arrivals by the same time interval, give added support to the hypothesis that these two records show the same reflection. As the Mohorovičić discontinuity is the most pronounced velocity contrast known to exist at such great depth and as no abrupt velocity changes are known to occur beneath it, a strong reflection this late, followed by no others, can be

assumed to be from the Mohorovičić discontinuity as a working hypothesis.

We have, then, the following vertical reflection data:

Monolith	first event (weak)	9.02 sec
	second event (strong)	10.59 sec
Both corrected to 1000 m datum		
Corona	first event	8.85 sec
	second event	10.54 sec
Uncorrected (quarry elevation 350 m)		

FIG. 5. Monolith quarry after August 1, 1953 blast, showing location of shotpoint (left side of top bench), material broken by shot (talus slope on second bench), and recording spread (left side of road, from figures in left center to where road disappears).

FIG. 6. Recording site for Monolith blast, August 1, 1953.

B. Reflections from Blasts beyond the Critical Distance

Considerations discussed in Sec. II B indicate that strong reflections are to be expected at and shortly beyond the critical distance for total reflection. Very strong second arrivals have been found on records from seven of nine stations at distances between 103.9 and 169.0 km from several blasts at Monolith. Records from the stations concerned are copied in Figures 32 and 33 in the Appendix. Complete readings of times are tabulated in the Appendix and a travel time plot is included as an insert.

As can be seen in the copies, the second arrivals are much stronger than the direct wave which in many cases is a small emergence. Despite lack of precise information on the absolute magnifications of the instruments used, some knowledge of the amplitude variations can be obtained from consideration of the ratio of amplitudes of second arrival to first arrival. A logarithmic plot of these ratios is given in Figure 7. Small variations in ratio could easily be due to errors in measuring the amplitudes of the small first arrivals. There are large irregularities, however, that may be instrumental or a function of position, more probably the latter. The vertical instruments of all the stations concerned have the same nominal characteristics; actually there can be some variations. Apparently these variations are not sufficient to account for the differences in the records. The seismometer at the Mount Wilson station was replaced between the Monolith blasts of September 6, 1952 and August 1, 1953, but the records are nearly identical in appearance and amplitudes. A reflected phase from an irregular

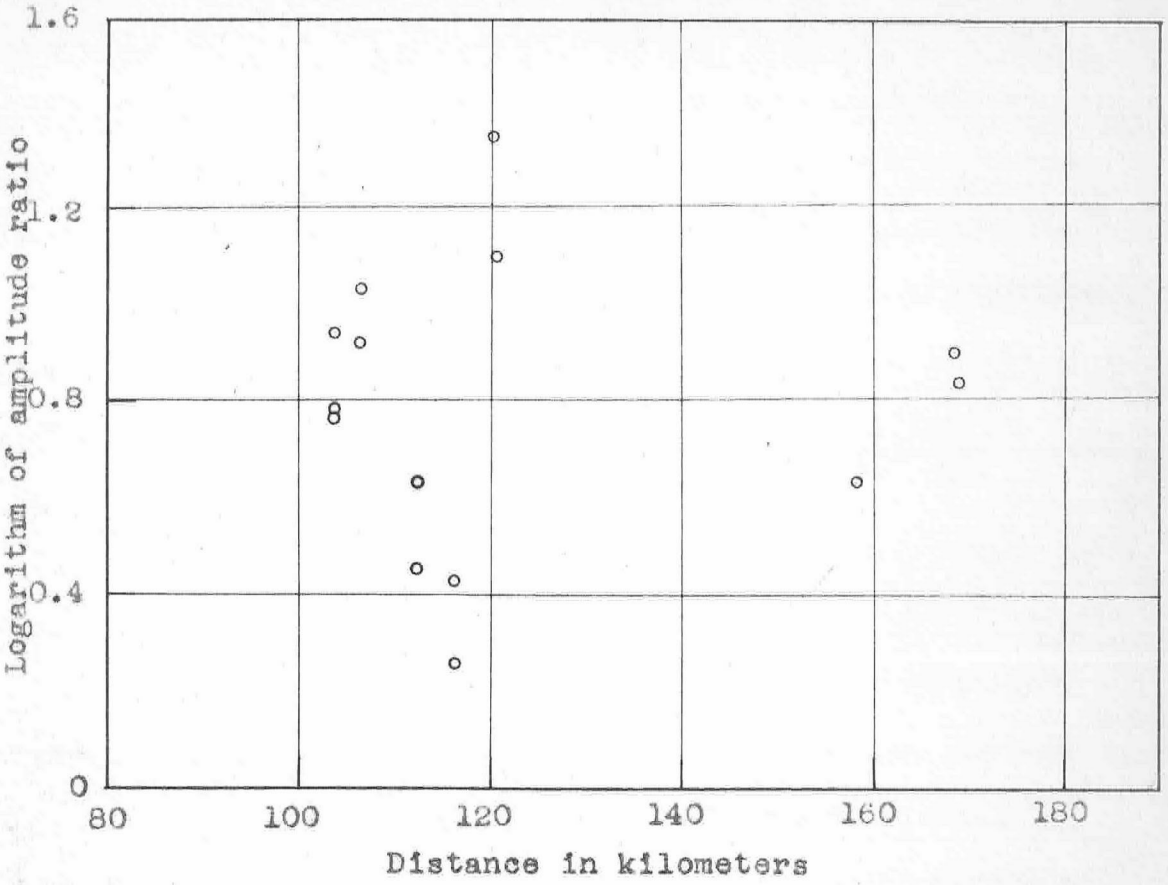

Fig. 7. Amplitude ratio of critical reflection to first arrival for Monolith blasts.

surface could be expected to have relatively large variations in amplitude with station position.

The travel times of these arrivals fit closely to a straight line with the equation $t = 5.1 + \Delta/7.0$ and might be considered to represent a refracted wave corresponding to P_m of earthquake studies. They fit equally well to a computed curve for a reflected wave. Because of the short distance covered by the seven records a decision cannot be made from the presence or absence of curvature. Positive identification of these events as reflections requires detailed amplitude measurements at a large number of points including critical distance.

Events similar to these have been reported by Tuve (1948 - 1952) from work in Maryland, Minnesota, and Tennessee. In most of the areas studied the strong arrivals were in the range of 90 to 130 km; in a few cases these have been found at distances as short as 80 km. By the use of calibrated instruments located at short intervals in this range of distance, recording repeated shots near Patuxent, Maryland, Tuve (1949) determined that the amplitude of the second arrivals varied in the manner to be expected of a critical reflection. In later work he has not reported whether detailed amplitude measurements were made.

From Corona and Colton blasts such a definite group of arrivals has not been found. Six stations have been within the proper range of distances from Corona blasts. Three of these -- Ramona, Lakeside, and Glencliff Camp -- were operated for the 1949 blast by the Carnegie Institution of Washington and the records

were not available for this study; Tuve (1952) has stated that critical reflections were not observed. On the Point Loma record there were two strong arrivals at 1.3 and 2.4 sec after first motion. The recording system used a Brush recorder with limiters to protect the pen and as a result the higher peaks are clipped, reducing the amplitude contrast. On the records at El Cajon and La Jolla there were weak second arrivals. The Point Loma times as given by Raitt are corrected for the sediment delay. If a similar correction is applied to the La Jolla data, the three records all have second arrivals early with respect to the observed curve for the Monolith blast as follows: La Jolla 0.6 sec; El Cajon 0.7 sec; Point Loma 1.0 sec. These arrivals may well represent the same phase as recorded from the Monolith blast; there is reason to believe, however, that the velocities are somewhat higher in the San Diego region (see Sec. III E) so that these arrivals should not be used with the Monolith data in a single solution. No such arrivals have been found on Colton blast records because of incomplete coverage of the critical distance.

On the hypothesis that the arrivals from the Monolith blast are reflections from the Mohorovičić discontinuity, computations can be made using them in conjunction with the vertical incidence record taken at the Monolith quarry. The first and simplest computation is by use of the hypothesis of a single-layer crust of constant thickness. The equations are:

$$V = \Delta / \sqrt{t^2 - t_0^2}$$

$$H = Vt_0 / 2$$

The values of k and of Δ^* can also be obtained if the velocity V_n below the Mohorovičić discontinuity is known, as follows:

$$k = t_o \sqrt{V_n^2 - V^2} \; / \; V_n$$

$$\Delta^* = t_o V^2 / \sqrt{V_n^2 - V^2}$$

For the Monolith blast of August 1, 1953 t_o = 10.6 sec corrected to 1000 m datum. Reflection times at the distant stations should be reduced by 0.1 sec to eliminate the effect of the limestone hill and to correct the origin to the same datum. For precise work corrections for the elevations of all stations should be taken into account; introducing such a correction properly requires knowledge of V and H and can therefore be done only by iteration. A numerical check shows that the effects of the height variations of the stations are small. The greatest variation, one kilometer, causes less than one percent change in computed values of V and H. The station effects are therefore small and, because the average elevation of the stations used is 1000 m, they tend to cancel. The computation is thus made under the simplest assumptions with only the correction for the known low-velocity material at the quarry. The results are given in Table II A.

Using the mean velocity of 6.20 km/sec and vertical reflection time of 10.6 sec gives a depth to the Mohorovičić discontinuity of 33 km below the Monolith datum or 32 km below sea level. The travel time curve computed from the mean velocity and the value of t_o may be compared with the observed points as shown in Table II A in column O - C. The residuals are very small. The residuals of +0.2 and +0.3 sec at Mount Wilson, compared with 0.0 sec for

Table II

Beyond-Critical Reflections

A. Monolith Blasts

Vertical reflection time t_o = 10.6 sec.

Station	Date	Δ (km)	t (sec)	V	O - C
China Lake	Aug. 1, 1953	103.9	19.5	6.35	-0.3
	Sept. 6, 1952		19.5	6.35	-0.3
Mount Wilson	Aug. 1, 1953	106.7	20.4	6.12	+0.2
	Sept. 6, 1952		20.5	6.08	+0.3
Pasadena	Aug. 1, 1953	112.4	21.0	6.21	0.0
	Sept. 6, 1952		21.0	6.21	0.0
Haiwee	Aug. 1, 1953	116.7	21.7	6.16	+0.1
	Sept. 6, 1952		21.7	6.16	+0.1
Dalton	Aug. 1, 1953	120.7	22.2	6.18	+0.1
	Sept. 6, 1952		22.2	6.18	+0.1
Riverside	Sept. 6, 1952	158.4	27.6	6.22	0.0
Big Bear	Aug. 1, 1953	169.0	29.2	6.21	0.0
	Sept. 6, 1952		29.4	6.16	+0.2
Average value of V				6.20	

If V_n = 8.2, k = 6.9 and Δ* = 76.
H = 31.9 km below sea level.

B. Corona Blast

Vertical reflection time t_o = 10.5 sec.

Station	Date	Δ (km)	t (sec)	V
La Jolla	Aug. 6, 1949	111.6	20.4	6.38
El Cajon	Aug. 6, 1949	124.1	22.1	6.38
Point Loma	Aug. 6, 1949	128.7	22.5	6.47
Average value of V				6.41

If V_n = 8.2, k = 6.6 and Δ* = 84.
H = 33.5 km below sea level.

Pasadena are explained by the height difference; the same effect explains the difference between Big Bear and Riverside. The early arrival at China Lake is explainable in terms of a single layer of constant velocity only if the reflecting horizon is 1.8 km shallower between China Lake and Monolith than at the quarry.

If these arrivals are considered to correspond instead to the reflection near nine seconds on the vertical incidence records, a similar computation would place the reflecting horizon 26 km below sea level and give a velocity of 5.99 km/sec for the material above it. Assuming a velocity of 7 km/sec for the material between this horizon and that giving the second reflection one obtains a thickness of 5⅔ km from the Monolith record and 6 km from the Corona record. The depth to the Mohorovičić discontinuity is again 31⅔ to 32 km below sea level. This shows that if there is such a layer 6 km thick with velocity near 7 km/sec immediately above the Mohorovičić discontinuity, the critical reflections from its upper and lower surfaces will practically coincide over the range of distance of these records. Possibly the variation in the strength of these second arrivals comes from reinforcement and cancellation of the two reflections.

The two other stations between 103 and 169 km from Monolith, King Ranch and Santa Barbara, are both on thick sedimentary sections. The second arrivals are either missing or late.

Applying the same computation to the three stations which recorded possible critical reflections from the Corona blast produces the results in Table II B.

C. Other Reflection Data from Blasts

When the reflection travel time has been determined at two points, as discussed in the previous section, it may then be computed for points between on the simple assumption of a single layer. Travel time curves computed for such hypothetical velocity layerings as will fit the observed refraction data (obtained in Sec. III E) coincide within the error of reading records with the curve computed on the single-layer assumption in the interval between the observed points.

Tabulated data and copies of some records of blasts between vertical and critical incidence are in the Appendix; the pertinent facts are in Table III. Blasts have been recorded at 21 distances between 8.2 and 70 km, and many stations have recorded several blasts from the same source. Of this number, eight show arrivals close to the computed reflection travel time curve for the reflection from the Mohorovičić discontinuity. At eight of the remaining stations, high amplitude of motion or confusion with the S group makes reflected phases unreadable. In five cases no identifiable reflections from the Mohorovičić discontinuity have been found, even though records are of low enough amplitude to read. In all these cases small events are present near the computed time and might be interpreted as the reflection.

Some points are observed that fit the travel time curve of a reflection from a horizon about six kilometers above the Mohorovičić discontinuity, corresponding to the weak early reflections near 9.2 sec on the Corona and Monolith vertical incidence records.

Table III

Δ (km)	Quarry	Station	Date	Reflections Present	Remarks
8.4	Colton	R	Nov. 3, 1949 (and others)	Yes	Small 2-cycle impulse; not present on all records.
20.3	Corona	R	Aug. 6, 1949 Mar. 31, 1951 July 26, 1952	Yes	Strong 1½-cycle impulse present on vertical in 1951 and on N-S for all 3 blasts; absent on E-W. Vertical records too faint to read late phases in 1949 and 1952 blasts.
21.2	Colton	Cr	Nov. 3, 1949 (and others)	?	No apparent reflection on first 1949 blast, possible weak reflection on second.
24.4	Monolith	PR	Aug. 1, 1953	No	Vertical shows no apparent reflection; instrument out of adjustment, peculiar long-period response; E-W (tangential) shows no reflection.
26.0	Monolith	WR	Jan. 23, 1953	?	Possible weak event among group of similar events.
26.4	Corona	Pe	Aug. 6, 1949 Mar. 31, 1951	?	Line disappears.
26.5	Colton	Corona	Dec. 23, 1939	Yes	Many high peaks in S group; one fits closely to reflection curve but looks no different from others.
33.0	Colton	Pe	Nov. 3, 1949 (and others)	Yes	Weak energy burst on first blast; strong impulse on second.
33.0	Corona	Po	Aug. 6, 1949	Yes	Strong energy burst in S group. Preceded by smaller burst that might be earlier reflection.
34.4	Colton	Po	Nov. 3, 1949	?	Dubious; weak record with many small impulses in quick succession.

Table III (cont'd)

Δ (km)	Quarry	Station	Date	Reflections Present	Remarks
39.4	Monolith	KxR	Sept. 6, 1952	?	Either absent, lost in S group, or very late.
45.1	Colton	D	May 22, 1952 (and others)	?	Cannot tell; phases present but may be S and cannot be separated with vertical instrument alone.
45.2	Corona	D	Mar. 31, 1951	?	Confused with beginning of S.
47.8	Colton	D*	Jan. 29, 1938	?	Two shots 0.8 sec apart; confused.
49.6	Corona	Cr	Mar. 31, 1951	Yes	One-cycle pulse.
60.8	Corona	SA	July 26, 1952	Yes	Small, ½-cycle upward pulse; preceded by weaker ½-cycle down which may correspond to earlier reflection noted on Corona vertical incidence record.
65.9	Corona	MW	Aug. 6, 1949 Mar. 31, 1951 July 26, 1952	Yes	Record of 1949 blast has strong ½-cycle upward pulse on vertical, preceded by weaker pulse that fits for earlier reflection. Line too faint on 1951 and 1952 records.
67.6	Monolith	Ch	Sept. 6, 1952	?	Energy burst, but no sharp phases.
68.5	Colton	MW	May 22, 1952 Nov. 3, 1949 (and others)	?	Many small pulses, only one that fits closely for reflection travel time curve..

* Portable station at Little Dalton Canyon.

Table III (cont'd)

Δ (km)	Quarry	Station	Date	Reflections Present	Remarks
69.9	Corona	BB	July 26, 1952	?	$\frac{1}{2}$-cycle upward pulse at time corresponding to earlier reflection; nothing at computed time for reflection from Mohorovičić discontinuity.
70.0	Corona	P	Aug. 6, 1949 Mar. 31, 1951 July 26, 1952	?	Large energy burst, starting at time corresponding to earlier reflection and continuing through time of reflection from the Mohorovičić discontinuity.

For stations at four distances between 70 and 81.6 km, there are no prominent reflections. Many small phases are present; some may be P_m, or reflections from a horizon six kilometers above the Mohorovičić discontinuity.

These points are on records from Big Bear, Pasadena, Mount Wilson, Santa Anita, and Pomona for Corona blasts. On the record from Santa Anita the direction of motion of this event is opposite to that of the reflection from the Mohorovičić discontinuity and to the first motion of the record; this is also the case on the Corona vertical incidence record. On the Big Bear record it is opposite to the direction of first motion of the record. On the Mount Wilson record the first motion, the first reflection, and the reflection from the Mohorovičić discontinuity all seem to have the same direction. On other records the direction of motion cannot be determined accurately.

The records of blasts at Monolith and Corona are completely reproducible; i.e., the same phases are present in records from different blasts at the same quarry recorded at the same station. This is especially noticeable on the Riverside records of the three Corona blasts. The Colton blast records are not so reproducible. This may be due to the occasional practice at the Colton quarry of firing two blasts with a delay of a few seconds or less between. There is also greater variation in location of the blasts than in the other quarries, as shown by variations in times of first arrival. For most of the later Colton blasts studied, firing data and blast locations were not obtained from the quarry. In several cases, pairs of blasts fired less than an hour apart produced records quite different in appearance.

Almost all events listed in Table III for both reflections are of the same type: short sharp impulses, usually a single cycle or

at most two cycles. This is in marked contrast with the records at distances just past critical, on which the arrival of the reflection from the Mohorovičić discontinuity marks the beginning of a prolonged wave train.

Such arrivals cannot, in general, be shown to be reflections on any evidence other than fitting to a travel time curve derived from other data. In the case of the Riverside records from Corona, corroboration that the arrival is a compressional wave is given by its greater amplitude on the vertical and on the N-S horizontal, nearly radial to the source, and its weakness on the E-W horizontal which is more nearly transverse. Other stations recording from short distances had vertical instruments only, except Piute Ranch. There a single horizontal instrument located transverse to the blast recorded no reflection.

At distances between 70.0 and 81.6 km, no identifiable events fall on or near the computed travel time curve. The presence of a zone of low amplitude is predictable on the basis of Figure 1 (p. 24), but the distance at which it occurs is greater than that obtained in the figure. The next records showing strong reflections occur at a distance of 103.9 km; hence the distance for critical reflection is not determined but apparently lies between 81.6 and 103.9 km.

Variations from the computed travel time curve do not appear to be significant in view of the inaccuracy of reading comparatively weak events on already disturbed records.

The reflected nature of these events is unproved. Moreover,

many similarly sharp impulses may be found at times which will not fit the computed travel time curves. At Williams Ranch and Knox Ranch, for example, the strongest pulse arrives too late to fit the reflection curve unless the Mohorovičić discontinuity is considered to be about 12 km deeper than at Monolith.

The conclusion that can be drawn from these data is that events can be found in the intermediate range of distances that will fit a reflection travel time curve derived from other data but that the attempt to use these arrivals alone to derive a curve is unrewarding in view of the large number of other events present. The need for recording with multiple-channel equipment is again indicated.

D. Reflections in Earthquake Records

Because of the difficulty of determining focal depth of shallow earthquakes, little information about the depth of the Mohorovičić discontinuity can be derived from reflected phases in earthquake records. Some information about velocities can be obtained, for the reflection travel time curve will be affected by the material between the earthquake focal depth and the Mohorovičić discontinuity while the travel time curve for the direct wave will not.

Extensive investigations of these phases have been made by Gutenberg (1944b; 1951b). The data for the 1944 paper came from fifty earthquakes scattered throughout southern California; only a portion of these were used in the 1951 paper. Because of the wide spacing of the stations at the time these shocks occurred, in no case were more than two stations represented for any one shock in the points studied for the curve P35P (the notation used in the 1951 paper for the untransformed P-wave reflected at the Mohorovičić discontinuity).

The scatter of the points is large, and examination of the plotted data (Fig. 6 in Gutenberg, 1951b) shows that the points for the phases P35P and P28P are quite close together. In only a few instances are points for both curves obtained from a single record. It is possible that most of the points plotted belong to a single travel time curve.

Because of the nature of the data used in Gutenberg's studies, the scatter might have been due in large part to variations in

both the focal depths of the earthquakes studied and the depth to the Mohorovičić discontinuity. For the present study it was therefore desired to obtain readings from a large number of stations for a single shock, or at least from shocks in a limited area. If all points were derived from records of a single shock, effects of variation of focal depth would be eliminated and effects of variation of reflector depth would be minimized; studying only points from shocks in a small area would minimize effects of variations of reflector depth but not of variations of focal depth.

The ideal situation, in which enough points could be obtained from records of a single shock to define the travel time curve of the reflected wave, has not been realized because the station network is not dense enough. In a search for records that might approximate this ideal, the most usable data were found to be the shocks used by Richter (1950) in his study of velocities of P at short distances. Of the eight shocks he used, numbers 2 to 6 have, at many of the stations, distinct second arrivals which form a reasonably smooth travel time curve. These shocks were recorded on a large number of near-by stations and the locations are unusually precise.

The data given by Richter for these five shocks, with a few additional readings made by the present writer, are plotted as Figure 8. Although these shocks are the same as the ones plotted in Figure 13 in Sec. III E, there is an important difference between the two plots. In Figure 8, the data are plotted with

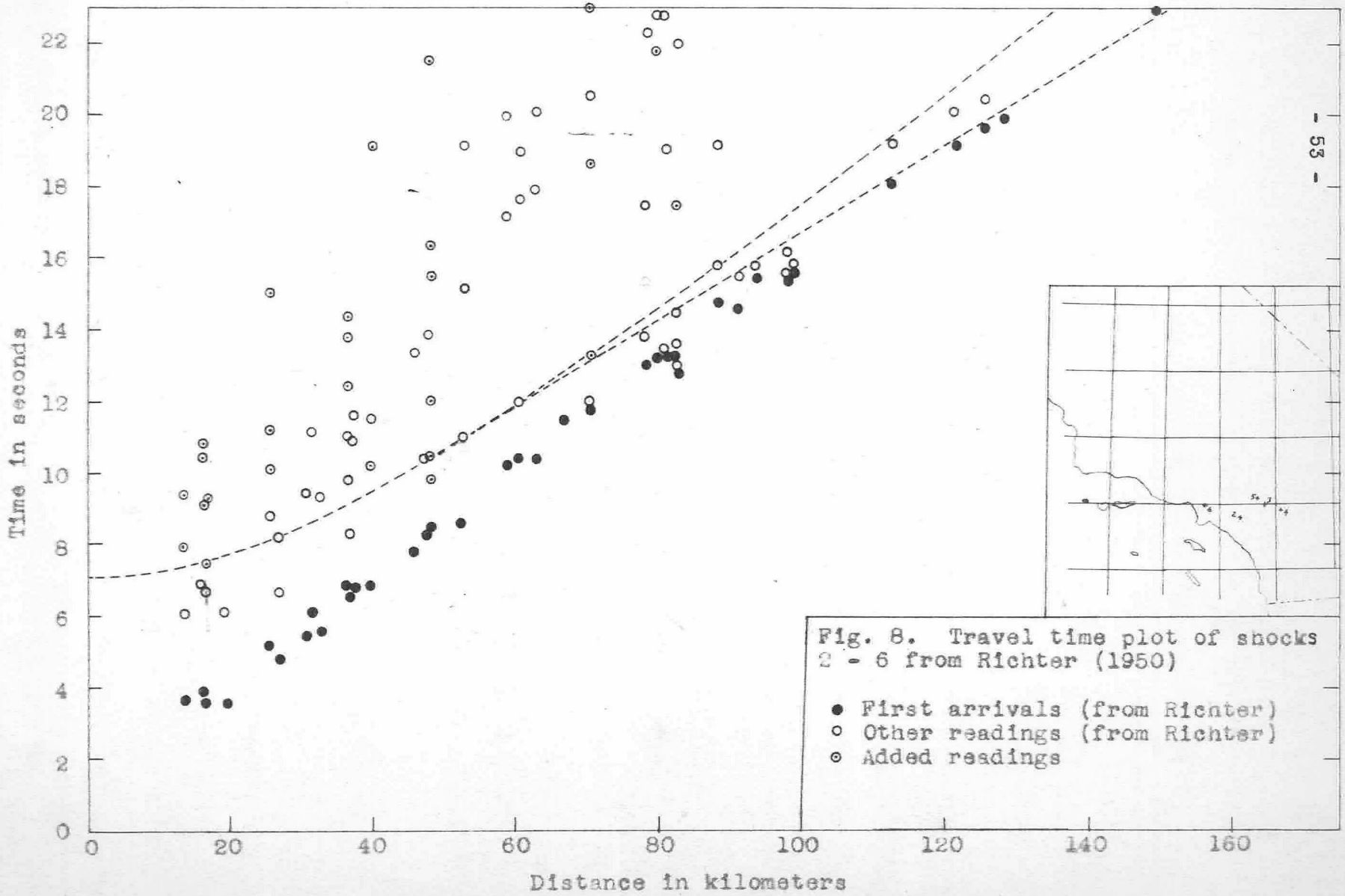

Fig. 8. Travel time plot of shocks 2 - 6 from Richter (1950)

- ● First arrivals (from Richter)
- ○ Other readings (from Richter)
- ⊙ Added readings

time read after the origin time determined from the S - P interval; in a note added to his paper Richter altered the origin times by small amounts in such a way as to reduce the constant residuals for each shock. This assumed that these residuals are due to errors in determination of origin time by use of S - P; but if a layered structure is assumed for the portion of the crust above the focal depth of the earthquakes, variations in focal depth will produce similar constant residuals. If the residuals are due to depth variations, the travel times of the reflected waves vary in an opposite sense to those of the direct waves, and such a change in origin times increases the scatter of the points on the reflection travel time curve. In Figure 13, because the direct waves are of interest, the origin time corrections are used.

Superimposed on the plotted points in Figure 8 is a computed travel time curve for the reflection from the Mohorovičić discontinuity based on the "mean velocity" of 6.20 km/sec and depth of 32 km to the reflector as obtained in Sec. III B. The focal depth of the shocks is assumed to be 20 km for this curve. The accompanying travel time curve for P_n with velocity 8.2 km/sec has an intercept time of 4.6 sec and a value for Δ^* of 51 km. Five of the second arrivals are close to both the reflection curve and the curve for P_n; five more are on the curve for P_n. In addition, the plot indicates that the first arrivals beyond 110 km may be P_n. Three of these shocks were recorded at stations sufficiently distant to give a value for the intercept time of P_n; if the velocity 8.2 km/sec is used, this average value of k is 5.3 sec. The check

is reasonably good if it is considered that these are small shocks and have weak first arrivals at the distant stations. The agreement here between observed points and computed curves is remarkably close.

Data of a slightly less precise nature can be obtained from the shocks used by Gutenberg (1951b). In Figures 9 and 10, for which Gutenberg's original readings have been used, shocks in two areas have been separated. The first area includes only shocks near Long Beach and the Palos Verdes Hills, segregated because they contributed a large number of the points near the calculated curves on Gutenberg's 1951 plots. The epicenters have been checked, using the velocities obtained in Gutenberg's later study (1951b); those of shocks 22 and 23 were shifted slightly. The precision of the epicentral locations is not as high as could be desired because the stations are all east of the epicenters. The velocities beneath the Los Angeles basin are not well known. In Figures 9, 10, and 11 times are plotted as time after first arrival, in order to minimize effects of errors in location.

The most striking feature on Figure 9 is the line of seven points that formerly were part of the cluster around the lines for P28P and P35P. They have an equation $t = 0.6 + \Delta/4.8$ and correspond to no known phase. All are arrivals at Pasadena and Mount Wilson and record strongly on vertical and radial instruments but not at all on transverse instruments, so the arrivals must represent a compressional wave. With such a travel time equation these cannot represent a reflection from the Mohorovičić discontinuity. They

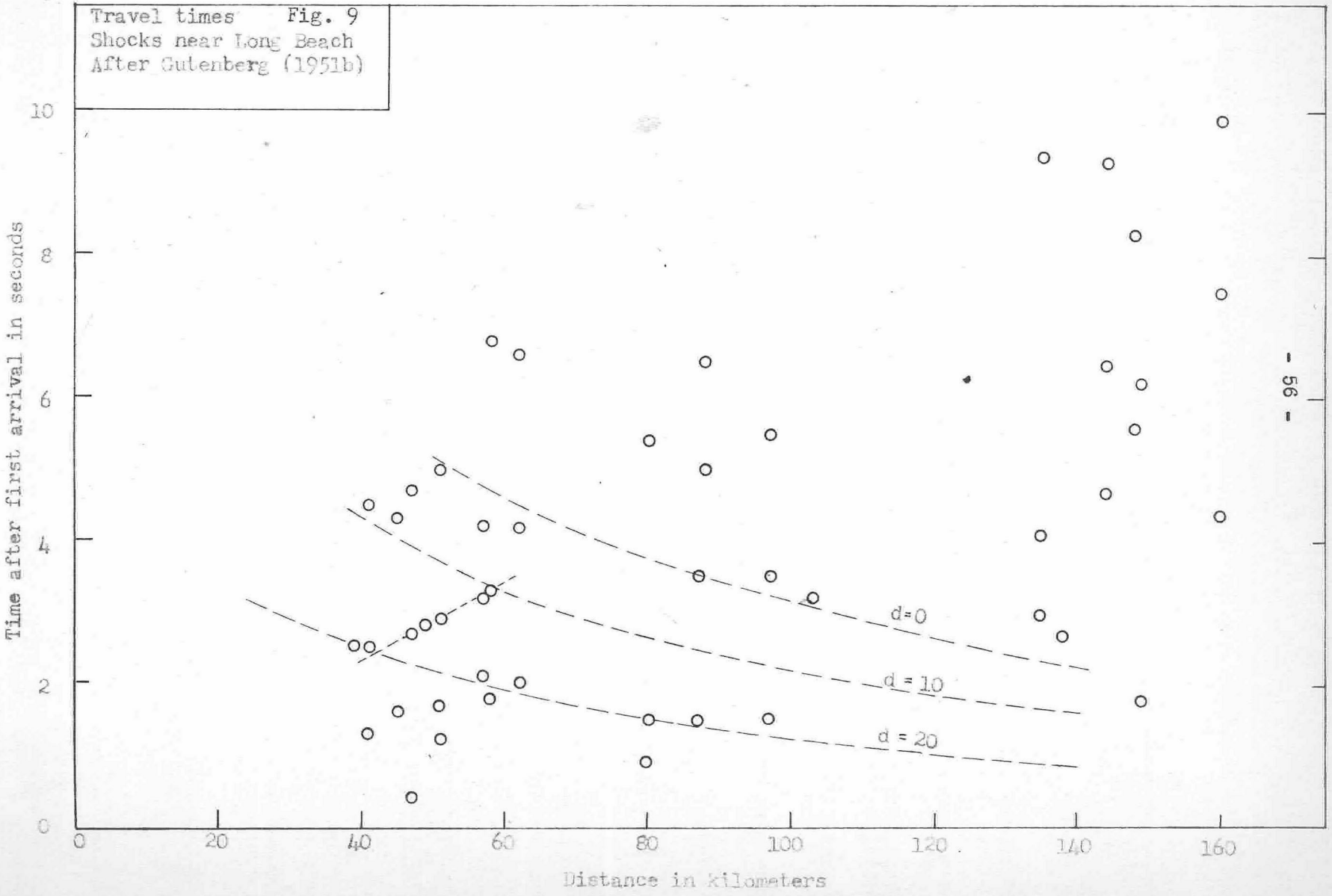
Travel times Fig. 9
Shocks near Long Beach
After Gutenberg (1951b)
Time after first arrival in seconds
Distance in kilometers
d=0
d = 10
d = 20
0
2
4
6
8
10
0
20
40
60
80
100
120
140
160

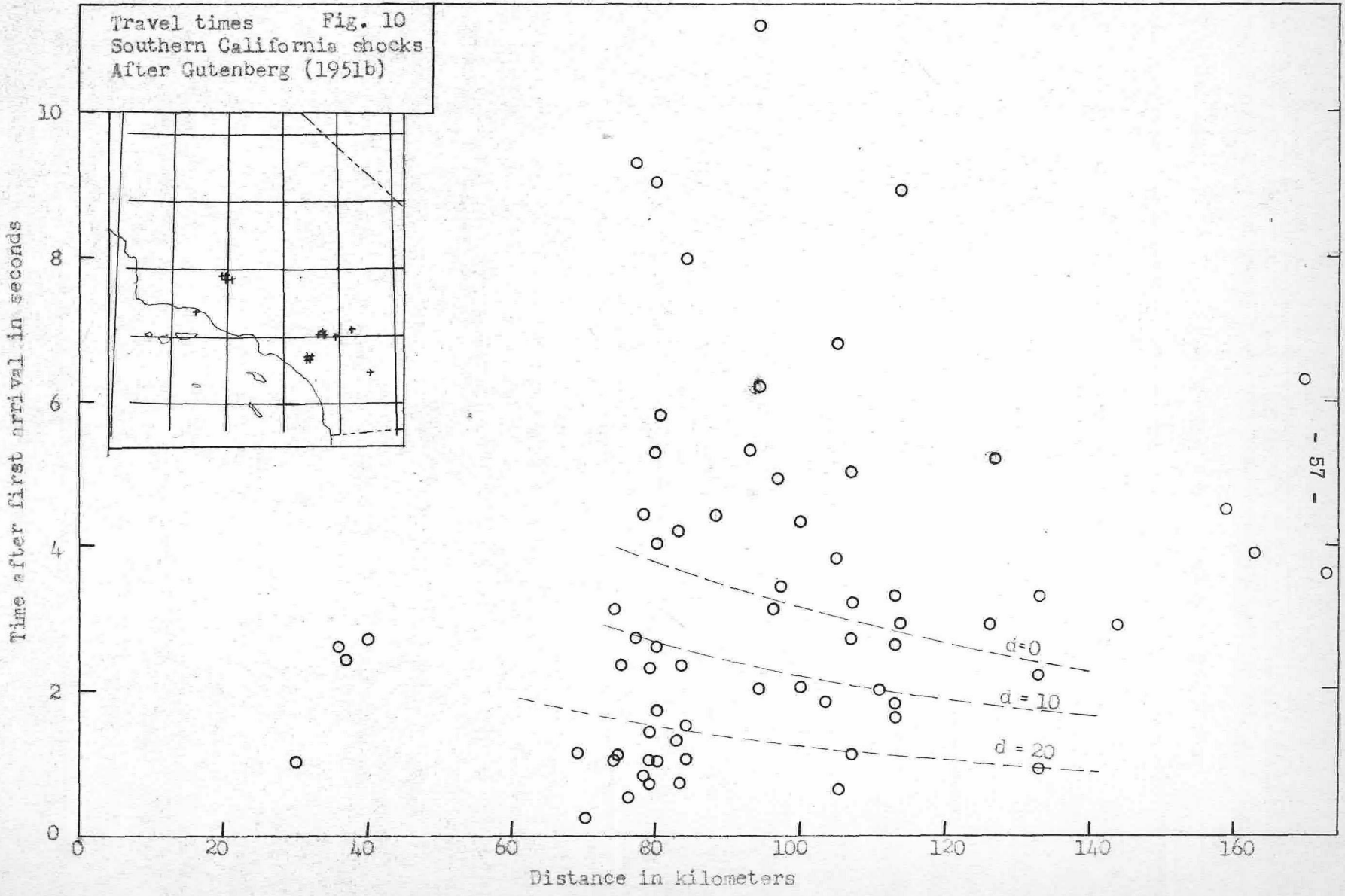
Travel times Fig. 10
Southern California shocks
After Gutenberg (1951b)
Time after first arrival in seconds
Distance in kilometers
0
2
4
6
8
10
0
20
40
60
80
100
120
140
160
d=0
d = 10
d = 20

may represent a wave traveling through the sediments of the Los Angeles basin. Other points on this plot, from the same shocks recorded at Mount Wilson, Riverside, and Santa Barbara, fall slightly below the travel time curve computed for a reflection from a depth of 32 km, if the focal depth of the shocks is assumed to be zero. This indicates that either the Mohorovičić discontinuity is much deeper under the Los Angeles basin or that the shocks are extremely shallow. If the phase with apparent velocity 4.6 km/sec is actually a wave through a sedimentary path, the shocks must be shallow. It should be noted that the observed points near the computed curve for h = 0 approach a constant time after first arrival more rapidly than does the computed curve.

Earthquakes in the second group taken from Gutenberg's fifty shocks (Fig. 10) all lie in or near the "Area of Study" marked on the base map and overlap the area covered by the shocks taken from Richter's paper (1950). The line corresponding to the "sedimentary wave" is completely missing on this plot; a few points lie near the reflection curve computed for zero focal depth, but the most outstanding group of points falls between the curves computed for focal depths of 10 and 20 km. The close fit in slope to the computed curve derived using a velocity of 6.20 km/sec for the reflected wave and 6.34 km/sec for the direct wave gives additional evidence that the average velocity of the material between the focal depths and the Mohorovičić discontinuity is not greater than the velocity of the material above the focal depths; it is probably slightly less.

Data from the Walker Pass earthquakes of March, 1946 and later (Chakrabarty and Richter, 1949) are plotted in Figure 11. In this case the locations are more doubtful. The Walker Pass shocks occurred such that almost all the seismograph stations at that time were north or south of them, very few east or west. As a result, the locations can be considered quite accurate in latitude and in relative position to each other, but the longitude of the entire group might be shifted as much as five minutes. For the present study Chakrabarty's locations were revised using newer velocity information; in most cases the shifts were small.

The only near-by station at suitable distance to record reflections from most of the shocks in this group was Haiwee; China Lake, established somewhat later, recorded a few of the last aftershocks. Records of the Haiwee and China Lake stations were completely re-read by the present writer and readings were rated for quality. Only the most definite readings were taken for plotting; all new readings are tabulated in the Appendix.

Most of the data roughly fit a line between the computed curves for focal depths of 10 and 16 km. This may mean either that the shocks are shallower than normal or that the Mohorovičić discontinuity is deeper. With only one near-by station it is impossible even to estimate the depth of these shocks. A greater depth for the Mohorovičić discontinuity in this area would not be unexpected. A few of the strongest phases fall on a line similar to that observed for the Long Beach area; this may represent a wave traveling through the sediments of Owens Valley.

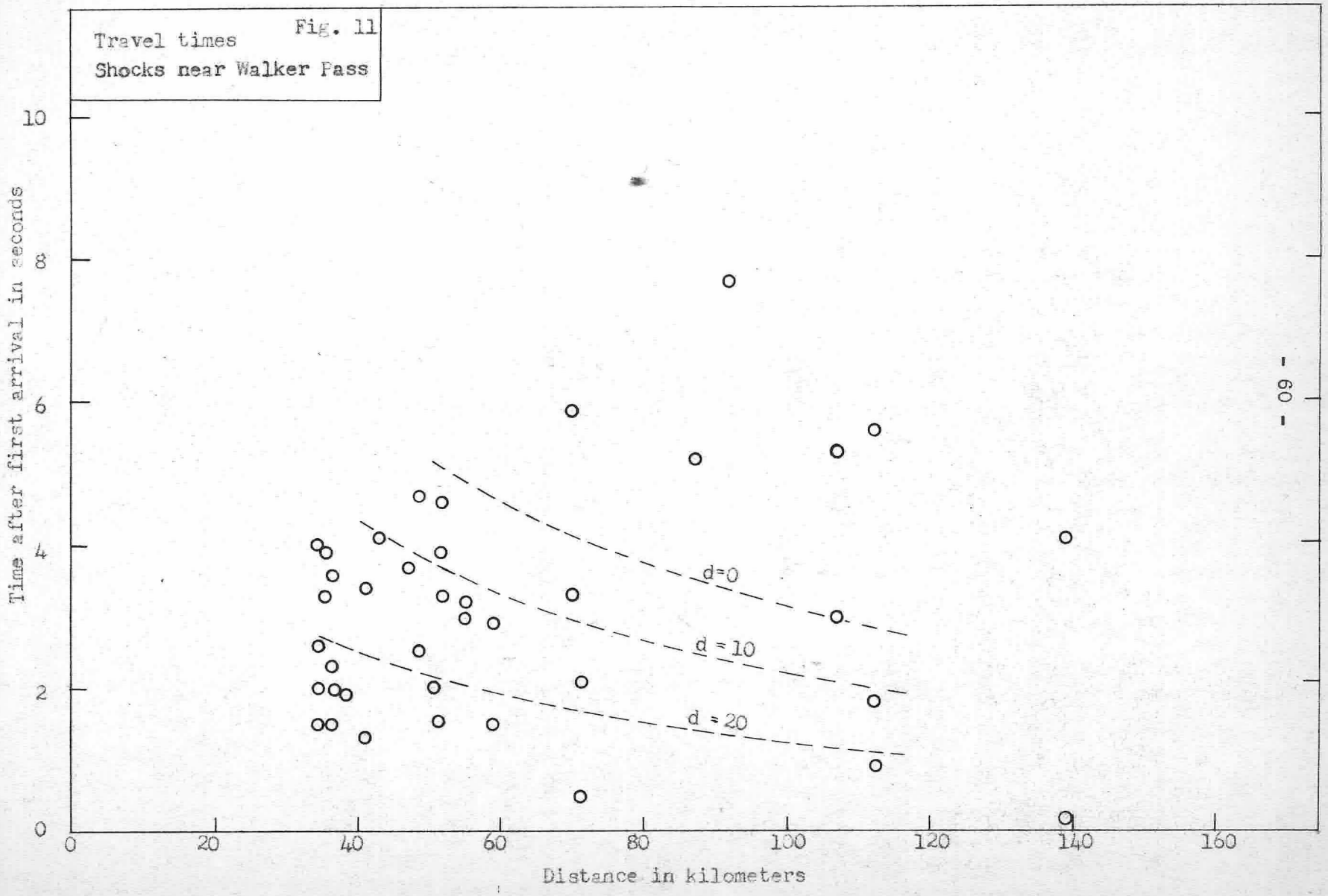
Travel times
Fig. 11
Shocks near Walker Pass
Time after first arrival in seconds
Distance in kilometers
d=0
d = 10
d = 20
0
2
4
6
8
10
0
20
40
60
80
100
120
140
160

In order to provide a check on the objectivity of the readings used in the previous plots, another type of information was plotted in Figure 12. In this, all the points represent readings made in the routine measurements of seismograms to locate epicenters; no attempt has been made to find phases corresponding to reflected waves. The plot includes all readings, within the ranges of time and distance shown, from shocks which occurred between September 2, 1951 and February 13, 1952 and which were given B-quality location ratings in the Pasadena local bulletin. The readings were made by Mrs. Violet Taylor for the laboratory and have not been re-read. The customary procedure has been to read the times of P and S whenever possible at all stations for all shocks and to read other phases only when outstanding. Any intermediate phases shown can therefore be considered to represent strong phases read without reference to expected arrival times. For the plot two symbols were used: one for shocks fitting closely the normal travel time curves with the assumption of a focal depth of 16 km and another symbol for shocks that could be located well only if shallower depths were assumed. These latter shocks include only those very close to at least one station; effects of depth on first arrival times become small at distances beyond about fifty kilometers. Some shallow shocks may have been included among the "normal" depth group because they were not within fifty kilometers of any station.

In this plot arrivals between P and S in the range from 40 to 90 km again follow the same general trend as on the previous

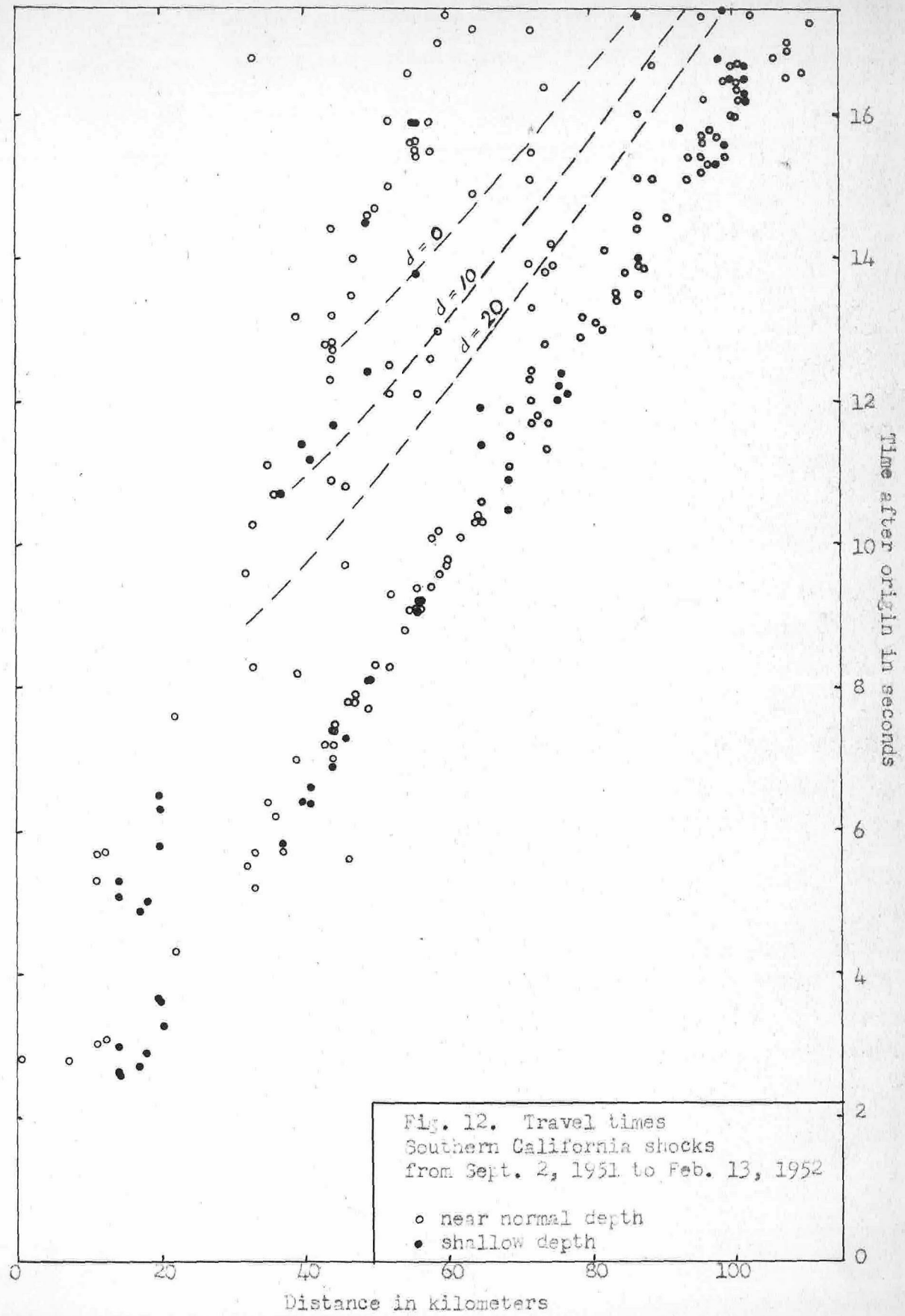

Fig. 12. Travel times
Southern California shocks
from Sept. 2, 1951 to Feb. 13, 1952

○ near normal depth
● shallow depth

plots. Shocks which include these phases represent only a small percentage of the total read, indicating that the reflected phase is not of uniform strength on all shocks. When strong second arrivals are present, they conform to the pattern expected for the reflection from the Mohorovičić discontinuity.

A few general conclusions may be drawn from the earthquake data. There does not seem to be any consistent discernable separation of the observed points into two parallel travel time curves as would be expected if there were two reflections of nearly equal strength. The scatter is great on all plots except that based on Richter's data and possibly that for the Long Beach area. This indicates that most of the scatter is caused by variations in focal depth rather than by variations in reflector depth. The plotted points fit reasonably well to the curves computed by assuming a single layer of constant velocity. It is not definite whether the reflection travel time plots parallel or approach the curve for the direct wave at long distances, but the approach is not rapid if present at all. This implies that the maximum velocity between the focal depth of the earthquakes and the Mohorovičić discontinuity is scarcely greater than that above the earthquake foci.

E. Crustal Velocities

Information about crustal velocities in the region studied comes from blasts at Monolith, Corona, Colton, and Victorville (Wood and Richter, 1933; Gutenberg, 1951a, 1952; and unpublished data) and from earthquakes recorded at short distances (Richter, 1950; and unpublished data). The data presented here refer to the igneous and metamorphic outcrop areas within the line marked on the base map "Area of Study". The area is bounded topographically by the Sierra Nevada, the San Joaquin Valley, the Los Angeles basin, the Peninsular ranges, and the San Bernardino Mountains. In terms of petrology, it covers the region from the southern end of the Sierra batholith to the northern end of the southern California batholith. The rocks exposed at the surface include large bodies of intrusive rocks ranging from granite to diorite, small and large bodies of metamorphics including gneiss, schist, and slightly metamorphosed limestones, and in some places a thin cover of Tertiary sandstones and shales (Jenkins, 1938; Larsen, 1948; Miller, 1934). Most of the stations are on igneous rocks. All the quarries are on either igneous rock or limestone; hence the low-velocity Tertiary sediments should have little effect on the velocities determined. The rock types present can be expected to have velocities between 3 and 7 km/sec on the basis of past reports on typical seismic velocities in igneous and metamorphic rocks (Heiland, 1940, p. 472). Contacts are definitely not the "uniform horizontal layering" normally postulated in deriving velocity from refraction first arrivals; in the areas of the

southern California batholith and the Sierra batholith near the quarries used for most of the work, the contacts between igneous and metamorphic facies are in general more nearly vertical (Larsen, 1948; J. P. Buwalda, oral communication). It would therefore be surprising if the combination of a heterogeneous group of data using stations in widely varying azimuths from different seismic sources, covering an area of nonuniform composition with nearly vertical contacts, should give a smooth travel time curve interpretable in terms of a simple series of layers or a linear increase of velocity with depth, even if the accuracy of timing were sufficient to ensure close determination of velocities. Such smooth curves were not obtained.

This study is aimed not at determining "the velocity in the granitic layer of the continents", but at determining a velocity-depth profile for computation of data within the area of study. The body of rock studied is limited in area. Immediately to the southwest and northwest of the area described, most of it is missing or deeply buried; sediments of the Los Angeles basin and of the southern San Joaquin Valley reach a depth of 10 to 15 km.

For the velocity in the material in the first five or six kilometers, travel time curves for stations out to 70 km can be used. (See travel time plot in pocket). There is a large and probably real scatter of the first arrivals in the range from zero to 70 km. Some consideration should be given to the accuracy of these data. The first arrivals from blasts at distances in this range are usually strong enough to ensure reading first

motion. At the individual stations times are read to 0.1 sec, but absolute timing of all (except the data from the Carnegie Institution stations for the 1949 Corona blast) may in many cases be in error by 0.2 sec or more because of variations in the rotation rate of the recording drum, variable lag in timing relays, non-uniform paper shrinkage, rate changes in chronometers, and inaccuracies of measurement. When distance intervals of only ten to twenty kilometers are used, such variations are causes of considerable error in computed velocities.

A cause of appreciable error in determining velocities at near-by stations and the intercept times of refracted waves at distant stations is the inaccuracy of determining blast firing time. For only one blast is the time of explosion established within a hundredth of a second; this is the Monolith blast of August 1, 1953, at which the signal from a loudspeaker (used as a microphone) placed three meters above the charge was compared with a time signal from radio station WWV. The time could be read to the nearest millisecond, and the only delay was the time of sound transmission to the speaker, which was not over 0.010 sec and probably much less. At one other blast, Victorville, the time of breaking of a wire within the loaded hole was recorded in comparison with a rated chronometer, ensuring accuracy of reading to 0.1 sec.

At most other blasts timed at origin, the signal from a seismometer located 0.15 to 0.6 km from the shot was either recorded directly in comparison with a rated chronometer or was

used to operate a relay to put a signal on the records at the Pasadena station. In these cases, origin time could be obtained by use of an assumed velocity for the rock between the shot and the seismometer. For the competent rock in the quarries studied, the velocity is probably between 3 and 6 km/sec, allowing errors in calculated origin time up to 0.1 sec. The accuracy of the chronometers after transportation to the quarry and rating with only a few time signals is questionable.

The one blast timed by two different methods has an uncertainty of 0.2 sec in origin time. This was the 1949 Corona blast, timed to 0.01 sec on the breaking of the cap wire compared with a signal from radio station WWV, and to 0.1 sec on the arrival of the seismic waves at a seismometer 0.3 km away compared with a chronometer calibrated with time signals from radio station NPG. There is a difference of 0.3 sec between the two measurements, assignable either to low velocities in the quarry floor, delay in detonation of the charge, inaccuracy of timing of the seismometer record, or a combination of the three.

Temporary stations were run by Tuve's party from the Carnegie Institution of Washington next to the permanent stations at Pasadena and Palomar; the temporary stations recorded time signals from WWV, and the permanent ones recorded signals from NPG. Published readings for the blast arrivals show differences between the temporary and permanent stations at each location not over 0.05 sec. Therefore, there was no discrepancy between the two timing systems. The timing of the cap break is not open to

question.

If the velocity of the rock in the quarry is assumed to be 3 km/sec or more, a discrepancy of 0.2 sec remains. Timing of later blasts with portable seismometers at the same quarry gives sufficient check with the 1949 blast to ensure that the error at the portable seismometer was less than 0.1 sec. Accurate recording of this blast at more distant stations in the same type of rock indicates that the velocity in the quarry should not be less than 3 and probably nearer 5.8 km/sec. The possibility of a delay in firing must then be considered, and all times from the 1949 Corona blast must be taken with an uncertainty of origin time of 0.2 sec. While this does not affect most of the calculations, it prevents accurate determination of shallow velocities and adds to the uncertainty of the intercept times of P_n at distant stations.

Curves could be fitted to the travel time plots using least squares methods under a variety of assumptions, including a single straight line, a series of straight lines, or a curve for linear increase of velocity with depth. Variations in reliability of the data and known lateral variations in rock type do not seem to justify these methods.

The best timing for velocity at short distances comes from the stations at Dawson Creek and Elsinore operated by the Carnegie Institution for the 1949 Corona blast (Rooney, Tatel, and Tuve, 1950). The times for these two stations are determined to 0.01 sec and the stations are in a straight line from the quarry with comparatively homogeneous rock between. Their differences should

give an accurate determination of the velocity at shallow depth; the result is 5.75 km/sec for a path almost completely in the Temescal Wash quartz latite porphyry, the material which is in the Corona quarry (Larsen, 1948). Other station pairs less than 30 km from the quarries concerned, but with less accurate timing, give the following velocities:

Blast	Date	Stations	Velocity
Corona	1949	Dawson Creek to Elsinore	5.75 km/sec
Corona	1949	Corona to Riverside	5.9
Corona	1951	Corona to Riverside	6.1
Corona	1951	Corona to Perris	5.6
Colton	1939	Colton to Corona	5.8
Colton	1939	Riverside to Corona	7.0?
Monolith	1953	Monolith to Piute Ranch	5.5
Monolith	1953	Monolith to Williams Ranch	5.9
		Average, excluding Riverside to Corona	5.8 km/sec

Velocities obtained from travel times between Colton and Riverside are low (near 4 km/sec) and variable. Some of the erratic effect is probably due to inaccuracies of timing combined with the short travel path; more is probably due to variation in the amount of the travel path that is in limestone and to errors in distance because of variation in position of the shots in the quarry. The effect of the size of the limestone bodies introduces an uncertainty into velocities obtained from Colton and Monolith blasts. At Monolith, however, the first arrivals on the reflection spread determine the velocity in the limestone body and give some idea of its extent.

Accordingly, the values of the velocity for shallow material as indicated on records at short distances from Monolith have been obtained by subtracting the arrival time and distance of the far-

thest geophone of the reflection spread from the arrival times and distances of the stations studied. This is tantamount to considering the limestone body as a hemisphere with a radius of 1 3/4 km from the blast site. This is a conservative estimate of the size of the limestone body (Fig. 2, p. 28) and, if an underestimate, will make the velocities appear lower than they actually are.

Examination of the blast travel time plot shows an apparent curvature, indicating an increase of velocity with depth. However, the points at which late arrivals indicate such a curvature are all beyond the range listed in the preceding tabulation, giving not a simple curve but an "S" shape, which indicates apparent velocity decreasing and then increasing again. If the velocities derived from stations at short distances as tabulated above are ignored, a fit is obtained for a velocity increasing with depth, starting at approximately 5.5 and increasing to 6.3 km/sec. A better explanation of these data is lateral variation of velocity, with certain stations consistently late. Crestline and Big Bear produce most of the late readings. Crestline is in the range of distance producing the apparent curvature on travel time plots for Colton and Corona blasts. Big Bear is in this range from Colton only; it is 70 km from Corona, at which distance other stations have early arrivals. Here again the Big Bear reading is 0.4 sec late. Since Big Bear and Crestline are at high elevation and near each other, it seems proper to assign their late arrivals to some cause associated with their position. Mount Wilson, also at high elevation, may have slightly late readings for the Corona

and Colton blasts; its readings are quite late for the Victorville blast. The Pomona record for the 1949 blast provides another late reading; this may be due to the alluvial material beneath this station.

If the velocity of 5.8 km/sec is extrapolated to greater distances, stations near 70 km from these blasts have early readings; a second line of the travel time plot is required, with velocity 6.0 km/sec and intercept 0.2 sec. Assuming uniform layering, this indicates a uniform surface layer 1.8 km thick with velocity 5.8 km/sec. Considering the known variation in surface elevations and types of rock exposed at the surface, the explanation seems absurd. It is more in accordance with the known inhomogeneity of the surface materials to combine them into a single surface layer and fit all data out to 70 km to a line with the equation $t = 0.1 + \Delta/5.9$. This agrees with the data from Corona and Colton blasts; agreement with Monolith blast data is good if 0.3 sec is added to the intercept time. The fit to this straight line is remarkably good in view of the known variation in rock types.

Beyond 100 km, first arrivals from blasts recorded north of Corona are very small emergences and may be late. The earliest is on the Dalton records of the Monolith blasts, on which the closeness of the second arrival to the line $t = 0.4 + \Delta/5.9$ suggests that an earlier arrival with velocity over 6 km/sec may be too small to be read on the other stations. This is verified by comparison with earthquake data presented by Richter (1950), from which the mean

velocity to a depth of about 16 km is found to be 6.34 km/sec. The earthquakes discussed by Richter all lie within the area of the present study as outlined on the base map; travel time curves for the blasts and the earthquakes should, therefore, show the same structure. A "mean velocity" of 6.34 km/sec (obtained by assuming a single layer for computation) implies that, if there is any variation of velocity at all, at some point between the surface and the earthquake focal depth the velocity exceeds 6.34 km/sec. Unless the layer with highest velocity is extremely thin, the inverse slope of the travel time curve closely approaches this highest velocity at comparatively short epicentral distances. Richter's data, plotted as Figure 13, show an asymptotic approach to velocity 6.5 km/sec. The data from blasts recorded north of Corona do not rule out such a high velocity; it is merely not observed because of weak first arrivals. At the time of the larger Corona blasts there were no stations within this area at a suitable distance from Corona to check the presence of such a layer of higher velocity.

The data from Corona south to the Mexican border show a different picture; a strong uniformly early arrival is found on records from stations in this area between 108.5 and 148.4 km. Most of these records were taken by Tuve and his co-workers and have not been available for examination. Records from Point Loma, La Jolla, and El Cajon for the 1949 Corona blast, and from Barrett for a Colton blast on May 22, 1952, are available and on examination show that the arrivals are strong and clear. The Point Loma

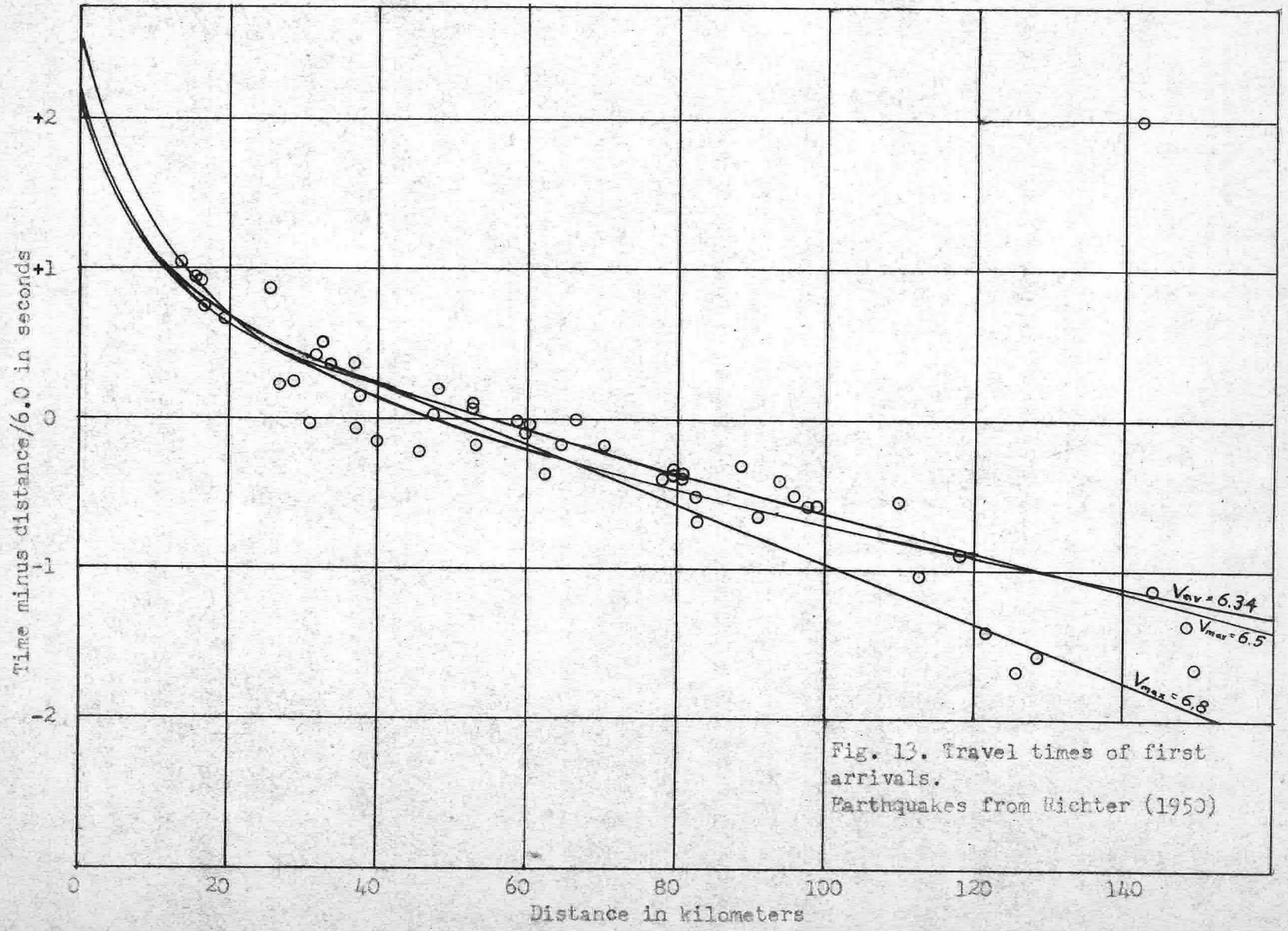

Fig. 13. Travel times of first arrivals.
Earthquakes from Richter (1950)

record has been plotted with a correction of 0.8 sec for the sediment delay as derived from previous refraction work in the area by R. W. Raitt (oral communication); this may be slightly large. The La Jolla station was also located on sediments at least two kilometers thick (Hertlein and Grant, 1944, pp. 38-39), and a similar correction (shown on the plot by a dashed circle) puts it near the same line. Any sediments below the El Cajon station are thin, and the reading cannot be adjusted in this way. These data can be interpreted only in terms of an apparent velocity of 6.5 to 6.8 km/sec. The readings from Ramona, Lakeside, and Glencliff Camp are the least subject to doubt because the stations were all on granitic outcrops and had high sensitivity; these stations fit the line $t = 0.9 + \Delta/6.64$. The entire group of data has been fitted by Gutenberg (1951a) to the line $t = 1.5 + \Delta/6.8$.

An attempt to treat the two groups of blast data and the earthquake data together leads to contradictions. If a simple system of uniform layers of constant thickness is assumed, the velocity structure consists of an upper layer, $8\frac{1}{2}$ km thick, having velocity 5.9 km/sec, overlying a layer with velocity 6.8 km/sec. Fitting this to the earthquake data and placing the earthquake foci in a lower velocity layer beneath that with velocity 6.8 km/sec in order to give the best possible fit to the observed travel times, one still finds an appreciable divergence between the observed points and the computed curve at distances near one hundred kilometers from the source.

It is apparent that the velocity structure cannot be obtained

on the simplest assumption of uniform horizontal layering extending to all stations which have recorded southern California blasts. If a completely heterogeneous variation of velocities, both laterally and vertically, is assumed, it explains all arrival times recorded but does not help in computation. The usual procedure with refraction data is to assume the simplest possible structure that will fit the observed travel times and to use it as a working hypothesis until more data are obtained. Because of this, the calculated velocity profiles for the earth's crust are in general simplest in those areas in which the least work has been done.

The simplest model that fits all observed data is a series of layers, each having constant velocity throughout southern California, with variations of thickness to account for the discrepancies between regions. For distances out to 65 km, all data fit most closely to a mean velocity of 5.9 km/sec. For the Corona data the intercept of this line is 0.1 sec. From 65 to 150 km, there is a second segment of the travel time curve which has velocity 6.5 km/sec and intercept time 1.0 sec and fits the data north of Corona. This takes account of the fact that several of the stations recording Monolith blasts in this range have small emergent beginnings that are probably late. This choice of velocity for this range is a compromise fit; it is the velocity that best agrees with the earthquake data and it is the lowest value that agrees with the data from the stations south of Corona. A single early arrival at China Lake from the 1951 Corona blast may be interpreted as indicating velocity 6.8 km/sec; it can be as logi-

cally combined with the arrivals at Havilah and Chuchupate and interpreted as P_n with velocity 8.2 km/sec and intercept near 7 sec, which leaves no data from these blasts indicating velocities over 6.5 km/sec north of Corona.

On this hypothesis, the layer with velocity 5.9 km/sec thins to zero south of Palomar; readings from the remaining stations to the south agree with small deviations to the line $t = 0.5 + \Delta/6.5$. For the area between Corona and Monolith, this indicates the following structure: a fraction of a kilometer of comparatively low-velocity material at the surface, underlain by six kilometers of material with velocity 5.9 km/sec and below that an undefined thickness of material with velocity 6.5 km/sec.

If the early arrivals south of Corona are ascribed to locally high velocity, and the solution for the area north of Corona is based solely on the northern stations and the earthquake data, a structure may be postulated of velocity 5.9 km/sec for the first six kilometers, and below this velocity 6.34 km/sec for an unspecified depth.

If, on the other hand, the earthquake data are omitted and all blast data are combined and solved for a simple system of horizontal layers, a model is obtained with velocity 5.9 km/sec in the first eight kilometers and velocity 6.8 km/sec below this.

The blast refraction data yield little information about the material between the layer with velocity 6.34 to 6.8 km/sec and the Mohorovičić discontinuity. They indicate only that there is no large increase in velocity immediately below this layer. From

studies of amplitudes of direct waves in southern California earthquakes, Gutenberg (1951b) has concluded that a velocity decrease exists above the depth of origin of most southern California earthquakes. The large amplitude phase $\bar{P}$ at distances over 150 km has been explained by him as a channel wave in a low-velocity zone near the earthquake focal depth. The velocity of $5\frac{1}{2}$ km/sec of $\bar{P}$ sets a minimum for the mean velocity within the low-velocity channel. The velocity in the material within this interval must be left as an unknown in computations, with only rough limits for its values.

There is some evidence for a zone with velocity near 7 km/sec immediately above the Mohorovičić discontinuity. The phases f and P_m in earthquake records have been interpreted by Gutenberg (1951b) as the beginning and maximum respectively of a refracted wave from a layer about seven kilometers thick with this velocity.

If material with this velocity and thickness exists anywhere in the crust above the Mohorovičić discontinuity with a low-velocity layer beneath it, a reflection from the discontinuity would, beyond critical distances, give a travel time plot identical with that assigned to P_m. If material with velocity 6.8 km/sec, as observed on blast records at stations 33 to 40 (base map), actually exists over the area of study, there is then no proof from P_m of the existence of the layer immediately above the Mohorovičić discontinuity. If the velocity above the earthquake foci is between 6.3 and 6.5 km/sec, the observations of P_m imply the existence of a layer with velocity near 7 km/sec immediately above the Mohorovičić

discontinuity. The inverse slope of the reflection travel time curve between 100 and 170 km is 7.0 km/sec; the maximum velocity above the Mohorovičić discontinuity must therefore be less than this, probably not more than 6.8 km/sec.

If such a layer exists, the event on the vertical reflection records 1.6 sec before the reflection from the Mohorovičić discontinuity corresponds closely to the time of a reflection from the top of the layer. If so, and if the velocity is 6.8 km/sec, the thickness is about $5\frac{1}{2}$ km. It is interesting to note that a layer 6 km thick with velocity 6.8 km/sec has been found overlying the Mohorovičić discontinuity over wide areas of the Pacific basin by Raitt (paper presented to Institute of Geophysics, Nov. 5, 1953, Los Angeles). The observations of P_m in earthquake records will not, however, agree with a velocity below 7 km/sec. If the timing of the reflections from Monolith blasts at Riverside and Big Bear were in error by 0.2 sec, which is quite possible, such a velocity would fit, so the possibility of this velocity must be kept in the models used. These models are shown in Figure 14.

Using these data, a more precise analysis of crustal thickness and velocity structure can be made. If the reflection at critical distance had been obtained, a rather simple analysis would be possible using the vertical reflection time, the critical reflection time, and the various models of crustal velocity structure. From the records of reflections beyond critical distance, a direct solution can be derived only by trial and error.

An indirect method is more feasible. The computation for a

h	Layer	V
½ km	1	5.0 km/sec
8 km	2	5.9 km/sec
? km	3	6.8 km/sec
? km	4	? km/sec
6 km	5	7.0 km/sec
		8.2 km/sec

Model 1

h	Layer	V
½ km	1	5.0 km/sec
6 km	2	5.9 km/sec
? km	3	6.5 km/sec
? km	4	? km/sec
6 km	5	7.0 km/sec
		8.2 km/sec

Model 2

h	Layer	V
½ km	1	5.0 km/sec
5½ km	2	5.9 km/sec
? km	3	6.34 km/sec
? km	4	? km/sec
6 km	5	7.0 km/sec
		8.2 km/sec

Model 3

h	Layer	V
½ km	1	5.0 km/sec
6 km	2	5.9 km/sec
? km	3	6.5 km/sec
? km	4	? km/sec
		8.2 km/sec

Model 4

Fig. 14. Models of crustal velocity derived from earthquake and blast refraction data.

single-layer case in Sec. III B gave a value for k of 6.9 sec. It can then be assumed that for any multiple-layer case that will fit the same observed points, the value of k will be close to 7 sec. It cannot be greater than 7.4 sec if it is to fit the reflections beyond critical distance. A small range of values of k is then possible. A set of models fitting the crustal velocity data of this section can be investigated, for a number of values of k within the range of possibility. If the value of k can then be established by a study of the travel times of P_n, a choice may be made of the model best fitting the beyond-critical reflection data.

If a vertical reflection time and a refraction intercept time for a surface source have been determined for the nth layer of a system of n horizontal layers, each of constant thickness and velocity, the reflection time t_o and the refraction intercept time k are defined by:

$$k = 2\sum_{1}^{n-1} h_j \alpha_{jn}$$

$$t_o = 2\sum_{1}^{n-1} \frac{h_j}{V_j}$$

in which h_j = thickness of any layer
V_j = velocity in any layer

$$\alpha_{jn} = \sqrt{\frac{1}{V_j^2} - \frac{1}{V_n^2}}$$

If the velocities in all layers and the thicknesses of all except layer (n-1) are known, h_{n-1} can be determined independently

from k or t_o by the equations:

$$h_{n-1} = \frac{\frac{k}{2} - \sum_{1}^{n-2} h_j \alpha_{jn}}{\alpha_{n-1,n}}$$

or $$h_{n-1} = \left(\frac{t_o}{2} - \sum_{1}^{n-2} \frac{h_j}{V_j}\right) V_{n-1}$$

The total depth to the nth layer is then:

$$H = \sum_{1}^{n-1} h_j$$

If the conditions of horizontal uniformity are not satisfied, and if the far end of the refraction spread is in an area with a completely different set of velocities and thicknesses, the equations can still be used with modifications. If the dip of the nth layer is sufficiently small that its cosine is approximately 1, the first equation can be replaced by:

$$k_{jr} = \sum_{1}^{n-1} h_j \alpha_{jn} + \sum_{1}^{n-1} h_r \alpha_{rn}$$

in which the summation over j refers to the point being studied and the summation over r refers to the point where the refracted wave is recorded. If a blast is fired at a third point s and is recorded at j and r, the equations will be:

$$k_{sr} = \sum_{1}^{n-1} h_s \alpha_{sn} + \sum_{1}^{n-1} h_r \alpha_{rn}$$

$$k_{sj} = \sum_{1}^{n-1} h_s \alpha_{sn} + \sum_{1}^{n-1} h_j \alpha_{jn}$$

$$k_{sj} - k_{sr} = \sum_{1}^{n-1} h_j \alpha_{jn} - \sum_{1}^{n-1} h_r \alpha_{rn}$$

$$k_{jr} + k_{sj} - k_{sr} = 2\sum_{i}^{n-1} h_j \alpha_{jn}$$

A corrected intercept time is obtained which refers only to the area near the point where the first blast was fired. The method fails if there is a large depression in the upper boundary of the nth layer at some point between the three stations.

Using this "corrected k value", a solution can be obtained for a case with as many postulated layers as desired. For the velocity layerings in Figure 14, there are three unknown quantities: the velocity and thickness of layer 4 and the thickness of layer 3. The computation is seemingly indefinite, with two equations and three unknowns. The item of principal interest, however, is the total thickness of all layers; this can be shown to be rather insensitive to variations in the assumed thickness of either one of the two unknown layers.

The equations previously given for the case of n layers become, when solved for h_3 and h_4 as a function of the third unknown V_4:

$$h_4 = \frac{V_4 V_3}{\alpha_{4n} V_4 - \alpha_{3n} V_3} \left[\frac{1}{V_3} \left(\frac{k}{2} - \sum^{j=1,2,3,5} \alpha_{jn} h_j \right) - \alpha_{3n} \left(\frac{t_o}{2} - \sum^{j=1,2,3,5} \frac{h_j}{V_j} \right) \right]$$

$$h_3 = \frac{- V_4 V_3}{\alpha_{4n} V_4 - \alpha_{3n} V_3} \left[\frac{1}{V_4} \left(\frac{k}{2} - \sum^{j=1,2,3,5} \alpha_{jn} h_j \right) - \alpha_{4n} \left(\frac{t_o}{2} - \sum^{j=1,2,3,5} \frac{h_j}{V_j} \right) \right]$$

A solution of these for layering 2, with the Corona reflection time of 10.54 sec and P_n intercept time of 7.0 sec, is shown as Figure 15. It will be noted that for any reasonable velocity, V_4, the total depth to the Mohorovičić discontinuity is nearly constant;

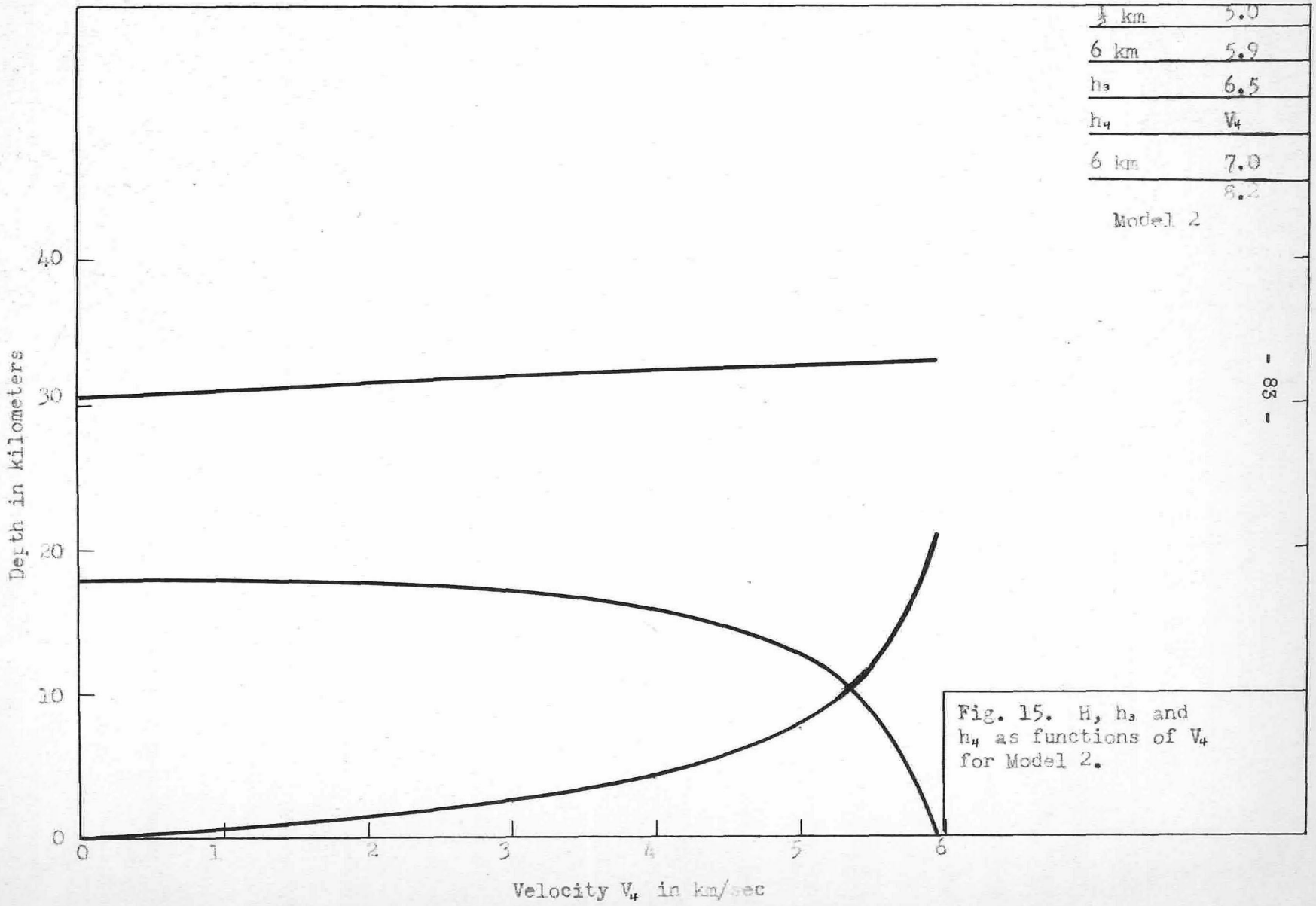

Fig. 15. H, h_3 and h_4 as functions of V_4 for Model 2.

the highest possible velocity of V_4 is reached when h_3 reaches zero. The depth is much more sensitive to variations in k. Plots of H and V_4 against k for the Corona reflection time and an arbitrary assumption of h_3 are in Figure 16, for models 1 to 4 of Figure 14. The equations are:

$$V_4 = \sqrt{1 - \left(\frac{\frac{k}{2} - \sum^{j=1,2,3,5} \alpha_{jn} h_j}{\frac{t_o}{2} - \sum^{j=1,2,3,5} \frac{h_j}{V_j}} \right)^2} \; V_n$$

$$H = \sum^{j=1,2,3,5} h_j + V_4 \left(\frac{t_o}{2} - \sum^{j=1,2,3,5} \frac{h_j}{V_j} \right)$$

with the summations in this case taken over all layers except number 4.

As can be seen from the curves in Figure 16, variations in the assumed velocity structure or the thickness of layer 3 have practically no effect on the computed total depth for values of k up to about $7\frac{1}{2}$ sec. Curves for all four models closely approach the curve computed for a single-layer crust. To find out more about the velocity structure the value of k must be determined closely.

The layerings of Figure 14 represent a choice of interpretations of the blast and earthquake refraction data at short distances. Choosing between them is not possible at the present stage of investigations. It is definite that below the surface material of variable velocity there are about six kilometers of material

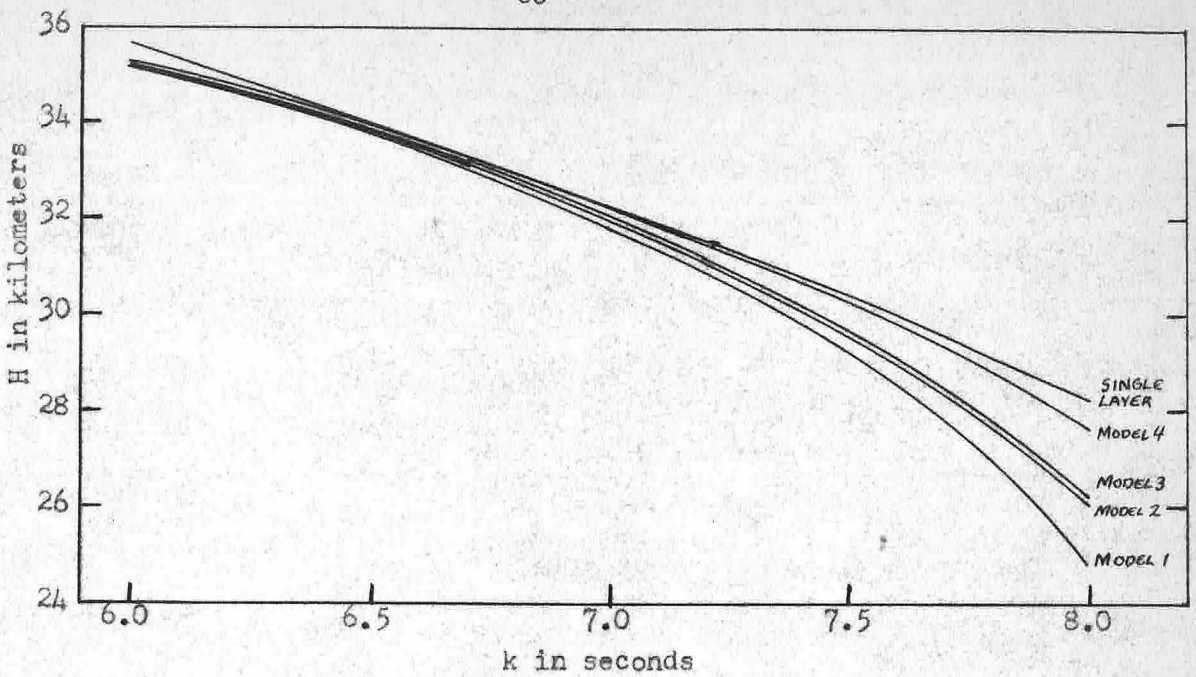

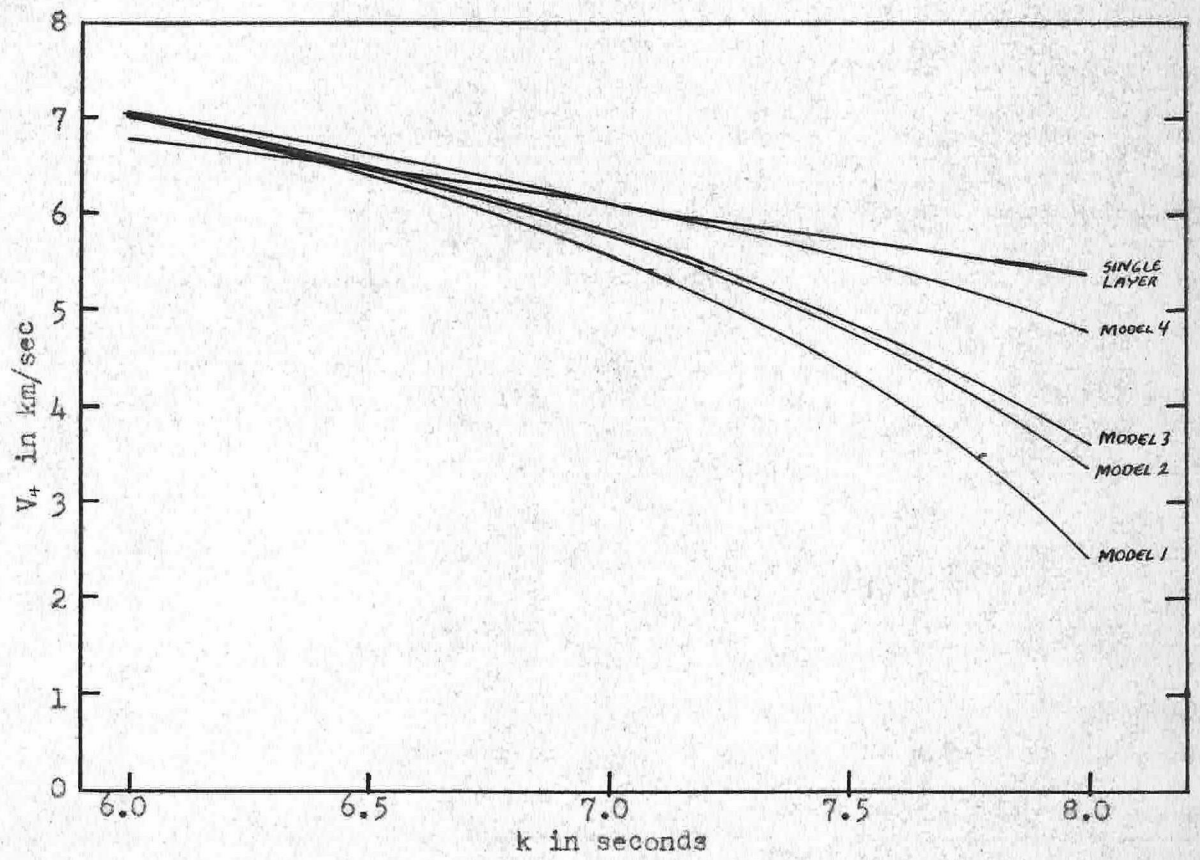

Fig. 16. H and V_4 as functions of k.

with velocity near 5.9 km/sec, and that below this there is either an abrupt change or a very rapid increase with depth to a velocity between 6.3 and 6.8 km/sec.

F. Velocity and Intercept Time of P_n

The velocity in the material below the Mohorovičić discontinuity seems to show greater uniformity than that in the material above. Recent findings by Gutenberg for California, Raitt for the Pacific Ocean basin, Tuve for the eastern United States, Ewing for the Atlantic Ocean basin, and Willmore for Northern Europe have all shown this velocity to be close to 8.2 km/sec (summarized by Gutenberg in unpublished manuscript for **Physics** Handbook, American Institute of Physics).

The P_n velocity for southern California has been obtained by Gutenberg from the study of a large number of local earthquakes; his most recent value, derived from the Arvin earthquake of July 21, 1952 and its larger aftershocks is 8.17 km/sec (personal communication). The value of 8.2 km/sec is sufficiently accurate for most computations and is currently used by Gutenberg. No completely independent check on this figure has been obtained in the present work, so the value 8.2 km/sec has been used throughout for computation.

The intercept time of P_n from southern California blasts is less definitely determined. Two blasts at Corona and two at Monolith have given a value of k, the intercept time, near eight seconds for distant stations. The first arrival can be definitely identified as P_n only at stations beyond 250 km; first arrivals from 150 to 250 km can be interpreted as P_n if one assumes the layering of numbers 2, 3, or 4 of the previous section (Fig. 14); but they can instead be interpreted as belonging to other waves if one assumes

the layering of number 1. First arrivals believed to be P_n are plotted in Figure 17. Since any depth computations using refraction data depend heavily on the intercept time for P_n in the area near the quarries concerned, a thorough investigation of the P_n intercept times must be made.

The stations at which the P_n intercept time is eight seconds, assuming a velocity of 8.2 km/sec, are all in Arizona and Nevada. Using this value for computations of Monolith and Corona data assumes that the structure is uniform from the quarries to the Arizona and Nevada stations and that the stations are at the same elevation above the Mohorovičić discontinuity as the quarries. This assumption of uniformity seems unjustifiable without additional evidence. The only value of the intercept time from such a distance that might apply to conditions at the two quarries is that from the record at Palomar for the August 1, 1953 blast at Monolith. The two reflection times indicate that the depth to the Mohorovičić discontinuity at Monolith is close to that at Corona, and Palomar is only 80 km south of Corona. This path gives an uncorrected intercept time for Palomar of 7.8 sec. When corrected from the high elevations of Monolith and Palomar to that of Corona, the intercept time is reduced to about 7.4 sec.

This single instance indicates that the refraction intercept times near eight seconds for the distant stations may not be directly applicable to the area of study. Some determination of possible delays to distant stations must be used.

Such delays in the arrival of P_n are of three general types.

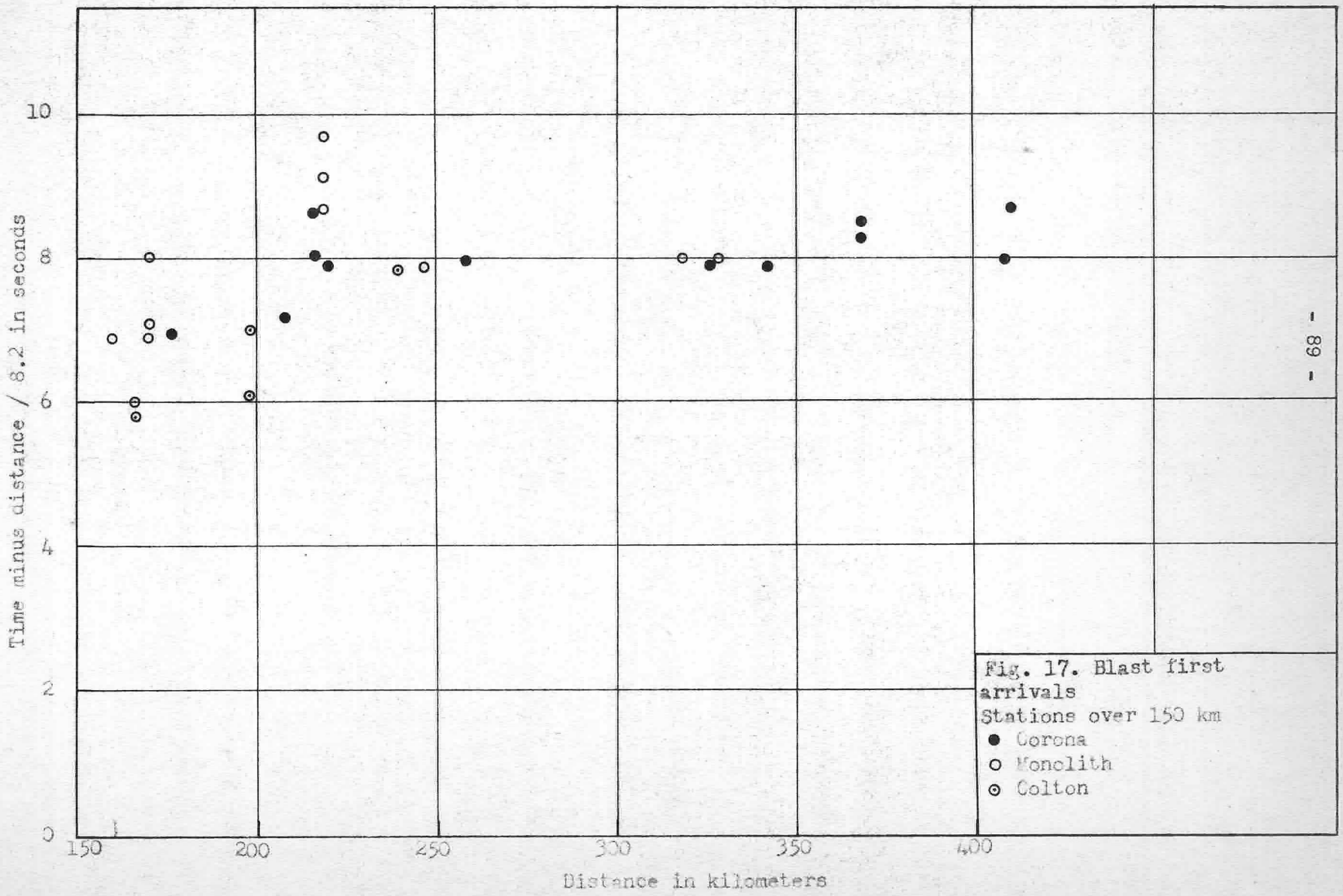
10
8
6
4
2
0
Time minus distance / 8.2 in seconds
150
200
250
300
350
400
Distance in kilometers
Fig. 17. Blast first arrivals
Stations over 150 km
● Corona
○ Monolith
⊙ Colton

The first includes delays caused by consistently late reading of small emergent beginnings; this cannot be checked without larger blasts or better signal noise ratio at the distant stations. The second includes delays caused by obstructions in the path from the source to the station. The third type includes delays associated with local conditions near the station.

Delays of the second type were first observed on records from Tinemaha of earthquakes in northern and central California; Byerly (1937) explained these as effects of depression of the Mohorovičić discontinuity beneath the root of the Sierra batholith. The existence of this root had already been postulated on geologic evidence by Lawson (1936). Byerly's observations have since been confirmed by many additional data. On records from Tinemaha of the Kern County aftershocks the delay of P_n is such that the direct wave arrives first for shocks at distances as great as 200 km.

Delays of the third type, associated with local conditions near a particular station or area, are not functions of the wave path. They are effects of variations in velocity and crustal thickness in an area around the station bounded by a circle with diameter equal to the critical distance. They may be distinguished from Sierra type delays by their independence from the path of the waves. Thus, if three stations are in a triangle, and there is a delay between stations A and B but no delay between B and C, a compensating delay should be found between A and C. If the delay is of the Sierra type, a delay can exist on one side

of the triangle with no delays on the other two sides.

The reflection data indicate that there is no Sierra root beneath Monolith; at any point north of this it may begin, and readings for waves traveling through the Sierra Nevada north of Monolith must be considered to have a possible delay associated with their paths rather than with the stations.

If it is assumed that the delays are of the third type for all paths considered, a solution for both the velocity of P_n and the intercept time differences can be obtained. If there are two stations, each recording P_n from the same two seismic sources, with stations designated A and B and sources designated C and D, the following equations apply:

$$t_{cA} = \frac{\Delta_{cA}}{V_n} + k_A + k_c$$

$$t_{cB} = \frac{\Delta_{cB}}{V_n} + k_c + k_B$$

$$t_{DA} = \frac{\Delta_{DA}}{V_n} + k_D + k_A$$

$$t_{DB} = \frac{\Delta_{DB}}{V_n} + k_D + k_B$$

in which t_{cA} = travel time from C to A
Δ_{cA} = distance between C and A
k_A = that part of the intercept time ascribable to conditions near A

We wish to find the velocity V_n and the station difference $k_A - k_B$. Combining equations and solving for V_n and $(k_A - k_B)$, we get:

$$V_n = \frac{(\Delta_{cA} - \Delta_{cB}) - (\Delta_{DA} - \Delta_{DB})}{(t_{cA} - t_{cB}) - (t_{DA} - t_{DB})}$$

$$k_A - k_B = (t_{cA} - t_{cB}) - \frac{\Delta_{cA} - \Delta_{cB}}{V_n} = (t_{DA} - t_{DB}) - \frac{\Delta_{DA} - \Delta_{DB}}{V_n}$$

The solution is most accurate when one source is on the extension of the line between the two stations and the other source is equidistant from the two. It will be noted that only differences in arrival times appear. The origin time of the seismic events need not be determined.

In general the source in line with the two stations may be an earthquake; small errors in location will not affect the result greatly. The source approximately equidistant from the two stations should be a blast because small errors in location cause large errors in the result.

Geography prevents full use of this method in the present case, for only one source area is available at sufficient distance for P_n to record at stations near one of the quarries as well as at the Arizona and Nevada stations. The velocity must be taken from other sources and only the station differences derived.

One blast source, the Monolith quarry, is available. A very weak recording at Nelson, Nevada of the blast of September 6, 1952 gives a k value of 8.0 sec if V_n is 8.2 km/sec; arrivals that may be P_n at Riverside and Big Bear give k values of 6.9 and 7.1 sec, indicating the possibility of a delay of about one second to Nelson.

More data are needed to confirm this. The only other source of information comes from earthquakes. Rather rigid requirements limit the use of earthquake data for this purpose: the earthquakes must be at such distances from one of the quarries (or a near-by station) and from the Nevada stations that P_n will record as a first arrival at both. Despite the fact that the depth and origin

times of earthquakes are not ordinarily known with sufficient precision to use the travel times directly for this purpose, the differences in arrival times and differences in distance may be used with fair precision, provided that the epicenters have been found to an accuracy of a few kilometers using near-by stations well distributed in azimuth and never using any station recording P_n. If stations recording P_n are used, the location will shift in such a way as to minimize the station differences.

The Kern County aftershocks are the only earthquakes available that satisfy these conditions. Over 200 of these have been located by Richter (1954) using four to ten near-by stations. Many of these shocks show P_n on records from the Nevada stations; almost all show it also at Riverside. Plots have therefore been made for all stations showing P_n on an appreciable number of well-located shocks of sufficient magnitude to record clearly; these are shown in Figures 18 to 27. Results are summarized in Table IV and Figure 28. In every case, the "error" shown is the standard error of the mean. Most of the readings were made by the laboratory staff; only the Mount Hamilton readings were made by the writer.

The most essential station for the purpose of this study is Boulder City, for it is the only one still in operation that recorded an undoubted first arrival of P_n from the 1949 Corona blast. The aftershock difference plots show an apparent delay of 0.8 sec in the arrival time of P_n at Boulder City when compared with Riverside (near the Corona quarry). This delay might be explained as the result of reading weak first arrivals consistently late from

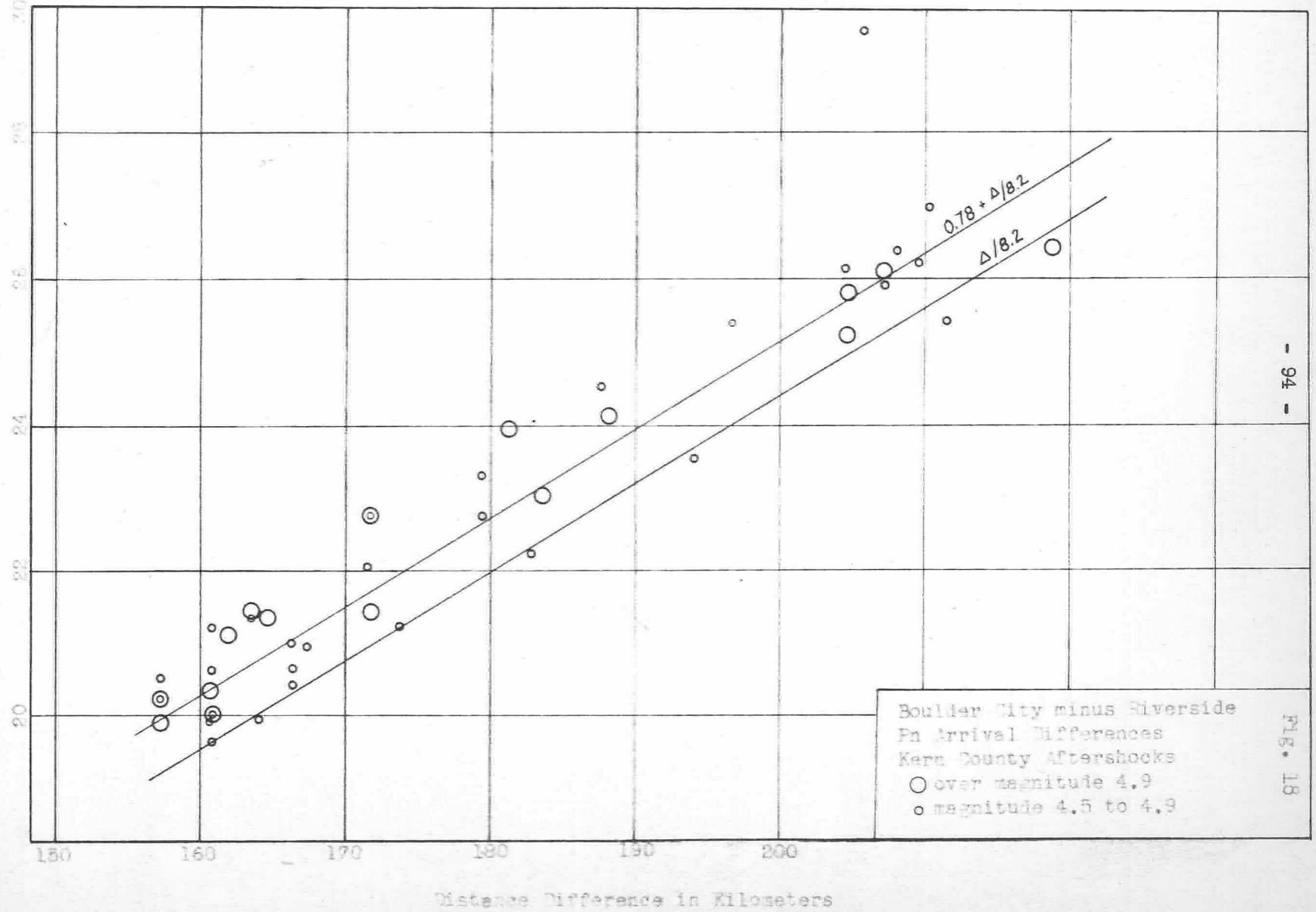
Time Difference in Seconds
20
22
24
26
28
30
160
170
180
190
200
Distance Difference in Kilometers
0.78 + Δ/8.2
Δ/8.2
Boulder City minus Riverside
Pn Arrival Differences
Kern County Aftershocks
over magnitude 4.9
magnitude 4.5 to 4.9
Fig. 18

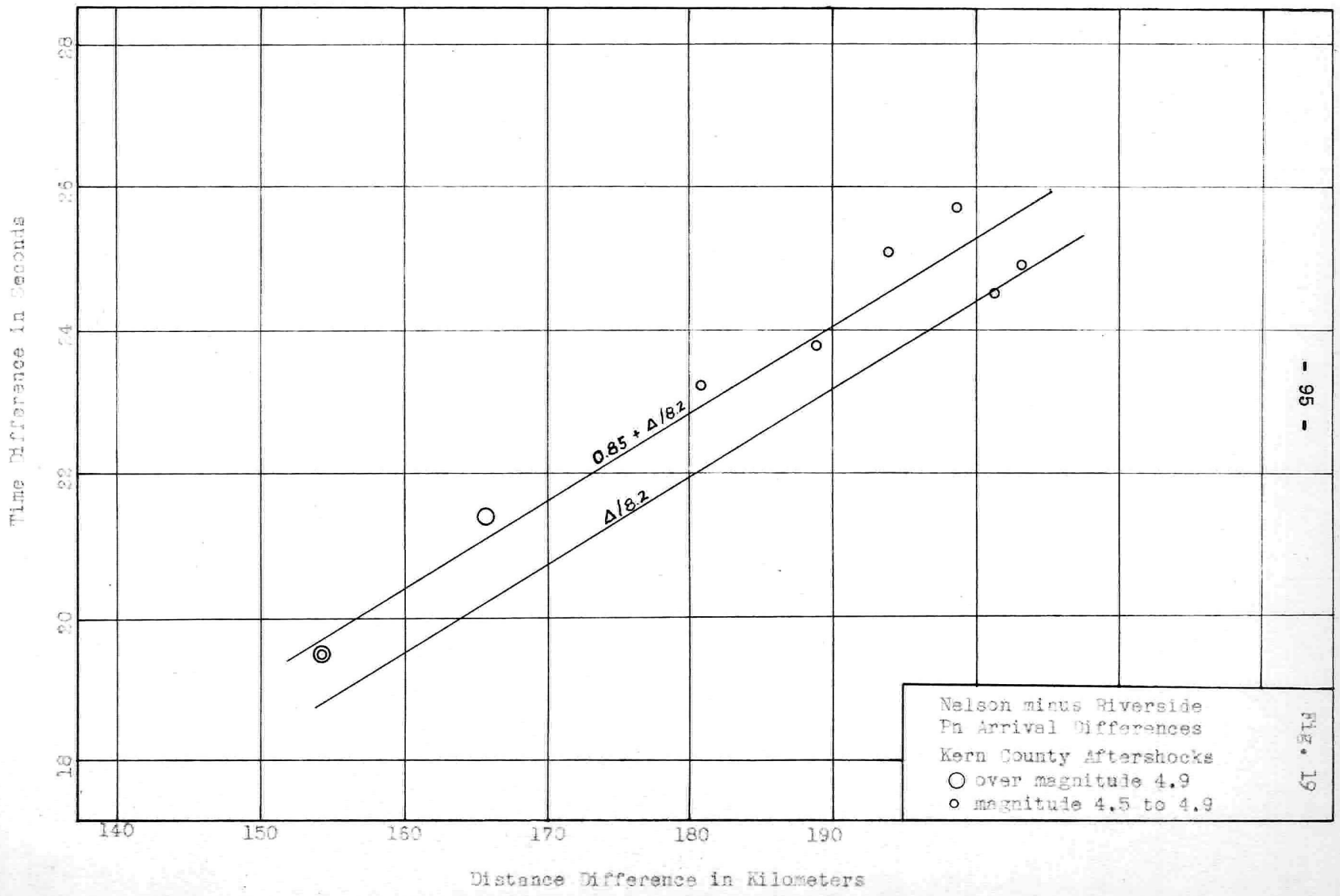
Time Difference in Seconds
18
20
22
24
26
28
140
150
160
170
180
190
Distance Difference in Kilometers
0.85 + Δ/8.2
Δ/8.2
Nelson minus Riverside
Pn Arrival Differences
Kern County Aftershocks
over magnitude 4.9
magnitude 4.5 to 4.9
Plate 19

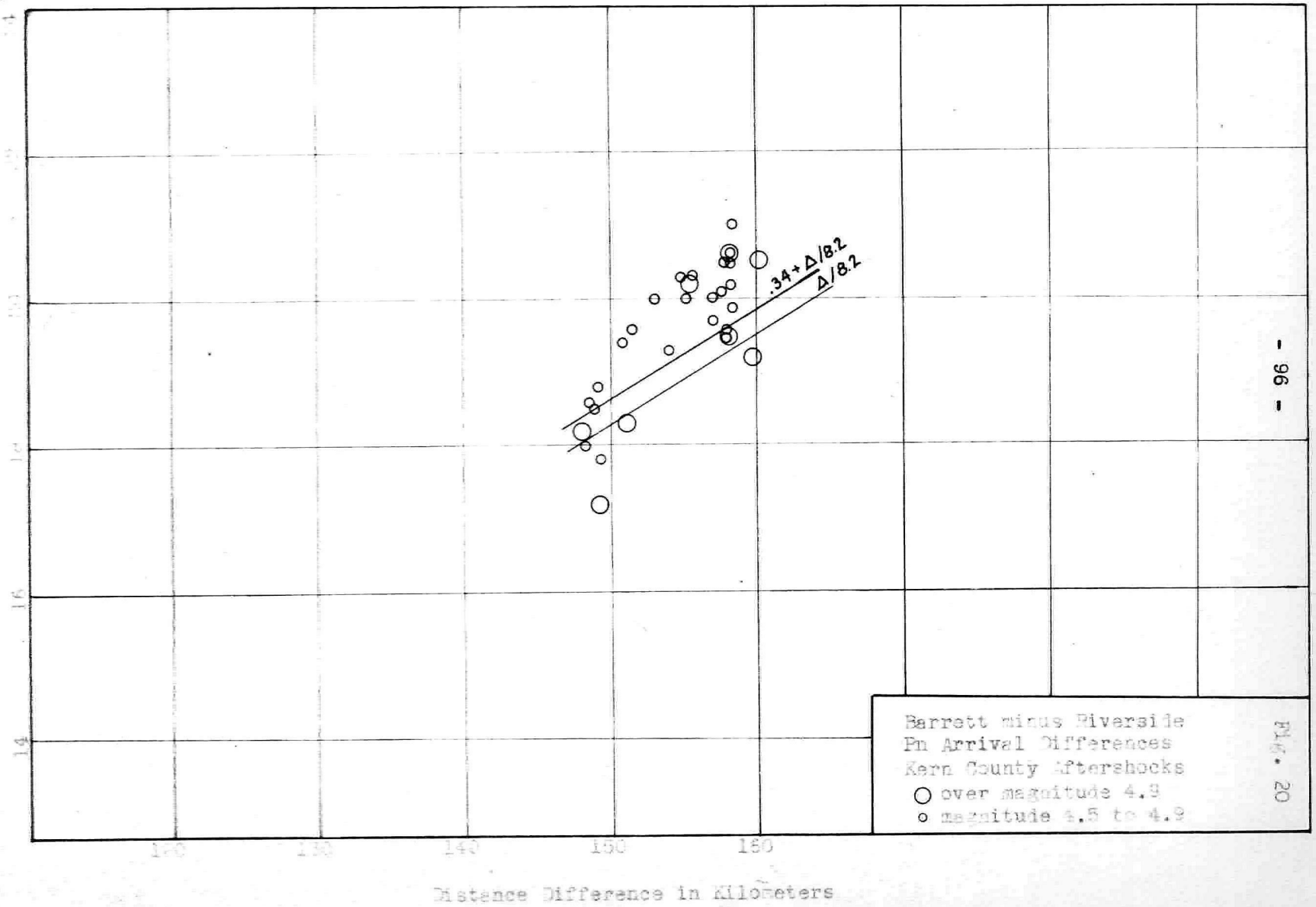
Time difference in seconds
14
16
.34+Δ/8.2
Δ/8.2
140
150
160
Distance Difference in Kilometers
Barrett minus Riverside
Pn Arrival Differences
Kern County Aftershocks
over magnitude 4.9
magnitude 4.5 to 4.9
Fig. 20

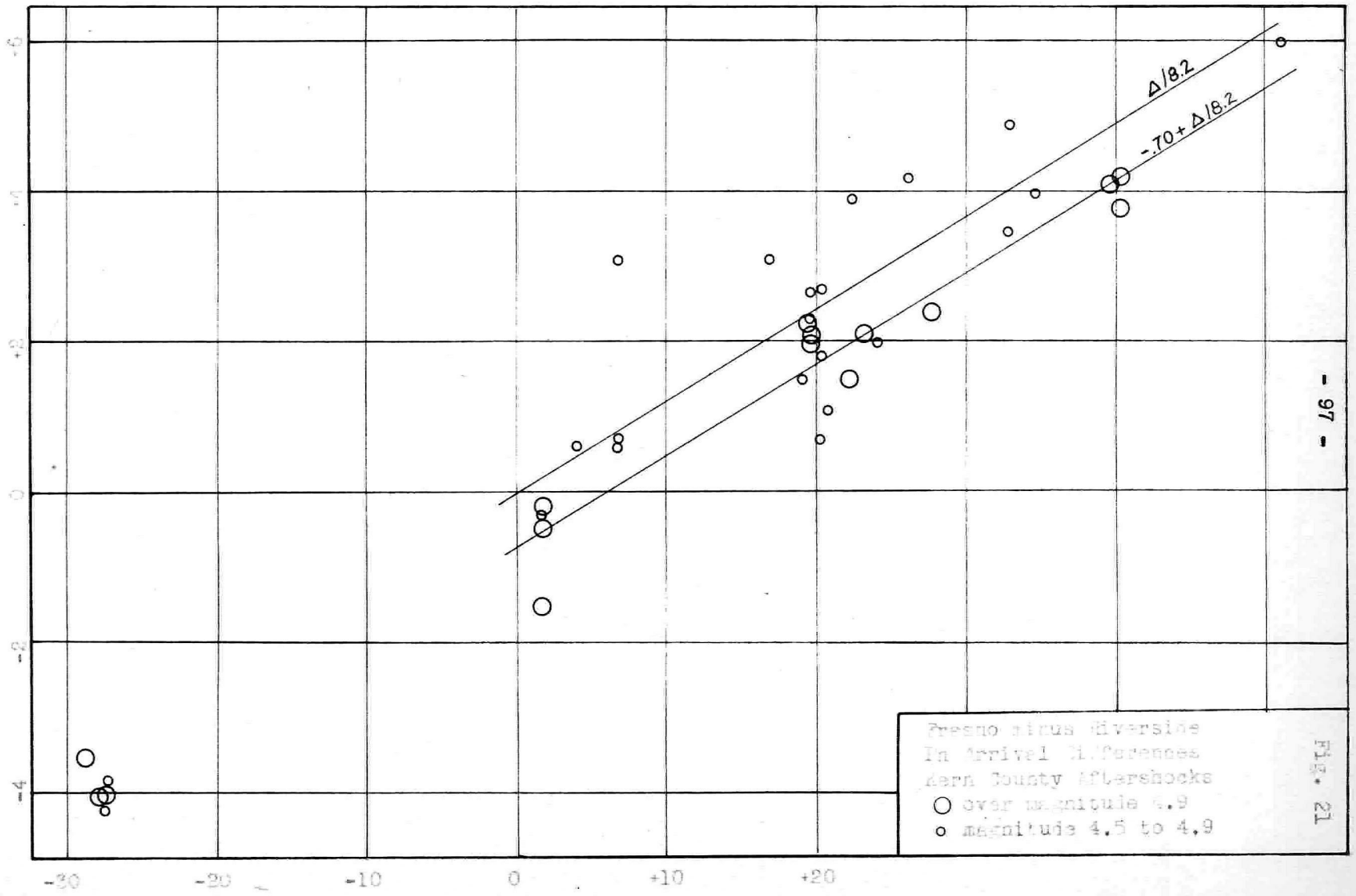
Time Difference in Seconds
-6
-4
-2
0
+2
+4
-30
-20
-10
0
+10
+20
Distance Difference in Kilometers
Δ/8.2
-.70+Δ/8.2
Fresno versus Diversion
In Arrival Differences
Kern County Aftershocks
over magnitude 4.9
magnitude 4.5 to 4.9

Fig. 21

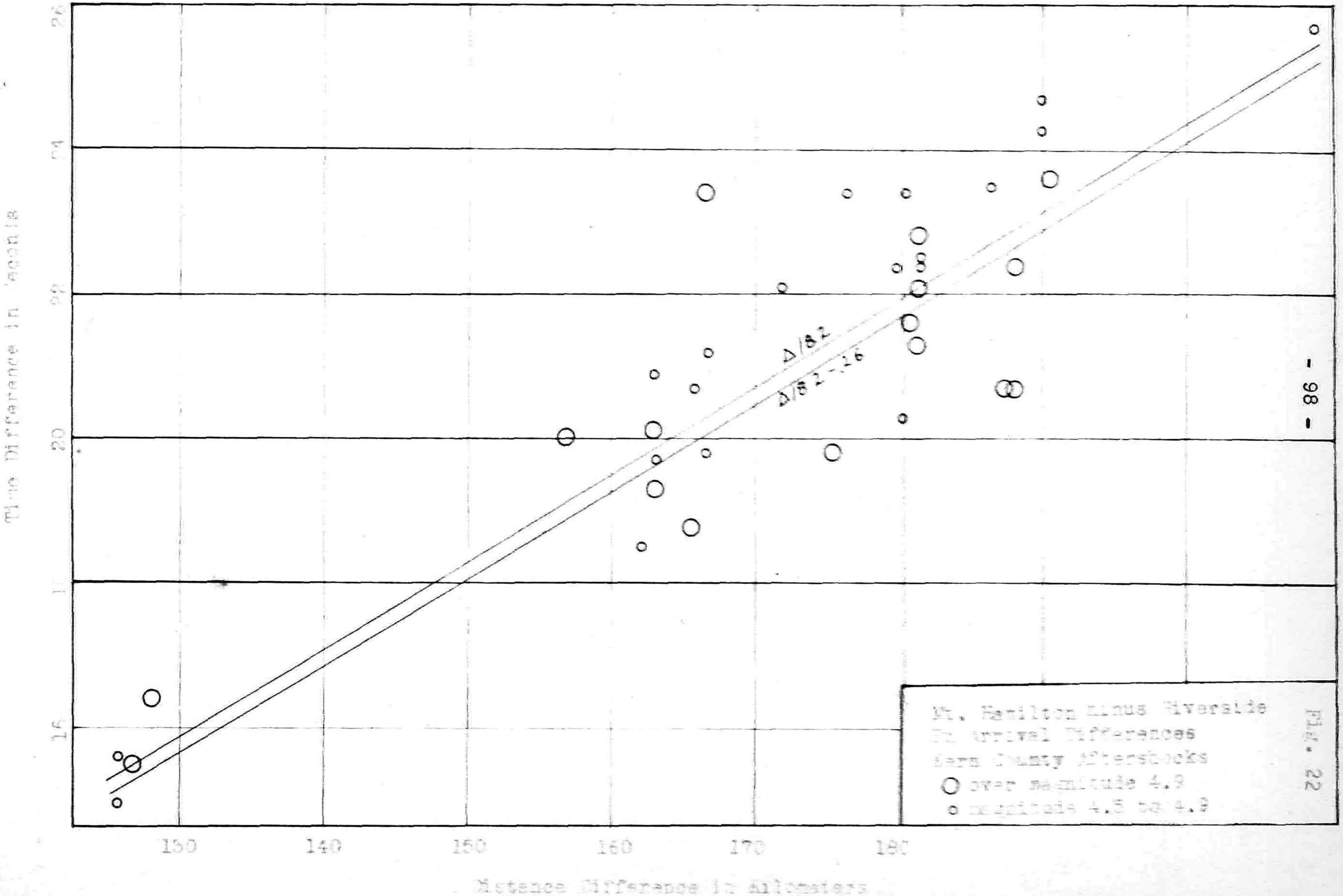
Mt. Hamilton minus Riverside
Arrival Differences
Kern County Aftershocks
over magnitude 4.9
magnitude 4.5 to 4.9
Δ/8.2
Δ/8.2 - 1.6
16
20
22
24
26
130
140
150
160
170
180
Time Difference in Seconds
Distance Difference in Kilometers

Fig. 22

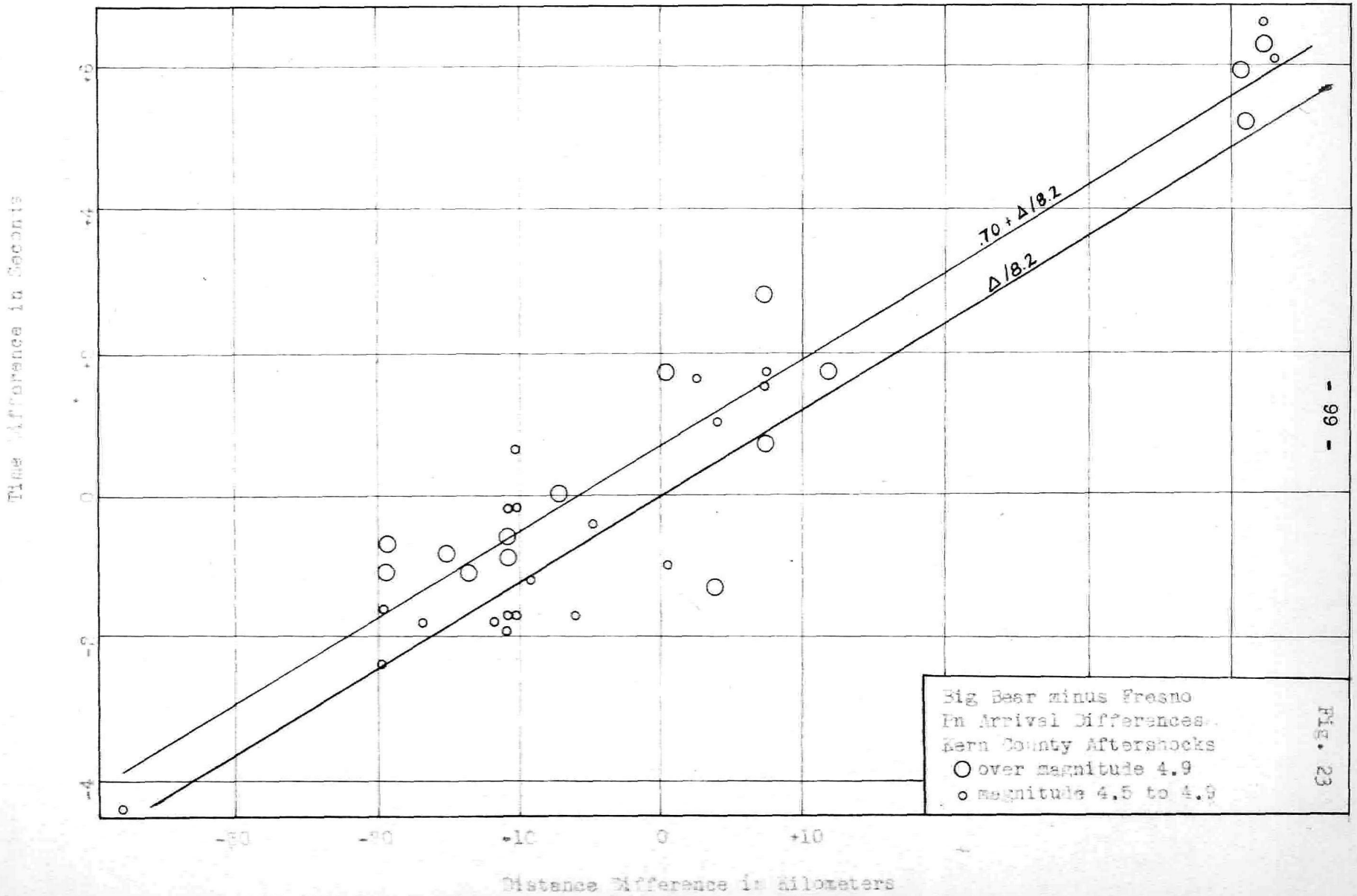
Time Difference in Seconds
+5
+4
+3
+2
+1
0
-1
-2
-3
-4
-30
-20
-10
0
+10
Distance Difference in Kilometers
.70 + Δ/8.2
Δ/8.2
Big Bear minus Fresno
Pn Arrival Differences
Kern County Aftershocks
O over magnitude 4.9
o magnitude 4.5 to 4.9
FIG. 23

Fig. 24

Boulder City minus Barrett
Pn Arrival Differences
Kern County Aftershocks
over magnitude 4.9
magnitude 4.5 to 4.9
6.2+Δ/8.2
7.8Δ/8.2
Time difference in seconds
Distance difference in kilometers
0
2
4
6
8
10
20
30
40

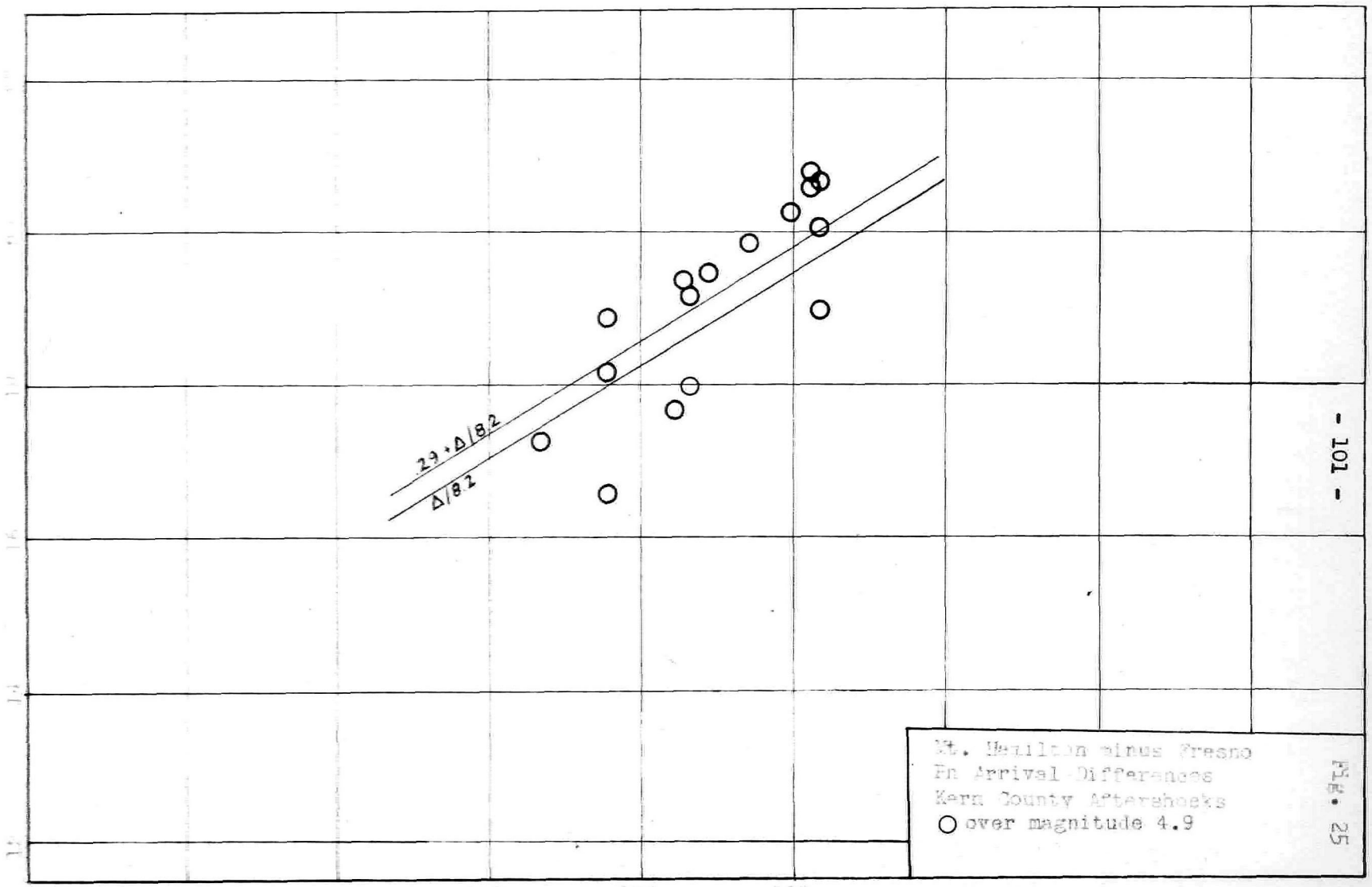
29+Δ/82
Δ/82
Mt. Hamilton minus Fresno
P- Arrival Differences
Kern County Aftershocks
○ over magnitude 4.9
160
Distance Difference in Kilometers

PLATE 25

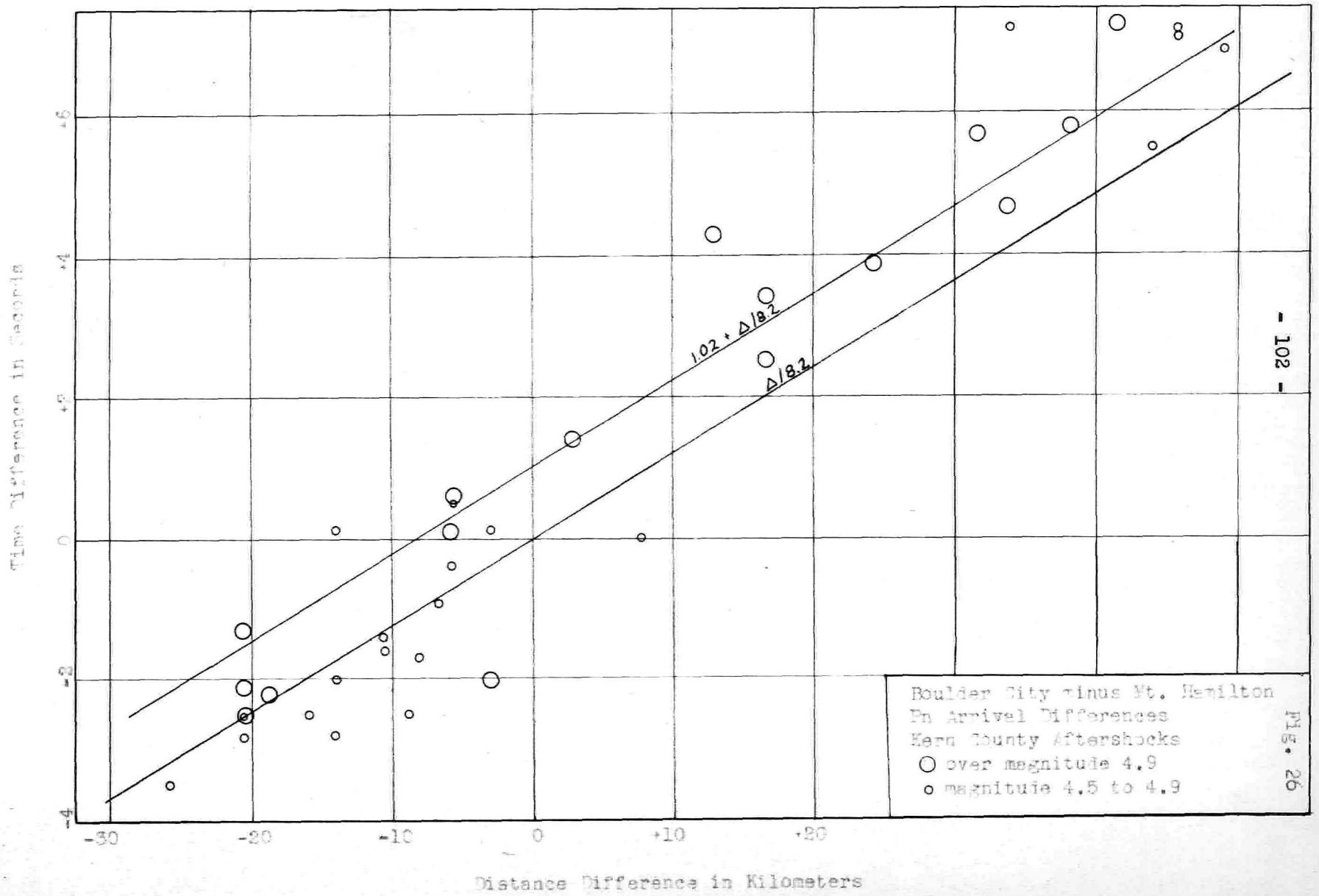
Time Difference in Seconds
+6
+4
+2
0
-2
-4
-30
-20
-10
0
+10
+20
Distance Difference in Kilometers
1.02 + Δ/8.2
Δ/8.2
Boulder City minus Mt. Hamilton
Pn Arrival Differences
Kern County Aftershocks
over magnitude 4.9
magnitude 4.5 to 4.9

Fig. 26

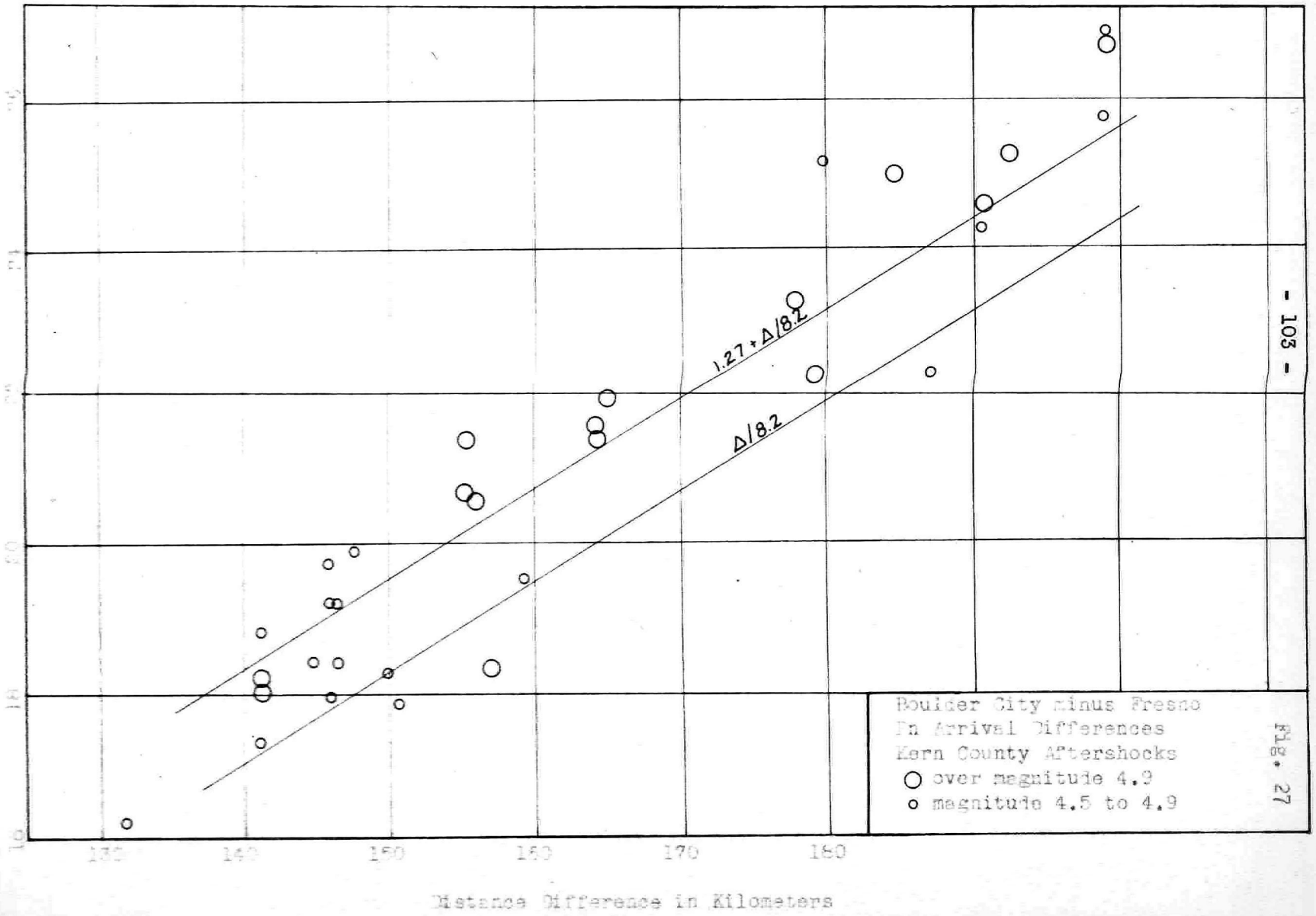
Time Difference in Seconds
Distance Difference in Kilometers
1.27 + Δ/8.2
Δ/8.2
Boulder City minus Fresno
In Arrival Differences
Kern County Aftershocks
over magnitude 4.9
magnitude 4.5 to 4.9
Fig. 27

Table IV

Station Pair	Shocks Mag. 4.5 - 4.9 Number	Mean	Shocks over Mag. 4.9 Number	Mean	Total Shocks Number	Mean
Boulder City minus Riverside	29	.76 ± .13	16	.81 ± .13	45	<u>.78 ± .09</u>
Nelson minus Riverside	7	.84 ± .22	2	.95	9	<u>.85 ± .18</u>
Barrett minus Riverside	23	.82 ± .11	8	<u>.34 ± .28</u>		
Fresno minus Riverside	21	-.07 ± .21	15	<u>-.70 ± .12</u>		
Mount Hamilton minus Riverside	21	.45 ± .19	16	<u>-.26 ± .35</u>		
Big Bear minus Fresno	22	.38 ± .17	16	<u>.70 ± .22</u>		
Boulder City minus Barrett	20	.08 ± .16	10	<u>.62 ± .29</u>		
Mount Hamilton minus Fresno	--		16	<u>.29 ± .20</u>		
Boulder City minus Mount Hamilton	23	.42 ± .17	15	<u>1.02 ± .20</u>		
Boulder City minus Fresno	21	1.16 ± .24	14	1.27 ± .22		

Underscored results are preferred values.
"Error" is standard error of the mean.

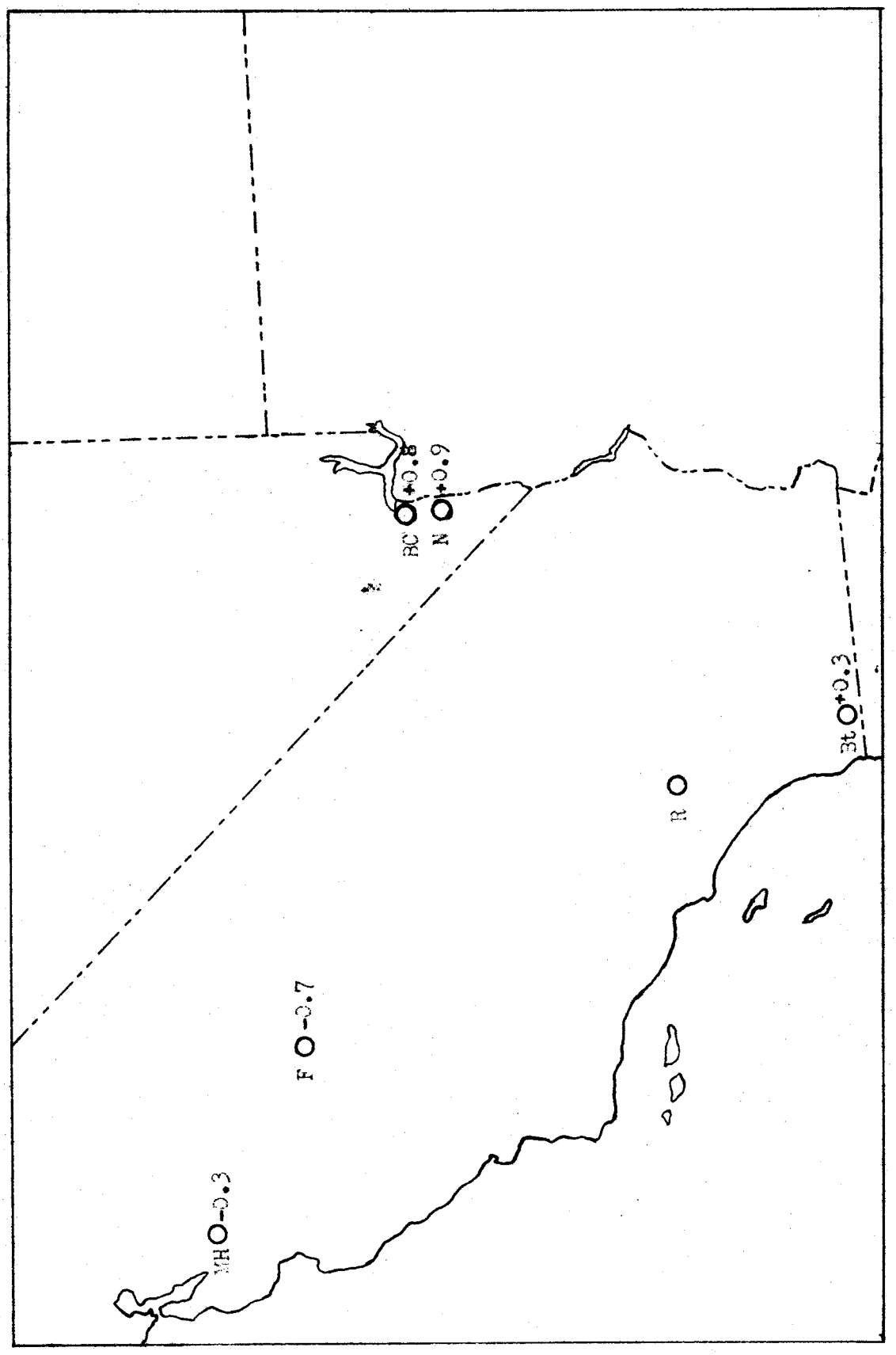

Fig. 28. Delays in Fn compared to Riverside

some of the smaller shocks, an effect of low-velocity material either directly under the station or over a wide region, a lower velocity for P_n than the value of 8.2 km/sec assumed, or greater depth to the Mohorovičić discontinuity near Boulder City than near Riverside.

A check on the possibility of late readings is provided first by separating the shocks by magnitudes. Kern County shocks over magnitude 4.9 have a beginning at Boulder City that is sufficiently strong to minimize the possibility of reading a weak arrival late. Riverside, the comparison station, is so close to the epicentral area that all Kern County shocks over magnitude 4.0 have clear first arrivals. Sixteen shocks over magnitude 4.9 were recorded at Boulder City and Riverside; they have a mean difference of 0.81 ± 0.13 sec. Twenty-nine smaller shocks, magnitude 4.5 to 4.9 have a mean difference of 0.76 ± 0.13 sec. Using all these shocks gives a mean difference of 0.78 ± 0.09 sec. The indication is, therefore, that there is no weighting of the mean by late readings of shocks of magnitude 4.5 to 4.9. Some shocks smaller than magnitude 4.5 show a greater delay at Boulder City.

A further check on the possibility of late readings as well as that of low-velocity material directly beneath the station is provided by the newly established station at Nelson, Nevada. Nelson, very near Boulder City, was established in August, 1952; it therefore recorded only the later Kern County aftershocks. It has less background disturbance than Boulder City, however, so that records of small shocks can be read with greater accuracy. Nelson

shows a delay of 0.85 ± 0.18 sec with respect to Riverside. A slightly greater delay at Nelson than at Boulder City can be expected because of the difference in elevation of the two stations.

The delay then must be due to some regional cause. If the entire delay is due to a lower velocity of P_n, this velocity must be 7.9 km/sec. If the velocity is 8.2 km/sec (as obtained by Gutenberg), the value of k is larger for the Boulder City area than for Riverside, explainable in terms of greater depth to the Mohorovičić discontinuity or lower velocities in the crust in the Boulder City area. Combining the observed delay of 0.8 sec with the intercept time of 7.7 to 7.9 sec at Boulder City for the 1949 Corona blast gives an intercept time of 6.9 to 7.1 sec corrected to Riverside.

The results from other station pairs confirm the existence of similar delays. In the plots for Fresno, Mount Hamilton, and Barrett, the smaller shocks show an appreciably different result from those of magnitude 5.0 and over. Examination of the records from Mount Hamilton shows the reason for this difference. The Mount Hamilton records of the Kern County shocks start with a rather small emergence, followed by a large impulse about one second later. On the records of the smaller shocks, the first arrival is often missed. As a result, the readings have a double-peaked distribution. Averaging the results from the two magnitude groups studied obviously gives an erroneous result, so the results for shocks over magnitude 4.9 are to be preferred. Even so, there

is some indication of a double-peaked distribution of arrival differences. In the Mount Hamilton - Fresno plot (Fig. 25) it will be noted that the mode and median of the delays for shocks over magnitude 4.9 are 0.7 sec while the mean is only 0.29 sec. This is the most pronounced difference between mode, median, and mean.

Such discrepancies are caused by the emergent nature of first arrivals on earthquake records at distant stations. An unbiased observer is more likely to read such arrivals late than early. The experienced seismologist is not unbiased, however. He recognizes this skewness of the observations and strains to read the earliest possible arrival. The effect of this attitude on the statistical distribution of readings of seismograms is a subject that should be investigated. What the effects are when two such readings by different observers are subtracted is hard to guess. The best that can be done in the present case is to present the mean and the standard error of the mean for each station pair.

The early small arrival on the Mount Hamilton records of the larger shocks suggests that the consistently late readings at Boulder City are due to low signal noise ratio. The relative quality of the two stations is indicated by the fact that in general Kern County shocks over magnitude 4.1 can be read at Boulder City; at Mount Hamilton shocks over magnitude 3.6 can be read. Since the early emergence is clear at Mount Hamilton on shocks over magnitude 4.9, it should be clear at Boulder City on shocks over magnitude 5.4, and these shocks should show no delay

at Boulder City. There are eight such shocks; Boulder City is on the average 1.2 sec late with respect to Riverside and 0.8 sec late with respect to Mount Hamilton. The delay cannot therefore be explained in this manner. It might be due to some geologic cause that prevented the small long-period first arrivals from reaching the Boulder City area.

Readings from Fresno show the same effect as those from Mount Hamilton. Fresno is near the epicentral area but it has high background disturbance and low sensitivity; comparisons with Riverside, Big Bear, and Boulder City show that only the readings from Fresno for shocks greater than magnitude 4.9 can be used with confidence. The result at Barrett is not so definite, partly because of the large standard error of the mean for the shocks over magnitude 4.9. Time corrections at Barrett were unreliable during the first few weeks of the Kern County aftershock series, the period when most of the larger shocks occurred.

The explanation of the delays at Boulder City and Nelson in terms of a velocity of 7.9 km/sec for P_n cannot be applied to the arrivals at Mount Hamilton and Fresno. A possible alternative explanation might be that the large second arrivals at Mount Hamilton correspond to the first arrivals at Boulder City and that this phase has a velocity near 7.9 km/sec; this implies that some mechanism prevents the small arrival with velocity 8.2 km/sec from reaching Boulder City or Nelson. If this is so, the same explanation applies to the Boulder City and Nelson records of

blasts. It does not explain the very early arrivals at Fresno, where arrivals would be expected to be late because of the low-velocity sediments underlying the station.

The Boulder City data indicate that if the velocity of P_n is 8.2 km/sec, k corrected to Riverside is about seven seconds. If the velocity is 7.9 km/sec, there is no delay to Boulder City and k is about 6.2 sec. In either case, the first arrivals at distances between 150 and 250 km come close to the travel time plot for P_n. They should therefore be considered. When corrected to an elevation of 675 m (the mean of Corona and the Monolith datum), the following are obtained:

Table V

Quarry	Station	Date	Observed k	k corrected to 675 m
Corona	Havilah	July 26, 1952	7.1	7.1
Corona	Chuchupate	July 26, 1952	6.9 to 7.1	6.8 to 7.0
Corona	China Lake	Mar. 31, 1951	7.0	7.0
Corona	Haiwee	Aug. 6, 1949	8.0	8.0 (Sierra delay?)
Monolith	Big Bear	Sept. 6, 1952	6.9	6.6
Monolith	Big Bear	Aug. 1, 1953	7.1	6.8
Monolith	Riverside	Sept. 6, 1952	6.9	6.8
Monolith	Palomar	Aug. 1, 1953	7.8	7.5

Agreement with the value obtained from the Boulder City arrival is apparent.

Data for Tinemaha and Santa Barbara are not included. At Tinemaha the arrival is definitely affected by the Sierra delay. Readings at Santa Barbara are late because of the great thickness of sediments beneath the station; the depth and velocity of the sediments are not known and no correction can be made.

Both these sources of information give intercept times for Corona and Monolith close to seven seconds. Because of the simplifying assumptions and the inaccuracy involved in using shocks with epicenters accurate only within one or two kilometers, the constant errors in the difference plots may be appreciable and are unknown; the agreement with the arrivals at the nearer stations gives sufficient corroboration that the combined data may be used with greater assurance.

A lower limit for the possible "corrected k" from blasts can be found by considering the earthquake data. The frequency distribution of k values at Riverside for 196 Kern County aftershocks located by Richter is shown in Figure 29. The distribution comes close to the shape of a Gaussian error curve, with mean value 5.58 sec and standard error 0.53 sec. This distribution represents the composite effect of the distribution of earthquakes in depth, the errors in timing at all stations, any error in the locations as a result of nonuniform distribution of stations as well as possible error in the travel time curves used in the locations, local variations of velocity, errors in determination of origin time, and the rounding off of location coordinates.

The error of none of these is known except the rounding off of locations. Locations were made by Richter by a method of reduction of residuals at all near-by stations, fitting to the nearest minutes of latitude and longitude. This means that the fit is to the center of a rectangle 1.5 by 1.1 km. The epicenter is assumed to be at the center of this rectangle; it can move over a range

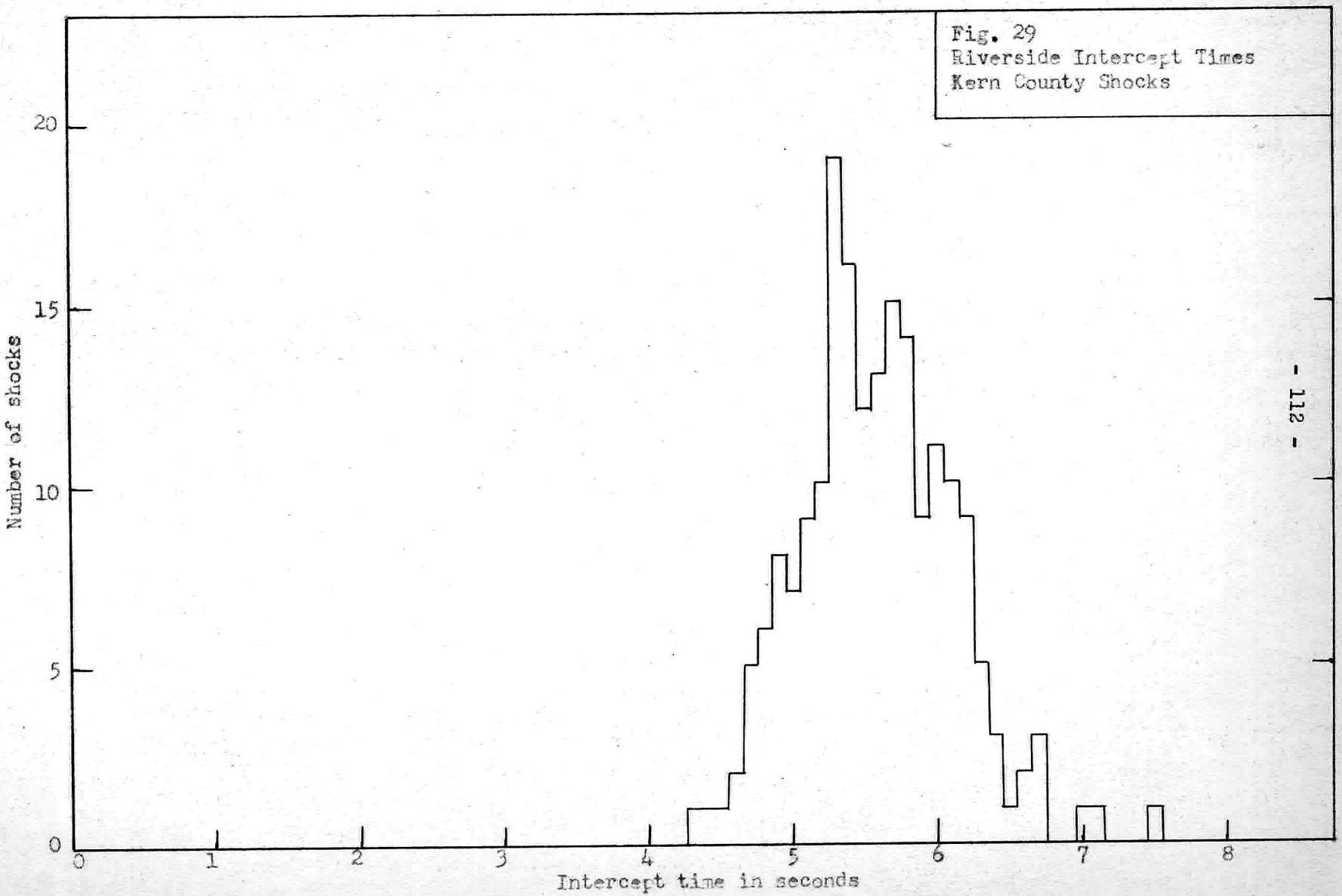
Fig. 29
Riverside Intercept Times
Kern County Shocks
Number of shocks
0
5
10
15
20
0
1
2
3
4
5
6
7
8
Intercept time in seconds

of ± 0.8 km and still stay within it. If it moves on the diagonal radial to Riverside, this makes a maximum change in k of ± 0.1 sec. Origin times are probably accurate to about 0.3 sec so, neglecting possible errors in the velocities used in the locations, the upper limit of k due to shallow depth of focus is approximately 6½ sec. As earthquakes do not occur above ground level, the value of k for a surface source should be greater than 6½ sec. This is in accordance with the results obtained above.

In Sec. III A, the event on the record at Corona was correlated with the reflection at Monolith because it arrived at nearly the same time. For this correlation, it was assumed that the structure was reasonably uniform from Corona to Monolith. We can now verify this assumption.

The intercept time for the Monolith blast recorded at Nelson is 8.0 sec; correcting this by 0.06 sec to bring it to the Monolith 1000 m datum gives a value of 7.94 sec. To correct for the height difference between Nelson and Boulder City another 0.04 sec must be subtracted, leaving a value of 7.9 sec for the intercept time that would be obtained from a blast at the 1000 m level at Monolith, recorded at Boulder City. The Corona blast recorded at Boulder City with intercept time between 7.7 and 7.9 sec. This, then, checks the reflection result and indicates that the Mohorovičić discontinuity is at nearly the same depth below the 1000 m Monolith datum as it is below the Corona 350 m quarry elevation.

The study of intercept times of P_n thus removes the anomaly originally found. The intercept time of P_n given by the reflection

data was near seven seconds; the intercept time given by stations over 250 km from the Corona quarry was nearer eight seconds. Comparison by means of arrivals from earthquakes brings the intercept time for the Corona-to-Monolith area to a value very close to seven seconds.

Using this value of seven seconds to obtain the velocity and thickness of layer 4 in Figure 16, one obtains the layerings of Figure 30.

h	Layer	V
½ km	1	5.0 km/sec
8 km	2	5.9 km/sec
	3	6.8 km/sec
17½ km		
	4	5.6 km/sec
6 km	5	7.0 km/sec
		8.2 km/sec

Model 1

h	Layer	V
½ km	1	5.0 km/sec
6 km	2	5.9 km/sec
	3	6.5 km/sec
19½ km		
	4	5.8 km/sec
6 km	5	7.0 km/sec
		8.2 km/sec

Model 2

h	Layer	V
½ km	1	5.0 km/sec
5½ km	2	5.9 km/sec
	3	6.34 km/sec
20 km		
	4	5.8 km/sec
6 km	5	7.0 km/sec
		8.2 km/sec

Model 3

h	Layer	V
½ km	1	5.0 km/sec
6 km	2	5.9 km/sec
	3	6.5 km/sec
25½ km		
	4	6.1 km/sec
		8.2 km/sec

Model 4

Fig. 30. Models of crustal velocity derived from reflection and refraction data.

IV. INTERPRETATION AND CONCLUSIONS

The presence of reflections from the Mohorovičić discontinuity in southern California seems firmly established. Observations of these reflections have been obtained at both vertical and near-critical incidence. The strength of the reflection at vertical incidence is not great; in general multiple-channel recording methods and large energy sources are necessary for recording an identifiable reflection. The few successes in recording such reflections in other areas lend confirmation to this. The reflection at critical incidence is more commonly observed but has large variations in amplitude. The necessary conclusion is that either the discontinuity is rough or interference effects are present.

Weak reflections from a horizon six kilometers above the Mohorovičić discontinuity may also be present. The shallower reflection is weaker than the reflection from the Mohorovičić discontinuity whenever observed; in most cases in which the direction of motion can be established, it has motion opposite to the reflection from the Mohorovičić discontinuity. If this is a reflection with an initial rarefaction, the material below the reflecting horizon has a lower acoustical impedance than that above. This requires a decrease in velocity or density or both. If there is a velocity decrease at this interface no critical reflections could exist. The reflections are weak; the beginning may be a compression that is not strong enough to read. In this case there will be critical reflections, but they will coincide so closely with the

reflections from the Mohorovičić discontinuity that they will not be distinguishable. They may cause pronounced amplitude variations by reinforcement and cancellation.

Information on crustal velocities from all sources indicates a rough approximation to a set of simple horizontal layers. The igneous material at very shallow depth has velocities varying between 3 and 6 km/sec. The material down to six or eight kilometers has an average velocity of 5.9 km/sec; below this the velocity gradually or suddenly increases to a value over 6.3 km/sec. The best interpretation from all data seems to be that this velocity is between 6.3 and 6.5 km/sec. Higher values obtained from blast refraction data in the mountains between Corona and the Mexican border may be explained in terms of some regional variation; either the thickness of the shallowest layer decreases or the velocity in the next lower layer increases to about 6.8 km/sec. More blast refraction studies with sensitive instruments in quiet locations are needed.

Values for the velocity in the material below the layer with velocity 6.3 to 6.5 km/sec depend upon the computations from reflection times and therefore on the value for the velocity in the material immediately above the Mohorovičić discontinuity. If a layer with velocity near 7 km/sec is assumed to overlie the Mohorovičić discontinuity, the velocity is quite low in the material between that layer and the material with velocity 6.3 to 6.8 km/sec. On the various assumptions of velocity distribution studied in

Sec. III E, the value in this low-velocity layer is 5.5 to 5.9 km/sec, if there is a layer with velocity near 7 km/sec. Evidence for the existence of the latter layer is very weak. The fact that this has been found in earthquake studies in many parts of the world is not sufficient evidence; the revision of the earthquake travel times in southern California by Gutenberg (1951b) shows that data from earthquake phases can be subjected to radical re-interpretation. The data from blast reflections do not extend to sufficiently great distances to determine definitely, by study of the asymptotic approach of the reflection travel time curves, whether this layer is present or not.

Reflection data from earthquake records supply a little more information on this point. Because of the shorter critical distance for reflections from earthquake sources, the reflection travel time curve approaches its asymptotic value at shorter epicentral distances. There is evidence from the earthquake reflection data that the reflection travel time curve approaches an asymptotic velocity not much, if any, greater than the maximum velocity in the material above the earthquake foci.

The apparent reversal of direction of the earlier reflection on the Corona vertical incidence record gives added reason to believe that the layer with velocity near 7 km/sec does not exist; this reversal is more in accordance with the assumption of a decrease in velocity five or six kilometers above the Mohorovičić discontinuity.

If there is no layer with velocity near 7 km/sec, the mean

velocity between the layer with velocity 6.3 to 6.5 km/sec and the Mohorovičić discontinuity is over 6 km/sec, but it is still lower than the velocity in the material above it.

Studies of travel times of P_n from blasts and local earthquakes have indicated either that the velocity below the Mohorovičić discontinuity is near 7.9 km/sec in southern California, or, if the velocity is near 8.2 km/sec as obtained by Gutenberg from other data, there are consistently larger intercept times at the stations in southern Nevada than at the stations in the portion of southern California studied. On either assumption, arrivals at Fresno are very early in comparison with southern California stations. Either interpretation eliminates the discrepancy between the intercept time for P_n as derived from records from Arizona and Nevada stations of Corona and Monolith blasts and the intercept time derived from the reflection data. This intercept time, for a surface source and station both in the area of study, is 7.0 sec for velocity 8.2 km/sec.

If the velocity of P_n is 8.2 km/sec, these delays (Fig. 28) indicate that the Mohorovičić discontinuity dips downward to the east as well as into the Sierra region and that its depth is less than normal under the Central Valley of California. The latter result is to be expected from isostatic considerations. If the Sierras cause a depression in the Mohorovičić discontinuity, the deep basin of the Central Valley must be compensated by a subcrustal hump. If the average velocity of 6.2 km/sec is used,

the 0.7 sec difference between Fresno and Riverside means that the Mohorovičić discontinuity is seven kilometers shallower at Fresno. Correction for the low-velocity sediments beneath the station would make the depth even less, although this may be counteracted by some regional velocity increase in the crust. A similar computation for Boulder City gives a depth eight kilometers greater than at Riverside, if the crustal velocities are the same.

Computations using reflections from the Mohorovičić discontinuity at vertical and critical incidence, and considering the crust as a single layer, give a depth to the Mohorovičić discontinuity of 32 km below sea level at both Monolith and Corona, and a mean velocity for the crust of 6.2 km/sec. Computations using these same data plus information from the intercept of P_n, assuming any velocity profile that will agree with the blast and earthquake refraction data, give the same depth to the nearest kilometer.

REFERENCES

Adams, L. H., Tuve, M. A., and Tatel, H. E.
1952. "Seismic Exploration of the Earth's Crust," Comptes Rendus des Séances de la Neuviéme Conférence, Union Géodésique et Géophysique Internationale, Association de Seismologie et de Physique de l'Interieur de la Terre, Strasbourg, pp. 113-116.

Benioff, H., Gutenberg, B., and Richter, C. F.
1953. "Progress Report, Seismological Laboratory, California Institute of Technology, 1952," Trans. Am. Geoph. Un., Vol. 34, pp. 790-791.

Byerly, P.
1937. "Comment on 'The Sierra Nevada in the Light of Isostasy'," Bull. Geol. Soc. Am., Vol. 48, pp. 2025-2031.

Chakrabarty, S. K. and Richter, C. F.
1949. "The Walker Pass Earthquakes and Structure of the southern Sierra Nevada," Bull. Seis. Soc. Am., Vol. 39, pp. 93-107.

Gutenberg, Beno
1944a. "Energy Ratio of Reflected and Refracted Seismic Waves," Bull. Seis. Soc. Am., Vol. 34, pp. 85-102.

1944b. "Reflected and Minor Phases in Records of Near-by Earthquakes in Southern California," Bull. Seis. Soc. Am., Vol. 34, pp. 137-160.

1951a. "Travel Times from Blasts in Southern California," Bull. Seis. Soc. Am., Vol. 41, pp. 5-12.

1951b. "Revised Travel Times in Southern California," Bull. Seis. Soc. Am., Vol. 41, pp. 143-163.

1952. "Waves from Blasts Recorded in Southern California," Trans. Am. Geoph. Un., Vol. 33, pp. 427-431.

Heiland, C. A.
1940. Geophysical Exploration, Prentice-Hall, Inc., New York.

Hertlein, L. G. and Grant, U. S., IV
1944. "The Geology and Paleontology of the Marine Pliocene of San Diego, California," Memoirs of the San Diego Soc. of Nat. Hist., Vol. II, Part 1: Geology.

Hodgson, John H.
1953a. "A Seismic Survey in the Canadian Shield, Part I: Refraction Studies Based on Rockbursts at Kirkland Lake, Ont.," Publications of the Dominion Observatory, Ottawa, Vol. XVI, No. 5, pp. 111-163.

1953b. Ibid., Part II: "Refraction Studies Based on Timed Blasts," Vol. XVI, No. 6, pp. 167-181.

Jenkins, Olaf P.
1938. Geologic Map of California, first edition, Calif. Div. of Mines.

Junger, Arne
1951. "Deep Basement Reflections in Big Horn County, Montana," Geophysics, Vol. 16, pp. 499-505.

Katz, Samuel
1953. "Seismic Study of Crustal Structure in Pennsylvania and New York," Tech. Report No. 32, Lamont Geol. Observatory, Palisades, N. Y.

Larsen, Esper S.
1948. Batholith and Associated Rocks of Corona, Elsinore, and San Luis Rey quadrangles, southern California, Geol. Soc. Am. Mem. 29.

Lawson, Andrew C.
1936. "The Sierra Nevada in the Light of Isostasy," Bull. Geol. Soc. Am., Vol. 47, pp. 1691-1712.

Miller, William J.
1934. "Geology of the Western San Gabriel Mountains of California," Publications of UCLA in Math. and Phys. Sciences, Vol. I, No. 1, pp. 1-114.

Reich, Hermann
1953a. "Über reflexionsseismische Beobachtungen der PRAKLA aus grossen Tiefen bei den grossen Steinbruch-Sprengungen in Blaubeuren am 4. März und am 10. Mai 1952," Bulletin d'Information de l'Union Géodésique et Géophysique Internationale, 2e Annee, N° 2, pp. 229-232.

1953b. "Über seismische Beobachtungen der PRAKLA von Reflexionen aus grossen Tiefen bei den grossen Steinbruch-Sprengungen in Blaubeuren am 4. März und am 10. Mai 1952," Geologische Jahrbuch, Band 68, S. 225-240.

Richter, C. F.
1943. "Calculation of Small Distances," Bull. Seis. Soc. Am., Vol. 33, pp. 243-250.

1950. "Velocities of P at Short Distances," Bull. Seis. Soc. Am., Vol. 40, pp. 281-289.

1954. Sections in publication on Arvin-Tehachapi earthquake of July 21, 1952, to be published by Calif. Div. of Mines.

Rooney, W. J., Tatel, H. E. and Tuve, M. A.
1950. "Surface Explosion -- Seismic Observations in Southern California," paper presented to American Geophysical Union, May 2, 1950 (abstract in Trans. Am. Geoph. Un., Vol. 31, p. 324).

Tuve, Merle A.
1948. Carnegie Institution of Washington Year Book No. 47, 1947-1948, Report of the Dept. of Terr. Mag., pp. 60-64.

1949. Ibid., Year Book No. 48, 1948-1949, pp. 61-63.

1950. Ibid., Year Book No. 49, 1949-1950, pp. 63-65.

1951. Ibid., Year Book No. 50, 1950-1951, pp. 69-73.

1952. Ibid., Year Book No. 51, 1951-1952, pp. 67-70.

Vestine, E. H. and Forbush, S. E.
1953. "Statistical Study of Waves from Blasts Recorded in the United States," Journal of Geophysical Research, Vol. 58, Washington, D. C., pp. 381-400.

Willmore, P. L., Hales, A. L., and Gane, P. G.
1952. "A Seismic Investigation of Crustal Structure in the Western Transvaal," Bull. Seis. Soc. Am., Vol. 42, pp. 53-80.

Wood, Harry O. and Richter, Charles F.
1933. "A Second Study of Blasting Recorded in Southern California," Bull. Seis. Soc. Am., Vol. 23, pp. 95-110.

APPENDIX

STATION INFORMATION

CGS = U. S. Coast and Geodetic Survey
CIT = California Institute of Technology
CIW = Carnegie Institution of Washington
SIO = Scripps Institution of Oceanography
UC = University of California

r = regular
t = temporary
p = portable
d = discontinued

Station	Symbol	Coordinates N	Coordinates W	Elev. (m)	Inst.	Status
Barrett	Bt	32 40.8	116 40.3	510	CIT	r
BED (1952)	--	35 05.7	118 24.7	1310	CIT	pd
Berkeley	B	37 52.3	122 15.6	81	UC	r
Big Bear	BB	34 14.3	116 54.8	2060	CIT	r
Boulder City	BC	35 58.9	114 50.0	776	CGS	r
China Lake	CL	35 49.0	117 35.8	766	CIT	r
Chuchupate	Ch	34 48.5	119 00.7	1590	CIT	td
Clear Creek (1952)	CC	35 15.1	118 36.6	820	CIT	pd
Clear Creek Ranch (1952)	CCR	35 14.8	118 36.5	825	CIT	pd
Corona (1939)	--				CIT	pd
Crestline	Cr	34 14.6	117 15.7	1400	CIT	td
Dalton	D	34 10.2	117 48.6	523	CIT	r
Dalton, Little (1938)	--	34 10.05	117 50.26	412	CIT	pd
Dawson Creek (1949)	--	33 46.96	117 27.92	320	CIW	pd
El Cajon	EC	32 47.6	116 57.3	135	CIT	td
Elsinore (1949)	--	33 38.00	117 21.22	457	CIW	pd
Fort Tejon	FT	34 52.4	118 53.7	980	CIT	r
Fresno	F	36 46.1	119 47.8	88	UC	r
Glencliff Camp (1949)	--	32 48.78	116 29.65	1205	CIW	pd
Haiwee	H	36 08.2	117 57.9	1100	CIT	r
Havilah	Hv	35 30.6	118 31.0	990	CIT	td
Isabella (1946)	--	35 39.6	118 25.9		CIT	pd
King Ranch	KgR	35 19.7	119 44.7	670	CIT	t
Knox Ranch	KxR	35 29.0	118 31.7	1090	CIT	td
La Jolla	LJ	32 51.8	117 15.2	8	CIT	rd
Lakeside (1949)	--	32 52.94	116 49.09	206	CIW	pd
Mojave (1946)	--	35 01.0	118 01.7		CIT	pd
Mount Hamilton	MH	37 20.4	121 38.6	1282	UC	r
Mount Wilson	MW	34 13.5	118 03.4	1742	CIT	r
Nelson	N	35 42.3*	114 51.2*	1160	CGS	r

*Coordinates used in present study; may be in error by as much as two minutes.

Station Information (cont'd)

Station	Symbol	Coordinates N	Coordinates W	Elev. (m)	Inst.	Status
Overton	Ov	36 31.9	114 26.6	395	CGS	rd
Palomar	Pr	33 21.3	116 51.6	1700	CIT	r
Palomar (1949)	--	33 21.23	116 51.55	1670	CIW	pd
Parker Creek (1952)	PC	35 26.4	118 43.8	910	CIT	pd
Pasadena	P	34 08.9	118 10.3	295	CIT	r
Pasadena (1949)	--	34 08.9	118 10.3	304	CIW	pd
Perris	Pe	33 46.8	117 14.0	440	CIT	td
Pierce Ferry	PF	36 07.2	114 00.3	417	CGS	rd
Piute Ranch (1952, 1953)	PR	35 21.8	118 22.9	1150	CIT	pd
Point Loma (1949)	--	32 42.00	117 17.82	-60	SIO	pd
Pomona	Po	34 05.9	117 42.6	350	CIT	td
Ramona (1949)	--	33 00.49	116 54.28	442	CIW	pd
Riverside	R	33 59.6	117 22.5	250	CIT	r
San Emigdio (1952)	SE	34 59.6	119 11.0	435	CIT	pd
Santa Anita (1952)	SA	34 11.08	118 01.18	440	CIT	pd
Santa Barbara	SB	34 26.5	119 42.9	100	CIT	r
Shirley Meadow (1952)	SM	35 42.5	118 33.8	2000	CIT	pd
Telegraph Pass (1949)	--	32 39.75	114 19.00	168	CIW	pd
Tinemaha	T	37 05.7	118 15.5	1180	CIT	r
Walker Dump (1952)	WD	35 24.3	118 29.0	760	CIT	pd
White Oak (1952)	WO	34 59.1	118 31.0	1510	CIT	pd
White Wolf Ranch (1952)	WWR	35 15.0	118 39.9	620	CIT	pd
Williams Ranch	WR	35 17.9	118 36.7	430	CIT	td
Woody	W	35 42.0	118 50.6	500	CIT	r

Seismogram Readings

Readings used in the text that are not already in print are tabulated in the following pages. Epicenters have been calculated by a method of reducing residuals to the standard travel time curves or by graphical methods. All distances have been calculated using the method of Richter (1943).

BLAST DATA

Colton

Station	Δ (km.)	Arrival times (Readings from files)
Apr. 17, 1937 15:30		
Quarry	0.22	59.8
R	8.4	iP! 62.0NEZ
MW	68.5	iP 71.9 eS? 81N
P	77.3	iP 72.8NEZ iS 82.8N iS 82.5E
LJ	133	eP 82.3N eS 97.5N
June 8, 1937 15:31		
R	8.4	iP! 41.0NEZ
MW	68.5	iP 52.1Z iS 61.3Z
P	77.3	iP 52.9Z i 57.8Z iS 62.7EN
Jan. 29, 1938 16:04		
Shipping office	0.64	15.6
R	8.4	16.9
Little Dalton	47.8	24.4
MW	68.5	27.3
P	77.3	28.4
Dec. 23, 1939 15:29		
R	8.4	iP 31.2NEZ
Corona	26.5	iP 33.8Z iS 37.8Z
MW	68.5	iP 41.2NEZ iS 49.0Z
P	77.3	iP! 42.3Z iS 52.2E eiS 54.7N
LJ	133	iP 51.2Z iS 08.2E iS 09.0Z
Pr	90.9	iP! 44.9Z
H	238	iP?? 66.1Z iP? 69.5Z iS 93.5Z
Sept. 6, 1941 15:15		
R	8.4	iP 47.4EZ
MW	68.5	eP 57.5N iP 57.6E
P	77.3	iP! 59.0NEZ iS 67.8Z eS 68.3NE
Pr	90.9	iP! 60.8Z
LJ	133	iP 67.5Z iP 68.5Z iS 83.0Z iS 85.4Z
Oct. 4, 1941 15:31		
R	8.4	iP 00.0Z
MW	68.5	iP 10.5Z
P	77.3	iP 11.7Z e 11.9NE iS(?) 23.5N
Pr	90.9	iP 13.6Z (indefinite)

Colton (cont'd)

Station	Δ (km.)	Arrival times
Jan. 10, 1942 15:59		
R	8.4	iP 31.0NEZ
MW	68.5	iP 41.2Z iP 41.3NE
P	77.3	iP 42.4NEZ iS 52.4NEZ
May 2, 1942 14:30		
Quarry	0.56	22.1
R	8.4	iP 24.0NEZ iS 25.9NEZ
P	77.3	iP 35.3NEZ iS 44.3Z iS 45.1NE
MW	68.5	iP 34.0NE iS 42.9
Pr	90.9	iP 37.2Z
Sept. 10, 1949 14:47 (2 shocks)		
R	8.4	04.3
Pe	33.0	08.5
MW	68.5	14.5
P	77.3	15.7
14:50		
R	8.4	32.7
Pe	33.0	35.8
MW	68.5	43.1
P	77.3	44.3
Nov. 3, 1949 07:45:28.4		
R	8.4	iP 29.9NE i 31.6NE i 32.2NE i 32.8N
Cr	21.2	iP 32.8 i 34.0 i 34.8 iS 35.5 i 38.4 i 43.4
Pe	33.0	iP 34.2 iS 38.4 i 40.1 i 42.1
Po	34.4	eP 34.4 iP 34.7 i 40.1 i 42.3 i 45.9 i 46.9 i 47.9
MW	68.5	iP 40.5 i 43.7 i 44.7 i 48.9 iS 49.5 i 54.4 i 58.5
P	77.3	iP 41.7EZ i 47.7E 51.3E 53.1NE 54.5NEZ 61.8NE 66.9E
Pr	90.9	i 43.3 i 43.8 i 44.2 i 54.2 i 55.7 i 56.5 i 57.5 i 59.0 i 62.8
07:48:37.8		
R	8.4	iP 39.3NE i 40.9NE e 42.1NE
Cr	21.2	iP 42.2 e 42.8 i 43.6 i 44.4 iS 44.9 e 47.9± e 49.7± i 52.7 i 54.9± i 58.3±
Pe	33.0	iP 43.6 i 44.5 i 45.6 iS 46.7 i 50.3 e 51.2
Po	34.4	iP 44.1 i 48.4
MW	68.5	i 49.8 i 53.0 i 53.9 i 59.0 i 61.0 i 63.0
P	77.3	i 50.9E 57.2E i 60.5NE i 61.0E 62.3N i 63.7NZ i 71.2EZ 76.2E

Colton (cont'd)

Station	Δ (km.)	Arrival times
Dec. 19, 1951 15:34		
R	8.4	i 45.2 iS 46.5 i 47.0 ei 61.3 i (air wave) 67.8
D	45.1	i 51.6 i 55.1 i 56.9 iS 57.4 i 62.8 e 65.1 i 72.3
BB	44.6	e 52.1
MW	68.5	i 55.7 i 58.0 i 58.7 i 59.1 i 59.7 iS 63.5 ei 70.0 i 73.9 i 79.9? i 82.7?
P	77.3	i 56.8 iS 66.6 i 69.0 i 70.5
Dec. 21, 1951 15:31		
R	8.4	i 56.9 iS 58.6 i 62.0? i 70.1? i 73.0? i (air wave) 80.0
D	45.1	i 63.1 iS 67.4 i 69.8? i 72.0?
MW	68.5	i 67.2 i 70.1 i 71.8 i 72.6 eiS 74.5 i 76.5 i 80.9 i 90.1?
P	77.3	i 68.5 eiS 78.0 i 81.3 i 78.7
Pr	90.9	ei 70.2 i 70.8 i 72.6 i 74.4 ei 81.2 iS 82.2 ei 82.6 e 84.5 e 88.2
CL	196.5	ei 85.5 ei 88.0 iS 112.8
Feb. 13, 1952 15:29		(Apparently 2 shots; only first arrivals usable)
R	8.4	i 41.4
D	45.1	i 47.8
MW	68.5	i 51.8
P	77.3	i 53.0
Pr	90.9	ei 55.2
Bt	165.6	i 66.1
May 22, 1952 14:19		
R	8.4	i! 26.6 iS 28.2 i 31.9 i 33.7 i 34.8 i 37.0 i (air wave) 49.4
D	45.1	i 32.9 i 34.5 i 36.5 i 37.4 iS 38.5
MW	68.5	i 36.8 i 39.7 i 41.1 iS 45.8 i 50.9
P	77.3	i 38.3 i 41.2 ei 47.6 i 50.8
Pr	90.9	ei 40.8 iS 54.8
Bt	165.6	i 51.1 i 54.7 i 56.4 i 64.3 i 66.2 iS 70.7
CL	196.5	e 56.0 i 58.2 iS 83.0

Corona

Station	Δ (km.)	Arrival times
Aug. 6, 1949	23:30:00.0	
Portable	0.3	00.3
R	20.3	iP! 03.7NEZ i 4.3NE i 4.9NE 5.6E 5.9N 6.5NE 6.7E 7.0E 7.4E 8.6E 11.0E 11.6N 12.0E 16.2N
Po	33.0	iP 06.2 i 07.0 i 08.5 iS 10.0 i 11.3 i 12.1 i 13.6 i 14.5 i 16.6 i 18.4 i 19.6
Cr	49.6	iP 9.0 i? 9.9 i 11.0 i? 12.1 i 13.2 i 14.9 e 16.8 (bad background; good to ± 0.2 sec).
MW	65.9	iP 11.5 i 14.5 i 15.1Z iS 18.7NEZ 19.1EZ i 20.3NEZ i 21.3NZ i 23.3Z i 24.6EZ i 27.6Z i 41.7Z
P	70.0	iP 12.0NZ i 13.5N i 14.0N i 14.5N iP! 15.3N i 17.0N 17.9N e 18.4NE i 19.8Z i 20.6N i 22.1N i 23.2Z i 23.6NE 24.6Z 27.1E i! 29.6Z i 33.3Z i 36.2Z i 38.5Z 43.1?E i 45.1N e 45.7Z
Pr	81.6	iP! 13.7
LJ	111.6	iP 18.5 i 21.2
EC	124.1	eP 20.3 iP 20.5 i 22.1 i 24.6 i 25.5 i 28.2 i 29.4 i 30.8 i 31.7 e 34.3 i 35.3 i 38.5 i 44.6± i 46.8
Readings from Gutenberg (1951a)		
SB	214.1	e 34.1? i 36.6 e 37.8 e 38.8 i 39.6 e 46.2 e 59.5 i 61.3 e 64 e 67.7
H	257.5	i 39.4 e 43.3 i 45.2 e 46.8 i 47.8 e 55.7 e 60.2 e 72.1 e 75.5 e 76.7 e 77.7 e 81.2
BC	340.3	i 49.4 e 57.4 e 60.5 e 64.5 e 71.5 i 79.9 i 98.7 i 99.4 e 101.4 e 107.5 e 115.4 e 120.5
T	366.8	i 53.2 e 54.6 e 55.4 i 60.6 i 65.1 i 76.6 e 103 e 105
PF	407.2	i 57.7 e 68.4 i 69.1 e 71.7 e 74.0 e 79.5 i 92.0 i 117 i 119.3 e 121 i 124½ i 127½ i 134½
Ov	408.1	i 58.5 e 69.2 e 115 e 119 e 122½ i 134 e 148
MH	539.2	e 74 i 84.4 e 89 i 92.8
Readings from Rooney, Tatel, and Tuve (1950)		
Dawson Creek	8.04	1.50 3.3
Elsinore	27.6	4.91
Pasadena	70.0	12.05 13.6
Palomar	81.2	13.64 14.0
Ramona	108.5	17.25 17.8
Lakeside	124.6	19.67

Corona (cont'd)

Station	Δ(km)	Arrival times
Aug. 6, 1949 (cont'd)		
Point Loma	128.7	20.1 21.4 (added by GGS: i! 22.5)
Glencliff Camp	148.4	23.26
Telegraph Pass	324.9	47.48 47.5 55.51
Mar. 31, 1951 23:30:33.5		
Portable	0.15	i! 33.5 i 42.3 i 44.0
R	20.3	iP! 37.0NEZ i 38.4NEZ iS 39.6NEZ i 45.3NZ
Pe	26.4	38.2
D	45.2	iP! 41.2 iS 46.7 i 52.4 i 54.2 i 58.0 i 67.4
MW	65.9	iP 44.9 i 47.8 i 52.5 i 72.3 i 74.9
P	70.0	iP 45.2NEZ 46.9N i 47.4N ei 48.7N i 51.8EZ iS 54.1N i(S) 55.0E i 57.1E i 59.1E i 60.6E 62.0E i 62.8Z i 67.3E 69.2E
Pr	81.6	iP! 46.9NEZ i 47.3NE i? 49.0NZ i 54.6E i 55.0N iS 57.3NZ e 70.7E
LJ	111.6	i?? 51.4Z iP 52.0Z i 58.8Z iS 65.6NEZ
Readings from files		
SB	214.1	i 68.2Z
CL	218.6	iP 67.0Z i! 69.6 iS 96.5
H	257.5	eP? 71.6 eP 72.7 ei 74.2
T	366.8	iP 86.5 i 95.5 iS 141.4

Corona (cont'd)

Station Δ (km) Arrival times

July 26, 1952 23:01:22.5

Seismometer 1000 ± 100 ft from the charge operated a relay controlling a tone signal transmitted by telephone to Pasadena. Automatic recording of telephone signal failed; manual operation of time-marker was used.

Recorded signal	23:01:22.8 GCT
Reaction time for manual signal	0.2
Assumed travel time, charge to seismometer	0.1
Calculated origin time	23:01:22.5 GCT

R	20.3	iP! 26.0NEZ i 27.3NE i 28.9E i 29.3NE iS 29.9NE i 31.8NE i 33.2E i 33.7N i 34.2E
D	45.2	iP! 30.5 i! 31.6 iS! 36.3 i! 38.3 e 46.3 i 51.8 i 56.7
SA	60.8	iP 32.9 i 36.5 i 37.2 i 38.9 iS 40.3 i 42.8 i 45.7 i 47.3
MW	65.9	iP! 33.7 i! 34.9 i 37.5 i 38.5 i(S) 41.3 iS! 42.1
P	70.0	iP! 34.3NZ i! 34.7N i 35.2N i 35.9N i 37.6N iS(?) 42.8N iS 43.0N e 44.3N i 49.5E e 50.6?N i 56.1N
BB	69.9	iP 34.6 i 37.6 iS? 42.6 iS 43.9 i? 45.2 e? 56.8
Ch	175.2	eP? 50.8 iP! 51.0 i! 52.2 i 53.5 i? 55.3
Hv	207.0	iP? 54.8 iP 56.9 eS 80.6±

Monolith

Station	Δ (km)	Arrival times
Sept. 6, 1952 20:25:01.2		
KxR	39.4	iP 08.2Z i 09.0Z iS 13.4Z i 19.2Z
Ch	67.6	iP 12.4 i 15.0 i 15.4 iS 22.4
W	73.8	iP 13.9Z i 19.4Z iS 22.8Z i 25.5Z
CL	103.9	eiP 18.7Z i 20.8Z i 30.5Z eiS 35.0
MW	106.7	iP 19.7Z i! 21.8Z i 28.4Z iS 37.2Z
P	112.4	eP 20.6NZ iP 22.3NEZ iS 35.9E eS 37.6Z
H	116.7	iP 21.1 i 23.0 i 25.4
D	120.7	eP 21.1 i 22.3 i 23.5! iS 38.4
SB	143.8	eP? 27.3Z i 27.7Z
R	158.4	eP 27.4Z i 28.4Z iP! 28.9Z i 30.1Z iS 48.5Z
BB	169.0	eP 28.7Z iP 30.7Z
T	216.7	eP 36.7Z i 41.9Z eS 63.5Z eS 65N
N	327.6	iP 49.2 i 56.4 eS 103.5
Jan. 23, 1953 22:53:55.8		
WR	26.0	iP 00.5Z iS 04.4Z
CL	103.9	eP 13.2Z iP 15.4Z eS 30.4Z
P	112.4	iP 16.2
D	120.7	eP 16.1Z iP 18.1Z iS 33.7Z
June 5, 1953 22:05:09.1		
Portable	0.17	iP 09.2Z
Inertia switch on charge	0.0	09.1
Geophone	0.06	09.15
Galvano-meters	0.21	09.23
CL	103.9	eP 26.7Z i 28.8Z e 42.9Z
MW	106.7	iP 27.9Z i 29.9Z iS 44.9Z
P	112.4	e? 28.5Z e 30.2NZ iP 30.5Z iP 30.6N e 44.6E
KgR	124.6	iP 31.1Z
BB	169.0	e? 37.7Z
T	216.7	ei(P) 45.2EZ i(S) 74.1NEZ
Aug. 1, 1953 15:08:47.219		
Refl.	1.082	47.503 near end
spread	1.753	47.674 far end
PR	24.4	iP 51.8EZ i 52.5Z i! 53.0E iS 55.1E i(S) 55.5Z
		i! 56.8E i 57.5Z i 58.1E i 59.9Z
FT	54.9	iP? 56.0±
W	73.8	iP 59.8Z i 65.3Z 68.8E iS 68.9Z

Monolith (cont'd)

Station	Δ (km)	Arrival times
Aug. 1, 1953 (cont'd)		
CL	103.9	eiP 64.5Z i 66.8Z i 76.3Z eS 80.6Z iS 82.0Z
MW	106.7	iP 65.5Z i! 67.7Z i 72.8Z iS 82.8
P	112.4	i(P)? 67.1Z i 68.3NZ i 80.6Z iS 82.2E iS 82.5N i 83.7Z
H	116.7	iP 67.4Z e 67.4N i 69.0Z eS? 84N eS 86.2Z
D	120.7	eP 66.9Z i 68.1 i! 69.5Z i 76.7Z eS 84.2Z
KgR	124.6	iP! 68.3Z i 69.1Z i 72.1Z e 79.6Z eS 83.4Z iS 85.0
BB	169.0	eP 74.9 i 76.5
T	216.7	eP 82.3 eS 109.3EZ
Pr	244.3	eP 84.8Z i? 88.1Z eS 116.3Z
Bt	316.5	eiP 93.8Z i? 102.5Z i(S) 140.9Z
N	327.6	eP 96.0Z iP 106.5Z eS? 150.9Z

EARTHQUAKE DATA

Earthquakes of August 16, 1949 (21:14) and August 31, 1949 (02:58). Readings used in Figure 8 in addition to those published by Richter as shocks 3 and 5 in "Velocities of P at Short Distances" (1950).

Station	Δ (km)	Travel Times
3		
R	16.5	7.5 9.1
Cr	25.4	10.1 11.2 15.0
Po	48.0	9.8 10.5 12.1 15.5 16.4 21.5 27.4
MW	82.3	17.5 25.3 26.6 27.2 28.0
5		
R	13.6	7.9 9.4
Cr	16.1	9.2 10.4 10.8
Po	36.8	12.5 13.8 14.4
Pe	39.9	10.2 19.1
MW	70.1	13.3 18.7 23.0 23.9 28.9
P	79.6	21.8

Readings by Gutenberg used in Figure 9.
Shock numbers as used by Gutenberg (1944b)

No.	Station	Δ(km)	Travel Times
20	P	49	7.7 10.5
	MW	62	10.0 12.0 14.2 16.6
	R	103	16.6 (19.8)
	SB	138	23.0 25.7
	LJ	149	24.5 26.3 30.7
21	P	47	7.8 8.2 10.5 12.5!
	MW	58	9.2 11.0 12.5 16.0
	R	87	14.3 15.8 17.8
	SB	155	28.1 30.2 32.2 33.9
22	P	45	7.0 8.6 11.3
	R	97	14.9 16.4 18.4 20.4
	LJ	144	22.8 27.5 29.3 32.1 35.0
	SB	147	25.7 27.8 29.2 32.0!
23	P	39	6.1 8.6
	MW	51	8.4 10.1 13.4
	R	88	14.0 19.0 20.5
	LJ	145	26.0 33.0
	SB	148	26.7 32.3 35.0
25	P	41	6.6 9.1! 11.1
	MW	51	8.4 9.6 11.3
	R	80	13.4 14.3 14.9! 18.8
	LJ	135	22.1 25.1 26.2 31.5
	SB	158	25.1 27.1 30.6 34.4
26	P	41	6.4 7.7
	LJ	131	24.5! 27.0
	SB	163	26.5 30.9 34.0! 36.4!

Readings by Gutenberg used in Figure 10.
Shock numbers as used by Gutenberg (1944b).

No.	Station	Δ(km)	Travel Times				
13	SB	80	13.3	14.3	15.0	15.9	18.9
	P	111	18.2	20.2			
	MW	113	18.3	20.1	21.6!		
14	SB	83	14.0	14.7	15.3	16.3	18.2
	P	113	18.5	20.1	21.1!		
	MW	114	18.7	21.6!	27.6		
	R	180	34.8				
15	SB	79	13.2	14.2	15.5!		
	H	169	31.3	33.0	35.5	43.5	
16	P	105	17.3	17.9	21.1	24.1	
	MW	107	17.5	18.6	20.7	22.5	
	H	166	28.1	31.0	35.7		
17	P	133	21.9	22.8	24.1	25.2	28.1
	R	209	34.1	38.5	44.2		
28	MW	69	11.5	12.6			
	LJ	130	24.3	26.2	26.8		
29	MW	76	12.6	13.1			
	P	84	13.8	15.3	21.8		
	LJ	126	20.7	23.6			
30	R	30	5.8	6.8			
	MW	96	15.6	18.7	29.8		
31	P	127	20.3	25.5			
	LJ	144	23.8	26.7	35.2	37.7	
32	MW	79	13.4	14.1	14.8		
	P	80	13.6	17.6	22.6		
	LJ	93	16.0	21.3			
33	R	40	6.7	9.4			
	MW	75	13.0	15.3			
	P	77	13.3	16.0	22.6		
	LJ	94	16.3	18.3	22.5	27.5	
34	R	36	5.8	8.4			
	MW	74	12.7	13.7	(15.8)		
	P	75	12.8	13.9			
	LJ	97	16.1	19.5			

No.	Station	Δ(km)	Travel Times
35	R	37	5.6 8.0
36	R	100	16.1 18.1 20.4
	MW	163	26.6 30.5
	P	173	28.3 31.9
46	R	103	16.6 18.4
	MW	170	28.0 34.3

Walker Pass earthquakes.
Readings used in addition to those published by Chakrabarty and Richter (1949).
Underlined readings are strong arrivals.

No.	Station	Date	Readings
1	Haiwee	Mar. 15, 1946 05:21:	09.2 15.9 17.3 20.1 20.9 25.1
2	Haiwee	Mar. 15 05:49:	44.8 (line disappears)
4	Haiwee	Mar. 15 07:00:	17.4
5	Haiwee	Mar. 15 11:18:	63.0
7	Isabella	Mar. 16 01:46:	iP 25.3 i 26.7 i 27.6 i 28.9 iS 30.1 i 32.1 i 34.3 34.8 45.2
8	Mojave	Mar. 16 22:03:	iP 59.9 i 60.4 i 62.0 i 63.9 eS 69.1 i 71.5 i 74.0 i 77.7
9	Haiwee	Mar. 18 02:05:	iP 04.3 i 06.8 i 09.1 i 10.8 (09.8??)
10	Haiwee	Mar. 18 07:49:	iP 33.6 i 34.9 i 37.0 i(S) 39.4 i 40.6 i 43.3
11	Haiwee	Mar. 19 00:45:	iP 51.0 iS 58.4 i 61.5 i 66.9 i 70.4
12	Haiwee	Mar. 23 21:17:	iP 36.5 38.0 40.0 iS 42.7 44.6 48.6 51.0 53.1
13	Haiwee	Mar. 24 12:00:	iP 11.9 i 15.6 iS 18.2 20.7 22.3 26.0 28.8 32.6 38.5
15	Haiwee	Apr. 22 23:11:	iP 49.0 i 49.4 i 51.2 e 52.2? iS 55.5 57.7 59.5
16	Haiwee	Feb. 6, 1947 09:20:	iP 50.3 i 53.6 iS 57.2
17	Haiwee	May 26, 1948 11:35:	iP 22.0 i 24.0 iS 28.8 iS 29.0 32.4 e 39.4
18	Haiwee	Apr. 16, 1946 02:37:	iP 12.4 i 13.2 i 13.9 i 15.2 i 15.9 i 18.0 i 20.6 iS! 17.3 i 21.3

No.	Station	Date	Readings
19	Haiwee	June 5, 1946 13:59:	iP 44.2 i 47.5 50.1 51.4 52.6 52.9 56.2 58.4 61.6 67.7 87.0
20	Haiwee	Aug. 31, 1946 01:10:	iP 23.7 i 28.6 27.7? i 31.3 iS 30.8 i 31.2 33.7 35.0
21	Haiwee	Feb. 1, 1947 05:30:	iP 67.2 i 69.9 i 73.4 i 76.2 iS 80.2 iS 81.4 i 85.2 i 89.4 83.5

Additional shocks near Walker Pass.
Earthquakes of August 29, 1952, 02:51 and 06:43.

Station	Δ(km)	Readings							
02:51:									
CL	14.0	15.6							
H	34.6	18.8	20.3	20.8	21.9	22.8			
Hv	87.2	27.0	32.2	36.8					
PC	107.4	30.5	33.5	35.8	42.7	50.3			
T	141.2	35.5	38.7	41.3	48.0	51.7	54.0	57.1	
Ch	172.0	39.9	41.9	44.4	48.8	63.6			
D	193.2	42.7	64.6	65.6	68.8				
BB	198.9	43.6	45.9	46.8	69.9				
P	200.2	43.0	45.7	47.7	48.6	61.2	69.1	70.2	71.2
R	214.6	45.3	48.3	72.4					
SB	245.2	53.7	83.1						
06:43:									
CL	14.9	31.0							
H	35.3	33.8	37.1	37.7	38.2	40.7			
Hv	92.0	42.2	49.9	52.4					
W	111.2	57.5							
PC	112.6	45.5	46.4	47.3	51.1	58.0			
T	139.4	51.2	51.4	55.3	68.5				
Ch	177.1	55.6	56.8	58.1	59.2	77.9	79.9		
BB	200.7	60.9	62.2	84.7	86.3				
R	217.9	63.7	87.9						

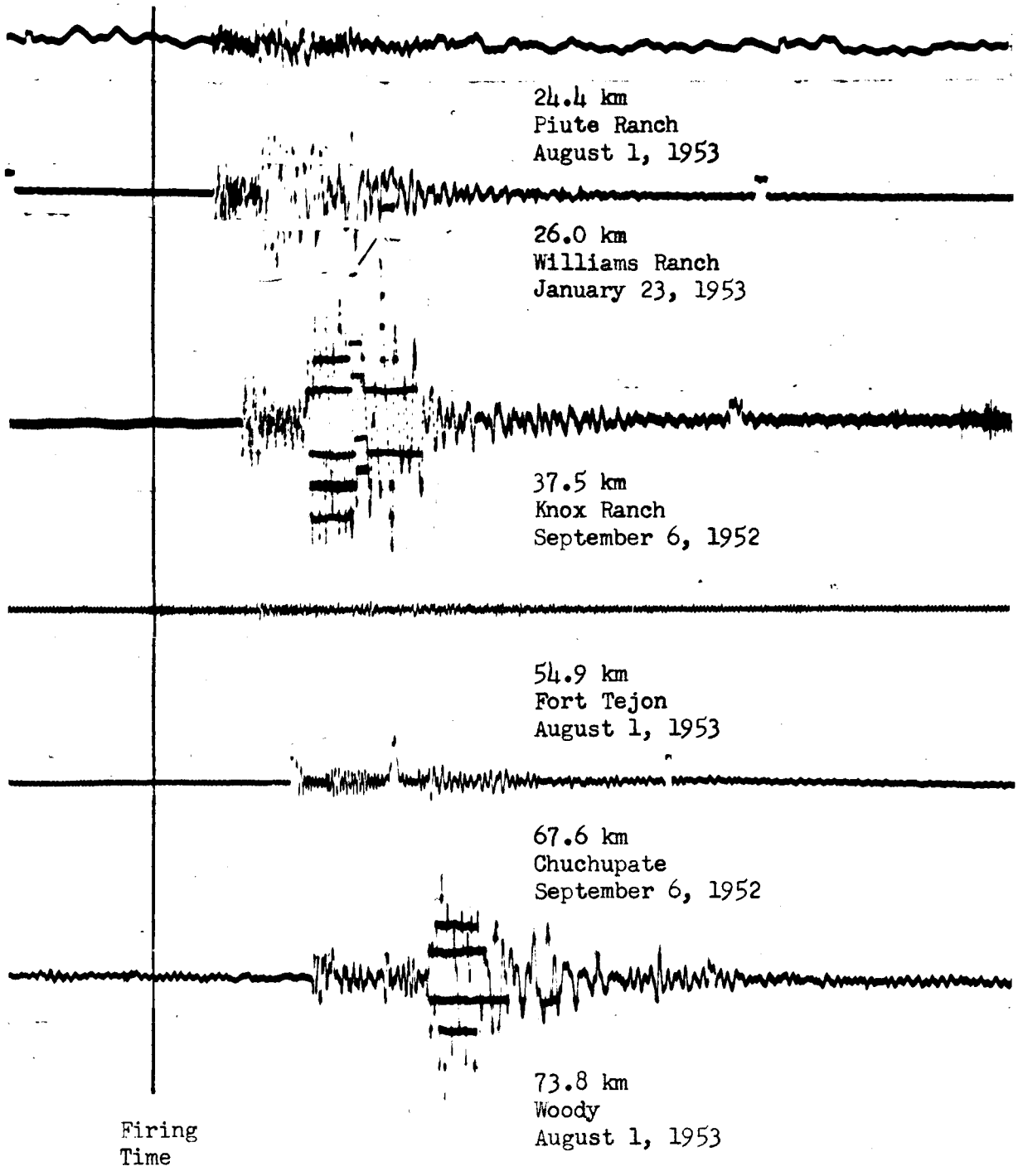

Fig. 31. Records from Monolith blasts at distances of 24.4 to 73.8 km.

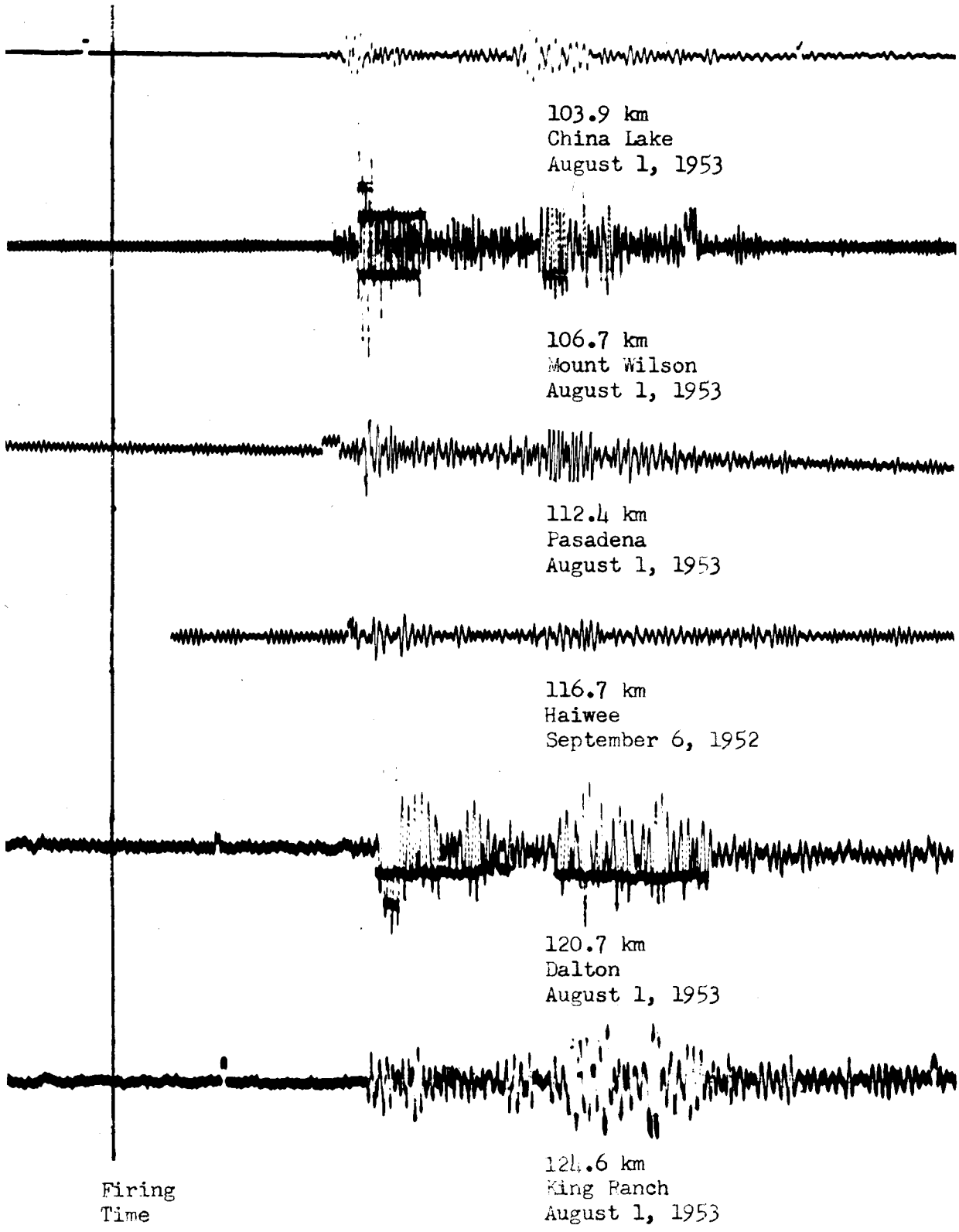

Fig. 32. Records from Monolith blasts at distances of 103.9 to 124.6 km.

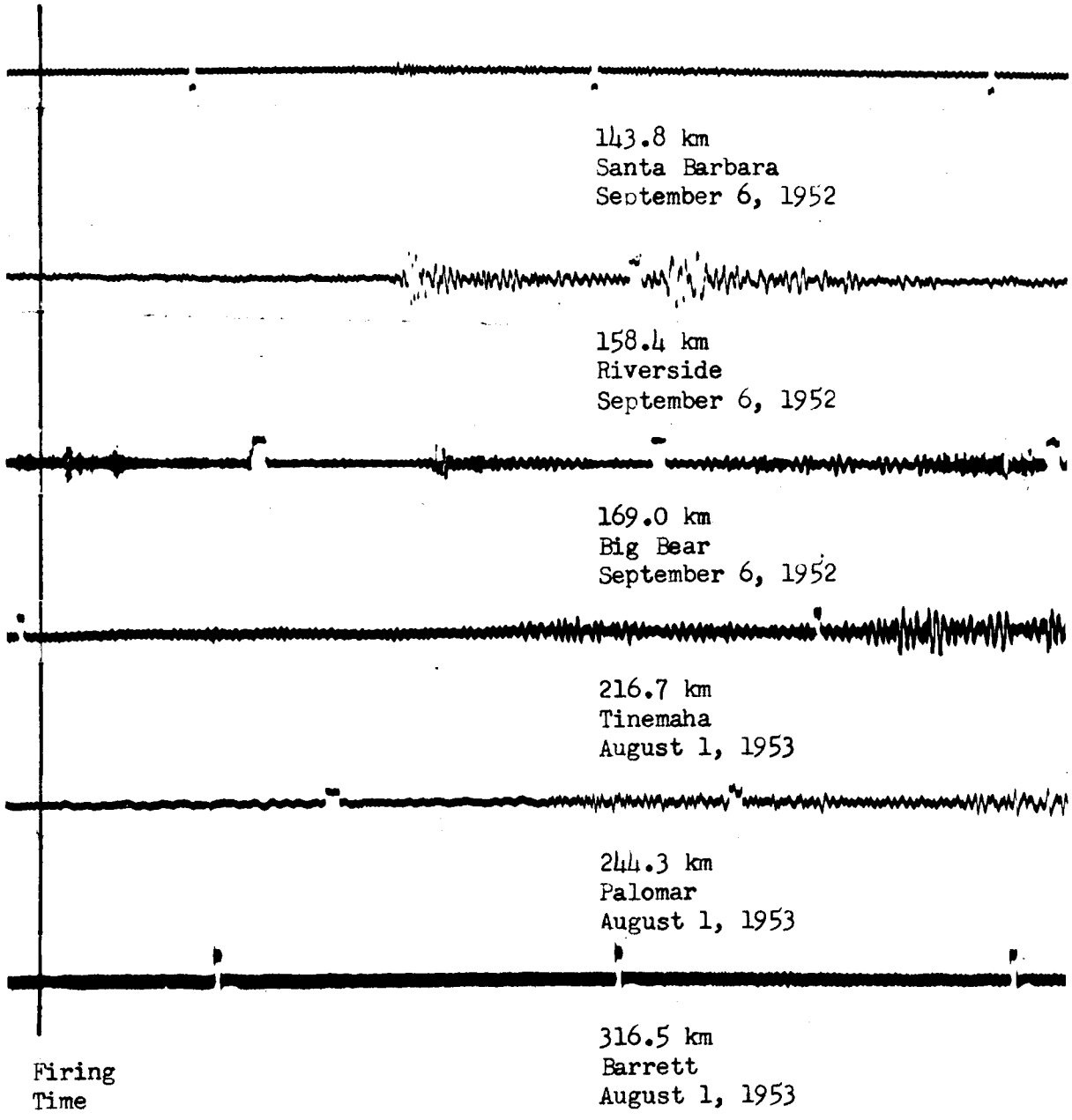

Fig. 33. Records from Monolith blasts at distances of 143.8 to 316.5 km.

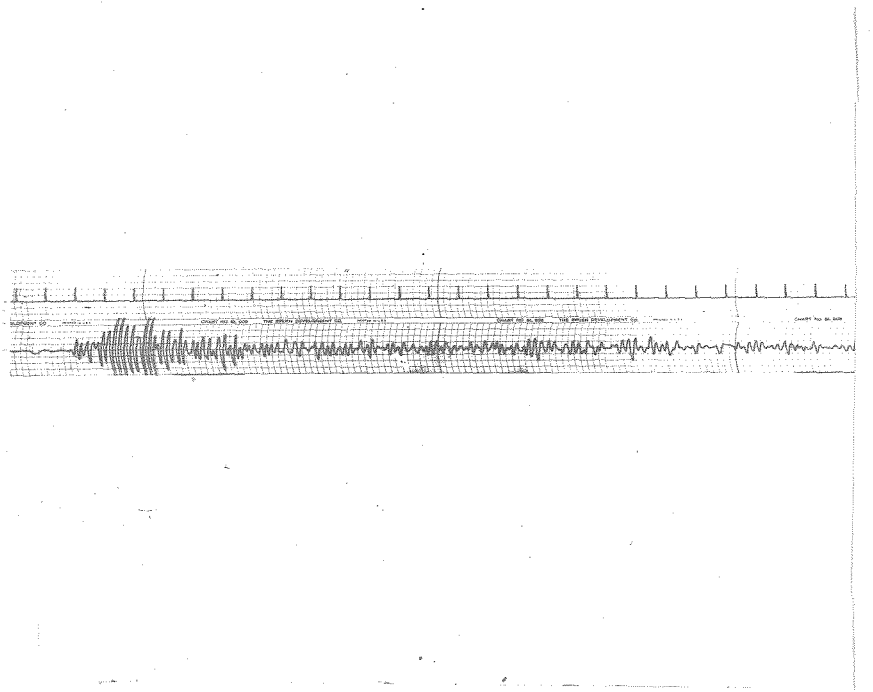

Fig. 34. Corona blast, Aug. 6, 1949.
Point Loma hydrophone; 128.7 km.
Reduced to 240 mm/min.

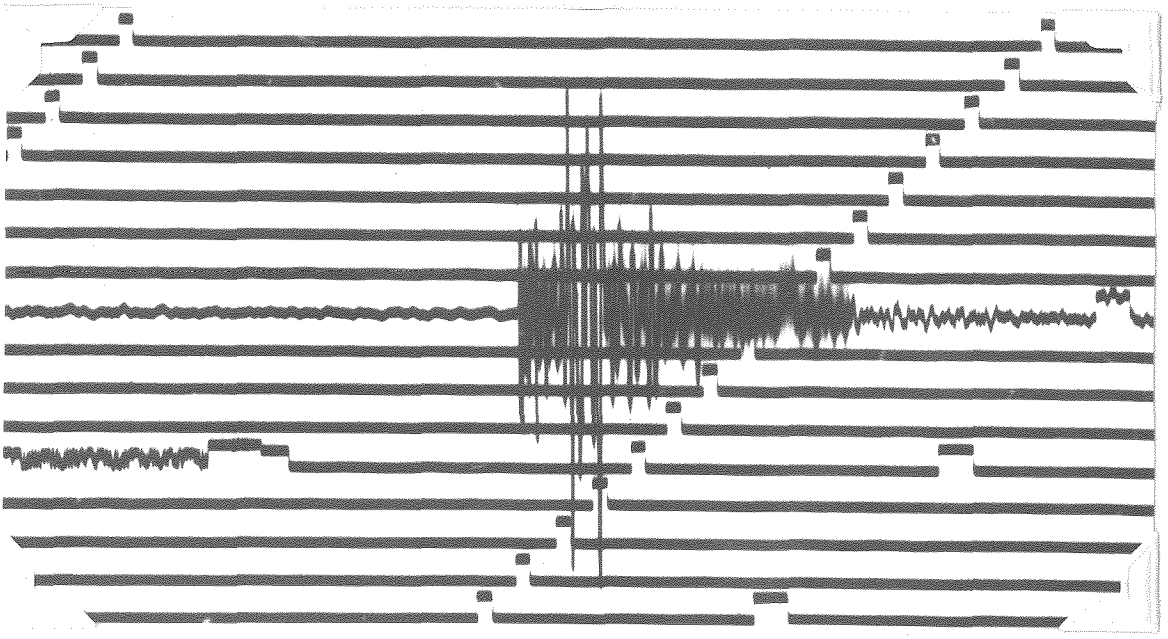

East - West Torsion

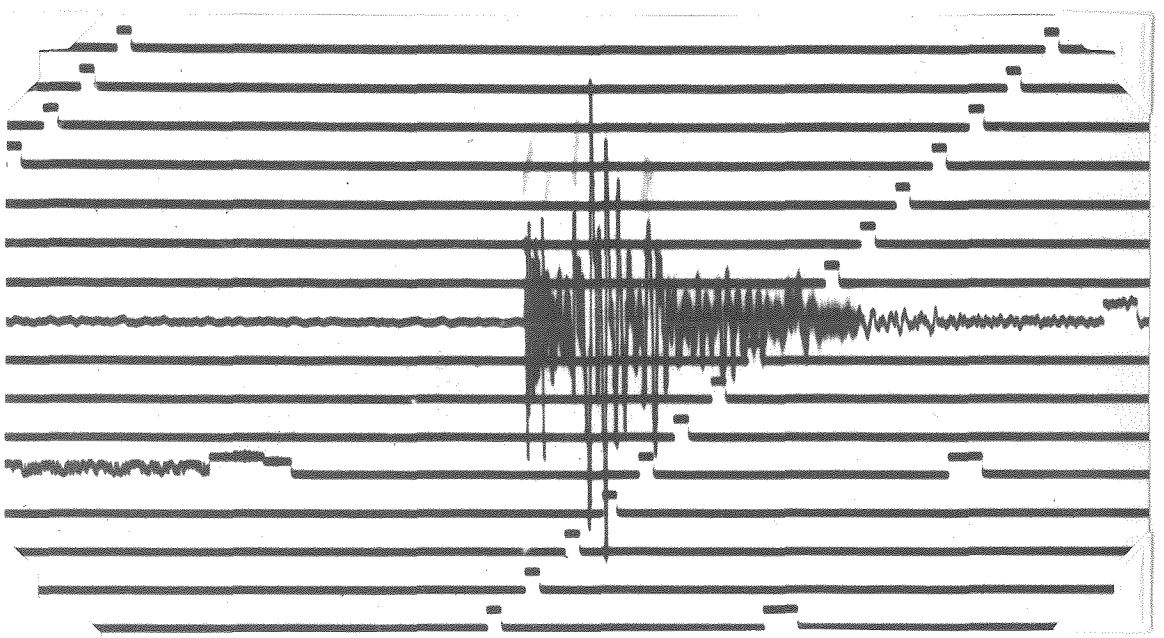

North - South Torsion

Fig. 35. Corona blast, July 26, 1952.
Riverside horizontals; 20.3 km.
Enlarged to 120 mm/min.

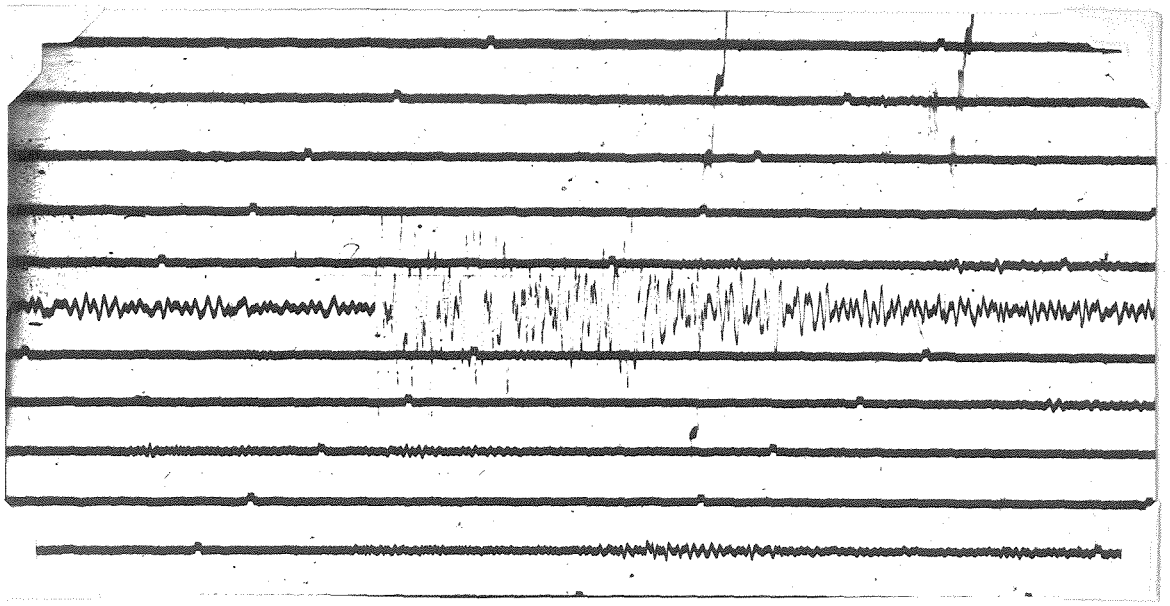

Dalton. 45.2 km.

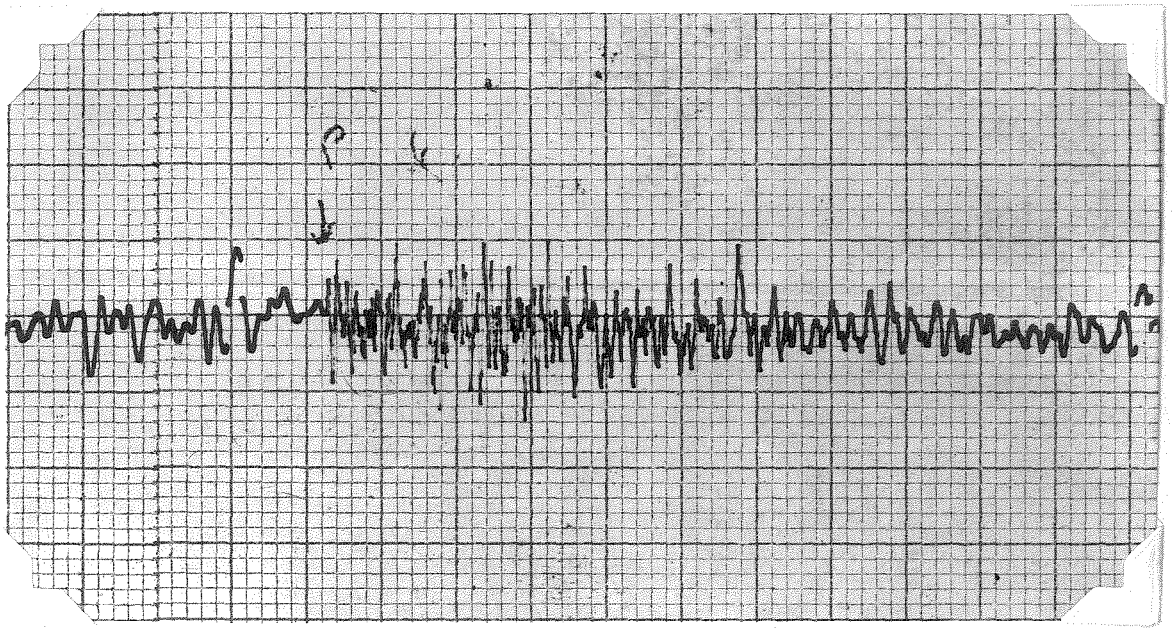

Santa Anita. 60.8 km.

Fig. 36. Corona blast, July 26, 1952.
Dalton and Santa Anita verticals.
Enlarged to 120 mm/min.

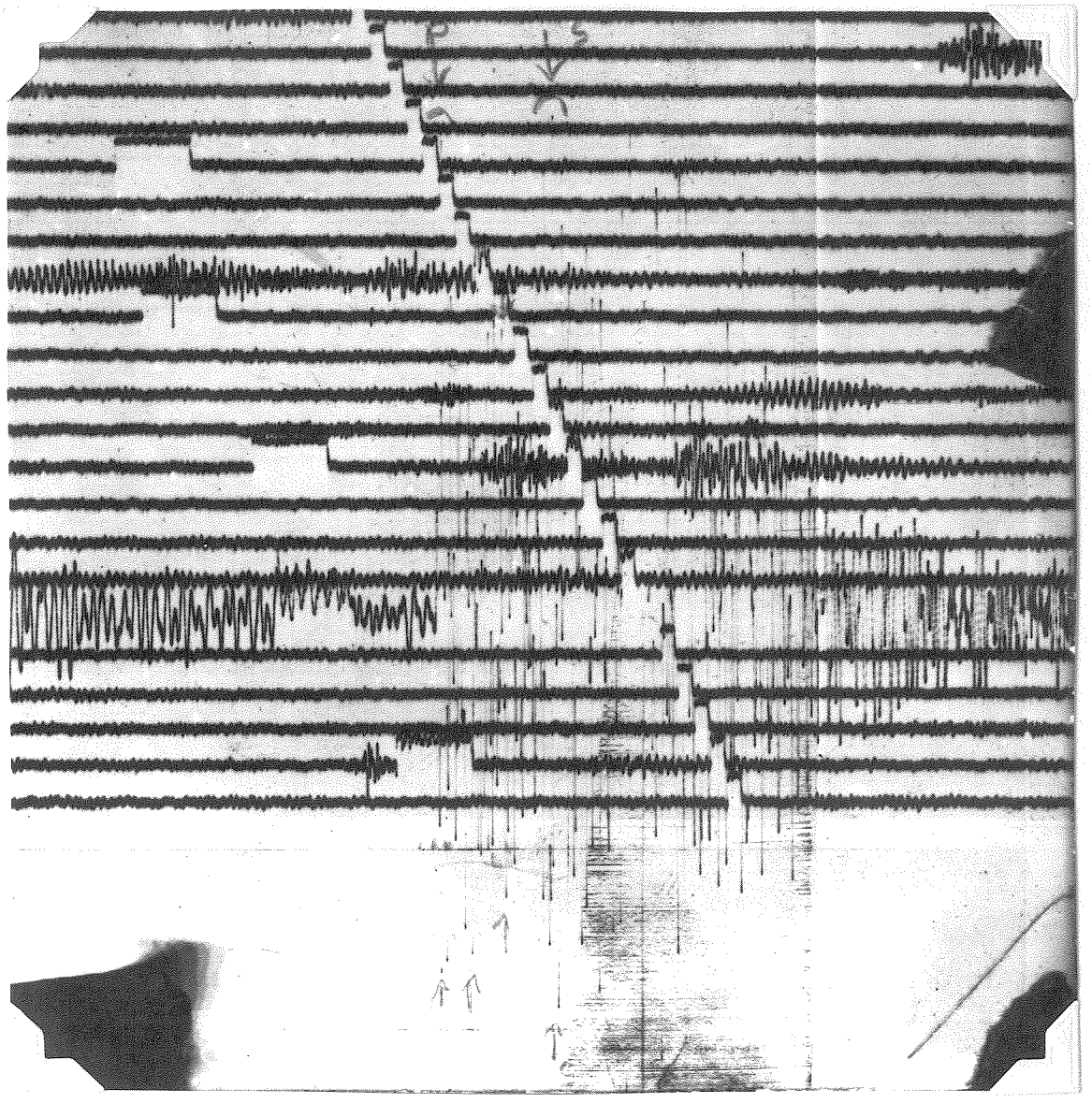

Fig. 37. Corona blast, July 26, 1952.
Mount Wilson vertical; 65.9 km.
Enlarged to 120 mm/min.

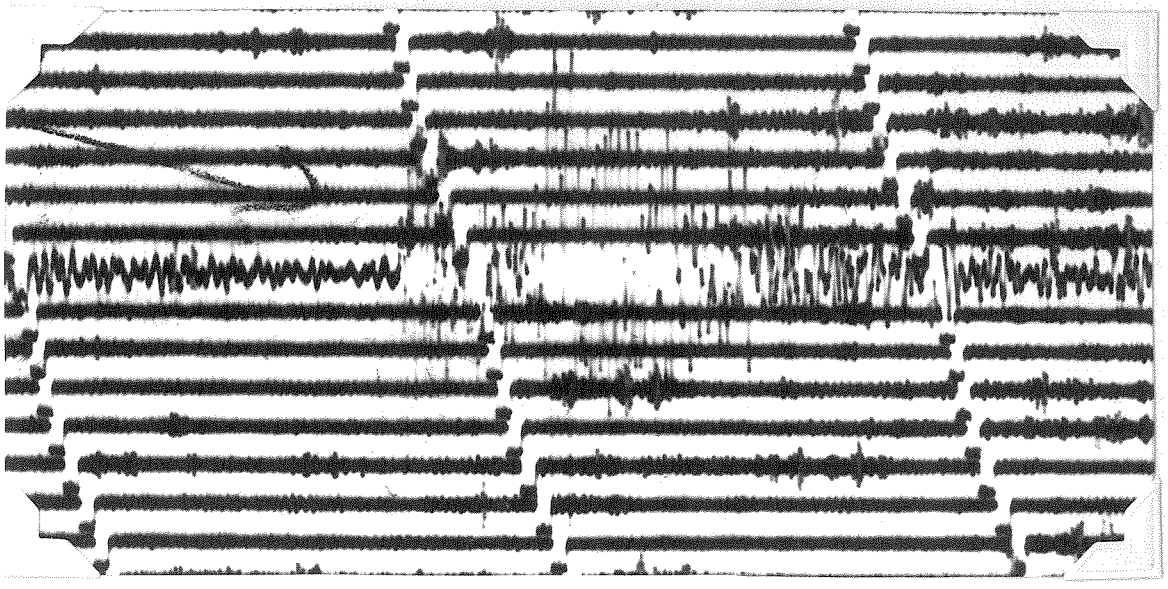

Big Bear vertical. 69.9 km.

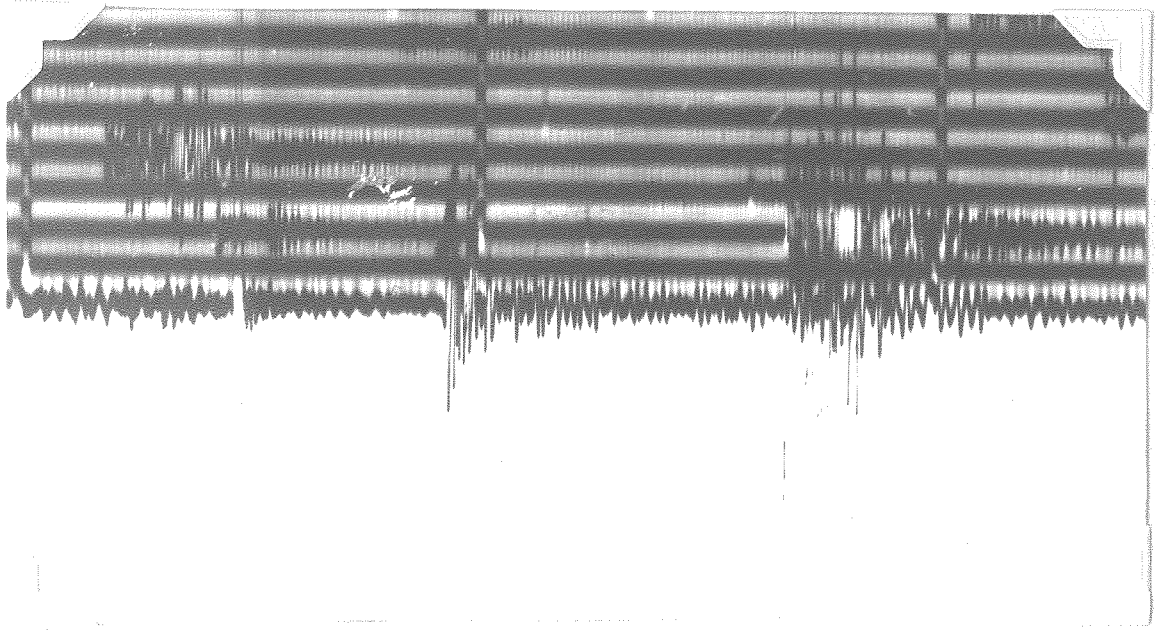

Chuchupate vertical. 175.2 km.

Fig. 38. Corona blast, August 6, 1949.
Big Bear and Chuchupate verticals.
Enlarged to 120 mm/min.

Kern County Earthquake Arrival Times

On the following pages are tabulated the times of first arrivals and epicentral distances of all located Kern County aftershocks from July 21, 1952 to May 25, 1953. These locations are the work of Dr. C. F. Richter and were used here for the study of differences of arrival times of P_n. Distances are all computed using the method of Richter (1943). The locations and arrival times but not the computed distances have been published by Richter (1954).

Additional readings for which there was no space in the table are:

No. 194.

Station		Fresno	Mount Hamilton	Berkeley	Tucson
Time	22:41:	50.5	68.5	79.2	131.3
Distance		177.7	330.9	410.9	823.1

No. 195.

06:03:	33.9	52.3	
	217.9	368.7	

No.	Time	Lat. N	Long. W	Mag.	SB	P	MM	CL	H	R	F	BB	T	Pr	Bt	MH	BC
July 21, 1952																	
1	09:43:03	35 00?	119 05?	3.1	17.1	22.3	23.3	29.1	31.9	34.1		37.4	41.4	40.6	49.3		
					04.8	120.3	127.6	162.6	161.8	192.6		216.2	244.1	274.9	340.6		
2	11:52:14.3	35 00	119 00	7.7	28.7	33.7	34.3	39.2	40.9	42.9	44.4	46.1	50.9	52.2	60.1?	61.7	69.0
					90.1	121.3	122.0	150.4	157.2	186.4	208.8	209.2	241.9	269.2	335.7	352.1	393.5
15	12:19:30.5	34 57	116 52	5.3	52.2	53.0		60.2	60.5±	62.4		65.8±	71				
					96.0	109.4		150.1	155.0	173.3		195.8	244.2				
20	13:25:11.6	35 00	119 00	4.5	20.7	30.2			35.9	39.5			48.4				
					90.1	121.3			157.2	186.4			241.9				
34	15:13:58.7	35 11	118 39	5.1	20.2	18.2			17.9	25.8	28.2	27.1±	32.5		46.0	47.4	48.8
					127.6	122.9			122.6	176.4	204.0	190.5	215.0		331.9	357.1	360.0
40	17:42:44.0±	35 14	118 32	5.0	08.5	03.0			02.6	11.3		13.5	16.9			34.9	32.7
					137.3	124.9			112.6	173.9		184.9	207.6			364.3	345.5
42	18:23:30.5	35 18	118 32	4.5	02.4	57.0		55.4	56.1	66.9	68.4	67.2	70.6	77.1	86.5	89.3	86.8
					144.0	132.0		102.3	106.1	179.7	198.7	189.4	200.7	265.5	335.5	359.5	343.5
43	18:20:27.5	35 18	118 32	4.1	50.8	49.0?			45.2				59.6				
					144.0	132.0			106.1				200.7				
44	19:12:08.0	35 13	118 20	4.3	10.0	31.0	20.0	25.0	20.7	36.2		38.4	40.6	46.1	55.0	59.3	56.1
					14.4	142.1	121.0	103.2	111.7	168.6		178.9	209.2	254.6	326.7	370.1	340.0
45	19:16:19.2	35 16	118 27	4.3	22.0	42.4	37.2	35.0	36.1	46.1	50.2	47.1	50.5		66.3	68.9	66.5
					17.1	147.5	120.0	90.5	106.0	172.3	201.0	181.2	203.6		330.6	367.7	337.0
46	19:41:22.3	35 08	118 46	5.5	20.2	40.6	41.0	44.7±	46.5	50.1	52.2	52.2	57.0	62.3	69.3	69.9	74.2
					32.7	115.0	122.2	130.4	132.9	180.8	203.9	186.8	222.5	264.6	340.5	356.1	360.9
47	20:21:05.9	35 13	118 28	4.2	00.0	27.9	25.0		23.5	33.2		35.7	37.9			55.0	53.7
					14.4	143.1	121.0		111.7	168.6		170.9	209.2			370.1	340.0
48	21:51:40.9	35 00	118 42	3.0	51.7	05.9	05.0	05.2	07.4	70.2	74.2	77.1	70.5	82.9	84.0	93.6	
					20.5	118.2	110.2	113.0	127.0	132.9	172.8	209.8	189.6	224.9	257.0	327.5	
49	21:53:09.3	34 52	117 01	4.3	19.1	22.3	27.0	27.3	33.8	35.4	36.3	40.8	39.6	48.0	40.3	54.1	57.4
					00.7	79.5	111.2	113.3	100.0	170.2	179.3	222.5	205.2	222.5	260.7	325.0	362.3
50	23:11:44.0	35 10	118 32	3.9	48.2	00.0	04.0	04.2		61.2	72.0		75.4	75.8		92.5	96.3
					25.3	144.0	132.0	120.9		106.1	179.7		189.4	200.7		337.7	359.5
51	23:53:20.1	34 59	117 02.5	4.5	37.0	41.9	47.0	47.5	53.8	54.6	56.4	57.5	59.1	65.6	66.8	74.4	74.9	81.8
					30.0	00.1	122.2	123.4	100.4	160.4	188.0	209.5	212.0	244.7	270.8	330.7	351.0	400.0
July 22																	
52	01:00:50.3	35 11	118 36	3.2	02.2	19.3	17.4	10.2									
					17.5	131.1	121.3	114.9									
53	01:10:43.0	35 11	118 30	3.9	40.7	05.1	02.0	02.5		62.1	72.2		74.1	70.7	81.4	90.7	92.8
					17.5	131.1	121.3	117.4		120.4	173.4		188.7	214.3	259.0	330.0	363.4
54	01:13:14.3	35 00	118 47	3.0	20.0	31.1	31.0						45.9	51.5			
					35.5	105.4	109.0						191.2	237.2			
55	01:41:02.0	35 08	118 31	4.5	04.1	24.7	20.3	20.4	20.1	22.2	28.4	34.4	30.0	36.3	38.8	48.1	54.1	50.0
					10.4	133.7	113.0	107.2	122.7	122.0	164.2	219.1	177.3	218.9	249.9	321.2	372.8	348.9
56	01:48:06.0	35 14	118 32	3	12.5	31.5	20.5	28.5	29.5		37.3			42.4	47.6			
					19.1	137.3	124.9	120.1	100.0		173.9			207.0	259.6			
57	01:51:50.0	35 17	118 33	4.4		14.8	11.5	11.4		08.5	19.9	21.9	19.5	23.1	29.0	30.1	41.7	30.7
						141.7	130.0	120.0		108.5	179.1	199.5	189.4	202.7	265.0	337.0	359.5	345.4
58	03:21:04.8	35 12½	118 37½	4.4		27.2	25.0	24.0	25.2	23.6	32.0	35.9	33.3	37.9	42.2	52.7	54.0	
						131.0	124.7	120.9	115.1	119.1	177.0	202.8	180.5	211.9	262.1	333.6	359.9	
59	07:44:55.4	34 52	118 54	4.1	02.2	10.2	11.5	11.0	12.0	21.9	21.4	27.8	24.0	35.0	30.7	39.4	40.5	48.4
					34.6	91.0	102.1	102.7	150.0	162.9	187.9	227.1	192.4	253.3	290.3	340.5	371.3	388.9
60	08:10:23.7	35 05	118 35	4.4	20.5	43.4	41.9	41.2	42.4	44.4	49.2	50.0	51.1	55.2	57.8	68.9	74.7	72.0
					12.7	125.7	110.4	100.0	120.9	129.6	182.7	210.7	177.5	225.1	249.5	320.0	372.1	354.4
61	08:21:21.7	35 00	117 00	4.1	20.7	30.1	41.0	41.4	47.7	45.8	49.5	50.2	51.9	57.2	57.4	69.2±	70.0	
					44.1	90.1	121.3	122.0	150.4	157.2	188.4	208.8	209.2	241.9	269.2	335.7	352.1	
62	08:47:34.3	35 05	118 45	4.7	30.5	52.5	53.0	52.9	55.7	57.0	60.8	64.8	63.0	69.9	71.0	80.1	84.3	84.3
					24.0	113.4	110.4	111.5	132.0	130.8	174.8	209.5	192.7	227.6	259.0	340.7	361.1	388.9
63	09:10:25.1	35 14	118 30	4.5	47.7	47.6	45.3	45.2	44.0	44.3	52.2	55.2	53.4	57.5	62.3	72.2	75.1	73.4
					20.7	138.5	122.7	122.2	111.0	115.5	177.6	201.6	189.9	208.9	263.2	332.0	359.7	351.5
64	10:19:30.0	35 02	117 00	4.1	40.3	52.4	50.0	52.7?	03.1	65.3	68.0	69.3	71.2	76.3	77.3	80.2	80.7	
					47.1	97.0	142.7	122.6	150.0	159.0	188.9	208.9	212.0	242.7	271.4	337.6	352.2	
65	10:44:05.7	35 03	118 30	3.0	00.7	20.3	22.2	21.7	24.3	27.0	30.5	41.2	35.1	43.0?	40.9	50.2	51.3	05.5
					7.4	130.1	104.4	100.1	110.1	130.0	156.2	22.7	171.1	220.0	241.8	312.0	300.1	348.3
66	13:31:42.7	35 00	117 00	4.0	51.5	57.3	02.1	02.3	01.7	69.8	71.1	75.0	74.0	82.2	80.5	88.9	91.8	97.3
					44.1	90.1	142.3	122.0	150.4	157.2	180.4	208.8	209.2	241.9	269.2	335.7	352.1	393.9
67	14:05:11.1	35 06?	117 00?	4.0	47.0	20.7	21.1	21.1		33.1	39.4	37.8	42.1	40.0	47.7	58.2	50.8	
					45.7	98.1	130.1	130.0		148.2	193.2	198.0	213.8	231.5	270.2	342.7	343.7	
68	14:30:10.3	34 54	117 03	4.3	20.5	31.0	30.1	30.7	43.2	45.0	45.9	44.5		50.8	50.0	02.3	00.4	12.1
					49.0	12.4	110.0	110.0	100.1	100.8	103.8	218.0		253.8	282.4	330.4	357.5	401.2
69	15:03:14.4	35 14	118 32	4.2		30.8	34.0	34.1	31.7	33.3	42.2	42.7	43.8	47.2	52.3	01.8	05.3	04.8
						139.3	122.7	120.1	100.0	112.6	173.9	208.3	184.9	207.0	259.0	331.4	364.3	345.3
70	17:52:30.3	35 00	117 00	4.1		40.9	55.3	50.3	01.4		04.7	05.0?	07.3	72.5	75.0	03.1	02.5	
						90.1	121.3	122.0	150.4		188.4	208.8	209.2	241.9	269.2	335.7	352.1	

No.	Time	Lat. N	Long.	n	mag.	Ch	SB	F	MM	D	CL	H	R	F	BB	T	Pr	Bt	MM	BC
July 22																				
71	19:08:59.3	35 13	118 26		4.3		21.8	10.8	10.7		15.5	17.4	4e.7	20.2	20.7	30.4	30.1	45.5	40.7	40.0
							143.1	121.0	110.2		103.2	111.7	108.6	209.0	170.9	209.2	254.0	320.7	370.1	340.0
73	21:02:10.8	35 04	118 46		4.2		20.4	29.2	29.3		32.2	3e.9	37.0	40.0	41.4	40.4	40.7	57.9	50.9	03.3
							111.1	115.6	113.8		134.8	139.2	174.7	210.4	193.2	229.7	249.4	320.1	360.7	370.9
74	22:31:33.4	35 01½	118 55½		4.7		48.9	52.4	52.0		57.0	59.1	60.2	04.4	04.0	09.4	70.9	79.0	02.3	09.6
							97.1	117.3	119.2		149.2	151.0	102.6	208.0	204.1	237.4	266.1	333.4	354.6	388.5
July 23																				
75	00:38:32.0	35 22	118 35		0.1		55.5	54.0	53.9		40.1	40.8	01.2	00.7	01.4	02.7	72.0	01.0	01.3	01.4
							145.7	140.4	135.0		102.3	102.1	100.3	190.1	197.5	194.0	274.3	340.4	351.3	345.4
70	00:43:08	35.0	119.0		4.4		23.1	20.5			33.67	33.6	35.7		41.5	46.1		55.0		
							90.1	121.3			150.4	157.2	100.4		209.2	241.9		335.7		
77	00:47:38.0	35 22	118 35		4.0		00.7	00.5	59.7		54.5	54.0	60.2	05.9	07.4	00.4	70.5	00.7	05.9	00.4
							145.7	140.4	135.0		102.3	102.1	100.3	190.1	197.5	194.0	274.3	340.4	351.3	345.4
78	03:19:23.1	35 22	118 35		5.0		40.1	45.4	44.7		39.3	39.4	51.7	50.2	53.0	52.7	01.0	71.2	71.0	71.6
							145.7	140.4	135.6		102.3	102.1	100.3	190.1	197.5	194.0	274.3	340.4	351.3	345.4
79	03:49:27.5	35 17	118 33		4.7		50.1	40.7	47.5		44	45.5	55.1	55.8	50.4	57.7	00.9		75.4	75.5
							141.7	130.0	120.0		104.7	100.5	179.1	199.5	189.4	202.7	265.0		359.5	345.4
80	04:01:39.6	35 22	118 35		4.7		02.7	01.1	00.7		55.8	50.1	07.6	07.4	09.1	70.1	78.4	07.8	00.5	00.1
							145.7	140.4	135.6		102.3	102.1	100.3	190.1	197.5	194.0	274.3	340.4	351.3	345.4
81	05:46:02.7	35 23	118 34		4.7		26.3	25.0	24.4		18.8	20.4		31.0	32.0	33.4	42.7	51.2	51.8	50.9
							140.0	141.3	130.7		100.1	99.7		196.7	197.5	191.9	274.9	347.2	351.3	344.4
82	06:10:45.8	35 16	118 27		4.2		00.7	05.7	05.0		01.9	03.0	12.6	10.3	13.3	17.3	23.1	32.1	30.0	33.3
							147.5	120.0	121.0		98.5	106.0	172.3	201.0	181.2	203.0	258.2	330.0	307.7	337.0
83	06:26:36.4	35 22	118 35		4.0		52.9	50.1	50.1		44.5	44.8	59.0	56.4	57.9	56.7	08.4	77.6	77.9	77.0
							145.7	140.4	135.6		102.3	102.1	100.3	190.1	197.5	194.0	274.3	340.4	351.3	345.4
84	06:53:42.3	35 22	118 35		4.2		05.1	04.2	04.1		58.0	58.6	67.2	70.4	71.4	72.5	81.0	89.0	91.1	90.4
							145.7	140.4	135.0		102.3	102.1	100.3	190.1	197.5	194.0	274.3	340.4	351.3	345.4
85	07:37:00.2	35 17	118 33		4.8		22.7	20.9	20.6		16.4	17.9	27.3	29.1	20.9	31.9	30.3	46.8	50.3	48.3
							141.7	130.0	120.0		104.7	100.5	179.1	199.5	189.4	202.7	265.0	337.0	359.5	345.4
86	07:53:18.7	35 00	118 50		5.4	25.4?	34.9	30.5	30.0		40.1	42.7	44.3	48.1	47.0	54.2?	54.9	02.0	07.0	09.5
						20.8	101.6	112.3	111.0		144.2	140.0	174.4	214.6	195.3	230.2	258.1	325.5	362.4	379.0
87	09:38:42.3	35 15	118 29		4.2	54.0±	05.3	02.2	01.7		58.4	59.6	07.3	73.6	09.3	74.7	79.4	00.7±	92.4	90.2
						00.7	143.0	125.5	120.2		102.0	109.0	172.5	205.9	182.4	205.5	258.4	330.6	366.6	340.5
88	10:54:13.4	35 19	118 30		4.1	20.5±	30.9	34.3	33.9		29.0	30.1	40.4	42.5	41.5	44.6	51.2	60.5±	63.3	60.9
						74.0	147.5	133.1	127.7		98.9	103.1	179.4	199.0	188.2	198.5	265.4	337.7	360.7	340.1
89	13:17:05.2	35 13	118 49		5.7		13.4	24.1	20.3	25.8		26.1	27.0	33.7	34.3	36.0	39.4	45.2	52.7±	53.7	57.6
							40.7	110.9	122.4	130.2		129.1	127.9	189.5	193.5	205.2	214.3	275.3	344.2	340.4	370.8
90	13:30:03.8	35 15	118 29		4.4		15.9	20.5	23.7	23.7		20.1	21.8	31.0	33.3	31.2	36.0	41.1	50.1±	53.9	51.8
							00.7	143.0	125.5	120.2		102.0	109.0	172.5	205.9	182.4	205.5	258.4	330.6	366.6	340.5
91	15:25:24.1	35 08	118 31		4.0		34.5	40.9	42.3	42.0		42.1	43.6	50.1	56.4	51.1	58.3	60.8	69.7±	75.7	
							57.0	133.9	113.0	109.2		112.7	122.0	164.2	215.1	177.3	210.9	249.9	321.2	372.8	
92	16:16:37.8	35 19½	118 30½		4.5		49.4	00.2	50.9	50.7		55.1	55.8	65.8	66.5	67.5	69.3	77.3	05.7±	87.0	87.1
							08.2	140.9	130.5	132.0		106.7	100.3	186.0	192.7	196.6	198.9	271.9	346.1	352.5	349.5
93	16:48:53.0	35 19½	118 30½		4.5		04.5	10.0	14.5	14.3		09.9	10.6	21.2	21.7	23.1	24.5	33.8	40.6±	41.0	
							08.2	140.9	130.5	132.0		106.7	107.3	166.0	192.7	196.6	198.9	271.9	346.1	352.5	
94	17:22:24.0	35 19	118 30		4.5+		36.0	49.2	44.9	45.1	46.4	39.0	40.9	51.8	54.5	52.6	55.1	63.5		74.3	71.8
							74.0	147.5	133.1	127.7	142.0	98.9	103.1	179.4	199.0	188.2	198.5	265.4		360.7	340.1
95	17:53:29.2	35 04	119 02		4.1		35.7	43.8	49.3	50.2	52.3	53.7	55.1	57.6	59.4	60.6	66.8	69.0		77.2	
							20.5	92.6	129.0	129.5	150.0	154.6	153.2	193.3	201.0	215.0	235.0	276.5		344.6	
96	18:03:27.6	35 19	118 30		4.0		40.6	52.2	50.4		50.5		45.1	55.6		55.6	60.2	66.4		73.7	
							74.0	147.5	133.1		142.0		103.1	179.4		180.2	198.5	265.4		360.7	
97	18:13:50.9	35 00	118 50		5.2		54.7	00.7	08.7	09.0	71.7	73.8	74.7	76.6	80.8	80.1	85.1	80.4		99.0	102.4
							20.8	101.6	112.3	111.6	131.7	144.2	148.6	174.4	214.6	195.3	238.2	258.1		302.4	379.0
98	19:51:33.8	35 22	118 32		4.0		45.9	57.0	55.6	54.5	56.8	49.8	50.9	01.7	02.0	03.2	04.4	74.0		83.1	
							75.0	149.0	139.2	133.9	142.1	98.4	99.7	185.7	192.7	194.0	193.4	271.0		354.8	
99	21:16:50.5	35 01½	118 55½		4.1			13.9	17.5	17.9	20.9	22.1	23.3	25.9	28.8	29.7	33.9	36.6		47.2	
								97.1	119.3	117.2	139.5	149.2	151.0	182.6	208.8	204.1	237.4	266.1		354.6	
100	22:32:20.1	35 04	118 56		4.1		24.9	33.9	39.8	40.2	43.1	43.2	43.8	47.7	49.3	50.3	55.7	56.6		66.6	
							29.0	99.5	123.5	123.2	143.2	147.1	147.6	186.1	204.2	206.7	233.1	269.8		350.7	
101	23:52:35.0	35 04	118 37		4.0		42.7	55.1	53.3	53.3	56.0	55.8	58.6	61.0	67.4	62.8	69.1	71.9		88.6	
							40.1	122.1	109.8	100.5	123.9	124.4	132.6	164.8	227.9	181.2	227.4	250.0		371.1	
July 24						Wnk														
102	03:11:07.2	35 00	119 00		4.1	13.5	11.9	24.5	27.8	27.5	30.9	31.4	32.4	36.1	36.2	39.2	43.8	45.9		54.0	
						34.7	32.4	98.1	130.1	130.0	150.2	150.1	148.2	193.2	198.6	213.8	231.5	276.2		343.9	
103	03:28:26.5	35 14	118 32		3.3	28.0	30.1	47.0	40.4	40.0	48.2	44.2	40.1	55.3	58.1	57.5		67.0			
						12.0	64.3	139.3	124.9	120.1	135.3	106.8	112.0	173.9	208.3	184.9		259.6			
104	03:29:27.5	35 00	119 05		3.6	30.7	31.3	41.5	47.1	47.5	51.2		57.2	56.0	60.2	61.9	68.1				
						53.3	22.3	84.8	120.3	127.6	148.8		161.8	192.6	206.5	216.2	244.4				
105	05:02:50.0	35 19	118 30		4.5	52.8	61.8	74.9	71.5	70.9	73.2	65.4	67.1	78.1	80.4	78.7	81.5	89.1		100.5	97.7
						10.6	74.0	147.5	133.1	127.7	142.0	98.9	103.1	179.4	199.0	188.2	198.5	265.4		360.8	340.1
106	09:50:32.3	34 59	118 54		4.3	30.8	30.3	47.4	50.7	50.2	53.9	55.8	58.5	59.4	62.6	62.3	69.7	69.2		80.5	
						36.5	20.3	95.9	134.1	134.3	134.7	150.2	153.5	178.0	214.0	200.2	241.3	261.0		359.6	

No.	Time	Lat. N	Long. W	Mag.	WHR	Ch	HV	SB	P	MW	D	CL	H	R	F	BB	T	Pr	MH	BC
July 24																				
107	11:47:55.0	35 24	118 35	4.4	58.4	67.8		79.1	78.6	78.6	80.6	71.6	71.8	85.4	82.5	86.4	85.3	95.3	103.1	105.7
					17.9	76.3		140.3	144.0	139.0	153.7	100.4	99.9	191.3	187.1	199.9	190.3	277.3	340.9	345.5
108	12:07:56.7	35 19	118 30	4.1	59.5	68.8		81.3	77.9	77.7	79.8	72.8	74.4	83.9	87.1	85.0	88.4	94.7	107.8	104.8
					16.6	74.0		147.5	133.1	127.7	142.0	98.9	103.1	179.4	199.0	188.2	198.5	205.4	360.7	340.1
109	14:05:26.3	35 19	118 30	4.3	28.8			50.9	47.5	47.0	49.0	42.0	43.7	54.0	50.6	54.5	50.1	65.2	77.0	74.3
					16.6			147.5	133.1	127.7	142.0	98.9	103.1	179.4	199.0	188.2	198.5	205.4	360.7	340.1
110	14:10:12.8	35 19	118 30	4.0	15.1			37.1	33.7	33.3	35.6	28.7	30.0				44.8	51.5	83.0	81.7
					16.6			147.5	133.1	127.7	142.0	98.9	103.1				198.5	205.4	360.7	340.1
111	17:35:06.0	35 14	118 32	4.2	88.0			28.5	28.1	25.7	27.7	23.1	25.0	32.9	36.7	33.9	39.3	43.0	56.3	
					12.0			139.3	124.9	120.1	135.3	106.8	112.6	173.9	208.3	184.9	207.6	259.0	304.3	
July 25																				
113	07:03:51.4	35 24	118 35	4.1	53.6	62.2		76.2	74.7	73.5		67.8	67.4	81.0	77.9	81.9	81.2	91.9	99.4	100.8
					17.9	76.3		140.3	144.0	139.0		100.4	99.9	191.3	187.1	199.9	190.3	277.3	340.9	345.5
114	10:22:53.6	34 56	119 02	3.3	61.1	55.8		80.5	72.3	72.6										
					48.0	14.0		82.9	117.6	119.2										
115	13:13:08.6	35 19	118 30	5.0	10.9	20.3		33.0	29.8	29.2		24.2	25.4	30.5	30.8	37.7	40.2	47.4	59.3	56.8
					16.6	74.0		147.5	133.1	127.7		98.9	103.1	179.4	199.0	188.2	198.5	205.4	360.7	340.1
116	14:34:42.0	35 08	118 46	4.4	45.7	49.3		80.5	81.1	61.5		64.1	65.0	69.0	72.9	72.1	77.8	80.3	91.7	94.1
					15.9	42.5		115.8	122.2	119.9		130.4	132.9	180.8	203.9	196.8	222.5	204.6	356.1	368.9
117	19:09:45.0	35 19	118 30	5.7	47.3	57.0		69.9	80.2	65.9		61.1	81.3	73.0	75.3	74.7	78.1	83.9	94.3	93.0
					16.6	74.0		147.5	133.1	127.7		98.9	103.1	179.4	199.0	188.2	198.5	205.4	360.7	340.1
118	19:43:23.3	35 19	118 30	5.7	25.7	35.4		47.7	44.5			39.8	40.4	51.3	53.3	52.0	54.4	62.0	73.4	71.3
					16.6	74.0		147.5	133.1			98.9	103.1	179.4	199.0	188.2	198.5	205.4	360.7	340.1
119	20:06:05.7	35 19	118 30	4.8	88.1	17.8		30.2	27.7?			21.3	22.3	33.7	34.8	34.6	30.7	45.2	50.1	53.6
					16.6	74.0		147.5	133.1			98.9	103.1	179.4	199.0	188.2	198.5	205.4	360.7	340.1
July 26																				
120	01:02:20.6	35 19	118 30	4 1/4		32.4	24.3	44.9	41.4	41.3	43.2	36.4	38.1	40.1	51.9	49.5	52.2	50.7	72.0	69.4
						74.0	21.5	147.5	133.1	127.7	142.0	98.9	103.1	179.4	199.0	188.2	198.5	205.4	360.7	340.1
121	01:04:45.5	35 22	118 32	3.5		57.8	47.4	70.1	67.1	66.9	69.2	81.0	62.2	73.7			70.5	85.2		
						75.8	15.9	149.0	139.2	133.9	142.1	98.4	99.7	185.7			193.4	271.6		
121a	06:38:50.1	35 11	118 36	4.0	55.2	50.7	55.9	72.7	70.0	69.2	72.0	68.6	69.7	77.0	81.2	78.4	83.2	87.8	100.6	
					9.4	50.1	37.0	131.1	121.3	117.4	133.7	114.9	120.4	173.4	206.3	188.7	214.3	259.0	303.4	
122	09:22:06.5	35 17	118 33	4.3	10.5±	17.3	10.8	31.8	28.7	28.1	30.1	23.3	24.7	35.0	30.9	30.3	38.8	45.3	57.9	55.4
					11.1	87.1	25.3	141.7	130.6	126.0	140.9	104.7	108.5	179.1	199.5	189.4	202.7	265.0	359.5	345.4
122a	15:08:30.9	35 05	118 45	4.4	34.5	37.0		49.7	49.4	49.1	52.0	52.7	52.7	57.3	61.3	59.0	65.3	67.5	80.2	
					20.0	38.7		113.4	118.4	114.5	133.0	132.8	136.8	174.8	209.5	192.7	227.6	259.6	301.1	
123	18:02:43.6	35 05	118 45	4.0	47.7±	49.1		61.7	62.5	62.5	65.4	64.0	65.3	70.5	72.1	73.2	77.1	81.0	92.2	94.8
					20.0	38.7		113.4	118.4	114.5	133.0	132.8	136.8	174.8	209.5	192.7	227.6	259.6	301.1	300.9
124	19:51:19.6	35 22	118 32	3±	21.3	30.7		43.6	41.3	40.8	43.3	35.1	38.1	47.9		51.2	50.4	50.2		
					17.4	75.8		149.0	139.2	133.9	142.1	98.4	99.9	185.7		194.0	193.4	271.8		
					SA															
125	22:28:21.5	34 54	118 57	3.4	40.3	23.8	33.0	34.9	39.0	40.1	42.4	47.8	40.1	47.8		53.0	59.5	59.2	70.8	
					116.6	11.7	78.3	88.8	109.8	111.1	132.3	159.5	165.8	170.2		200.[illegible]	251.4	258.4	303.5	
126	22:41:03.1	35 11	118 36	4.6	22.8	11.3	09.8	24.0	22.4	22.1	24.0	20.9	23.2	29.1	34.0	31.8	30.8	41.6	53.0	52.4
					122.9	50.1	37.0	131.1	121.3	117.4	133.7	114.9	120.4	173.4	206.3	188.7	214.3	259.0	303.4	352.7
127	22:58:56.5	35 19	118 30	4.3	17.8	07.8	00.3	19.8	17.4	16.9	19.1	11.0	13.9	23.9	28.1	25.5	28.2	35.0	47.3	44.5
					133.1	74.0	21.5	147.5	133.1	127.7	142.0	98.9	103.1	179.4	199.0	188.2	198.5	205.4	360.7	340.1
July 27																				
127a	00:09:15.8	35 19	118 30	4.2		27.8	19.0	40.7	37.1	36.5	38.4	32.3	32.9	44.0	45.7	45.3	47.2	52.5	67.0	63.9
						74.0	21.5	147.5	133.1	127.7	142.0	98.9	103.1	179.4	199.0	188.2	198.5	205.4	360.7	340.1
127b	02:49:11.6	35 30	118 30	4.0		25.7	10.0	37.8	35.9	34.9	38.8	25.7	25.4	41.5	38.9	41.8	39.0	51.8	80.4	50.4
						89.8	1.9	101.5	152.9	147.1	160.4	89.0	85.5	196.3	182.8	201.8	170.3	202.2	340.[illegible]	330.0
128	07:18:11.3	35 02	119 03	4.1		18.2	23.0	25.1	31.1	31.6	34.7	38.1	38.1	40.4	40.0	43.8	48.3	50.7	57.7	
						25.2	71.8	89.5	128.1	127.9	148.7	158.7	157.0	192.3	204.0	214.9	239.7	275.1	346.3	
129	07:35:39.3	35 22	118 35	4.2		50.7	41.0	82.4	81.4	61.0	63.1	55.7	56.1	88.3	60.8	69.3	69.2	78.5	87.6	87.5
						73.2	17.0	145.7	140.4	135.6	150.4	102.3	102.1	188.3	190.0	197.5	194.0	274.3	351.3	345.4
130	11:34:38.4	35 04	119 02	4.1		43.7	49.2	53.3	50.8	59.2	62.3	62.9	63.5	67.4	68.8	70.3	74.3	77.2	85.8	
						28.5	68.0	92.8	129.0	129.5	150.0	154.6	153.2	193.3	201.0	215.0	235.8	278.4	344.8	
131	16:18:07.5	35 22	118 35	3.8		18.9	10.0	30.9	29.8	28.9	31.7	23.8	24.3	30.0	30.0	37.4	38.1	47.2	50.5?	55.0?
						73.2	17.0	145.7	140.4	135.6	150.4	102.3	102.1	188.3	190.0	197.5	194.0	274.3	351.3	345.4
132	18:26:43.9	35 08	118 46	3.9		51.4	51.4	64.3	63.8	62.8	65.9	64.8	68.0	71.8	74.7	74.5	79.2	82.4	93.5	94.6
						42.5	47.0	115.8	122.2	119.9	138.3	130.4	132.9	180.8	203.9	196.8	222.5	104.6	350.1	368.9
133	17:37:43.3	35 19	118 31	3.8		55.0	46.9	87.5	84.1	63.9	66.0	59.0	61.0	71.3	73.8	72.4	74.7	81.6	93.8	91.4
						72.3	21.4	148.4	133.4	128.2	142.7	100.1	103.8	180.3	198.1	189.3	198.9	208.2	359.5	342.0
134	18:56:23.8	35 18	118 30	3.9		34.8	27.5	40.8	44.8	44.2	46.5	40.8	41.8	51.3	52.8	52.9	55.5	82.3	74.0	72.1
						78.0	24.5	139.5	133.7	129.2	144.7	107.5	109.1	183.4	195.4	194.2	201.5	209.2	354.9	349.4
July 28																				
135	02:21:04.4	35 06	118 34	3.9			11.5	20.5	22.3		23.9	23.7	24.8	29.8	30.0	32.2	37.5	40.5	57.9	53.4
							45.7	120.0	111.8		124.3	118.8	127.3	164.4	215.8	179.2	223.1	249.9	371.9	340.5
136	05:45:54.0	35 08	118 31	4.2			80.0	18.0	12.4		14.5	12.5	14.7	20.0	27.7	21.9	28.1	30.8	47.4	43.5
							41.8	133.9	115.8		125.0	112.7	122.0	164.2	215.1	177.3	218.9	249.9	372.8	346.9
137	07:29:02.7	35 05	118 52	3.7			12.0	19.4	22.2		25.3	25.1	28.2	30.2	30.8	33.7	37.8	40.8	50.2	
							57.0	105.3	121.8		140.2	141.0	142.8	182.8	205.0	202.1	231.3	288.9	353.0	
138	15:41:19.7	35 22	118 35	4.0			22.1	43.2	41.6		43.2	38.2	38.5	48.0	48.9	49.5	50.3	50.8	88.2	
							17.0	145.7	140.4		150.5	102.3	102.1	188.3	190.0	197.5	194.0	274.3	351.3	

No.	Time	Lat. N	Long. W	Mag.	Gn	Av	n	Sb	P	Mn	D	Cl	H	R	F	Bb	T	Pr	Bt	Mh	Sc	Lu
July 28																						
139	15:43:11.7	35 22	118 35	3.7		14.0		35.7	34.0		37.0	28.2	28.1	41.4		44.2	42.2	54.9				
						17.0		145.7	140.4		150.5	102.3	102.1	188.3		197.5	194.0	274.3				
July 29																						
140	05:50:23.4	35 23	118 51	3.9	33.0			44.4	46.8	46.5	49.2	42.9	43.0	53.7	50.1	56.0	54.9	64.8	72.9±	69.5	75.3	
					63.8			131.0	130.4	146.5	164.8	123.4	115.8	205.1	177.2	216.0	197.3	290.5	361.1	331.7	309.7	
141	07:03:40.8	35 23	118 51	0.1	56.8			66.4	70.0	70.2	72.0	66.5	66.0	77.2	73.2	79.1	76.3	86.1		92.7	96.5	90.7
					63.0			131.0	130.4	146.5	164.8	123.4	115.8	205.1	177.2	216.0	197.3	290.5		331.7	309.7	315.9
142	07:50:23.1	35 23	118 46	3.0	33.0			44.0	40.5	46.2	58.8	41.5		53.7			54.2	64.4	72.5±	70.0		
					67.0			135.0	147.5	144.0	160.6	116.4		200.1			195.3	285.0	350.9	330.6		
143	08:01:46.4	35 24	118 49	3.1	57.1			68.2	69.9	69.7	72.3	65.0	64.0	76.7	73.2	76.4	77.4	87.9	96.0±	93.1	97.8	91.3
					68.0			134.3	150.9	147.7	164.0	119.0	112.3	204.5	175.0	216.6	194.7	290.1	360.9	332.7	310.3	316.2
144	08:07:47.5	35 20	118 47	3.8	00.0			11.4	12.8	12.5	14.5	07.5	07.7	20.1	16.1	21.7	20.0	30.7	38.6±	35.9±	40.1	
					72.4			139.1	148.3	149.6	166.1	115.0	107.5	205.3	174.0	216.4	190.3	291.1	362.3	332.0	302.5	
145	09:37:38.0	35 07	118 38	3.9	45.9			50.7	50.6	56.5	58.4	57.1	50.9	64.1	66.9	65.7	73.1	74.1	82.7±	88.0		
					47.0			124.2	115.5	112.1	129.3	122.0	120.4	189.9	211.2	185.3	222.1	255.3	325.5	305.8		
146	10:19:32.7	35 21	118 32	3.7	44.5			57.0	54.2	53.9	55.9	40.5	49.2	60.5	61.7	61.9	63.4	71.3	80.6±	83.5	80.2	
					74.2			147.7	137.4	132.2	146.7	99.4	101.3	184.2	194.2	192.0	195.2	270.2	342.5	356.0	338.1	
147	12:50:37.2	35 20	118 44	3.5	40.5			57.4	59.8	60.1	62.7	55.0	55.6	66.9	62.9	68.6	66.0	77.8	86.0±	83.0		
					63.5			133.5	141.2	137.7	154.3	116.1	113.0	193.9	185.8	206.2	200.1	279.6	350.0	343.3		
148	15:49:50.3	35 11	118 30	4.9	59.3			72.5	69.6	69.6	72.1	66.5	70.1	77.1	80.6	79.0	83.9	88.3	96.5±	101.4	99.8	
					50.1			131.1	121.3	117.4	133.7	114.9	120.4	173.4	206.3	186.7	214.3	259.0	330.0	303.4	352.7	
149	17:36:43.0	35 14	118 32	4.4	53.1	47.2		65.5	62.7	62.7	64.8	60.0	61.7	69.0	72.6	71.9	75.7	80.5	89.6±	92.9	91.7	
					64.3	30.0		139.3	124.9	120.1	135.3	106.0	112.0	173.9	200.3	184.9	207.6	259.0	331.4	304.3	345.5	
150	19:51:32.4	35 20	118 55	4.5	41.4	30.9		52.9	55.7	56.0	58.2	53.9	53.2	63.1	50.9	65.5	64.0	73.7	82.2±	78.7	85.9	
					58.8	41.5		122.9	140.1	146.0	164.0	131.1	123.9	205.1	177.7	220.0	204.3	290.3	360.0	330.9	376.0	
151	09:59:28.9	35 10	118 32	4.0	39.8	32.8		53.0	50.0	49.5	51.8	44.9	40.5	50.5	59.0	54.9	60.5	66.9		79.5	77.0	
					69.9	23.3		144.0	132.0	126.9	141.8	102.5	100.1	179.7	190.7	189.4	200.7	265.5		359.5	343.5	
152	11:02:55.0	34 58	118 57	4.1	57.0	07.2		69.5	73.1	73.5	76.5	79.7	82.4	82.4	85.3	85.4	93.0	92.1		103.3	108.0	
					16.4	73.5		91.2	115.5	116.2	137.0	154.9	157.5	180.8	205.8	203.5	244.3	282.1		357.9	392.0	
153	14:46:50.1	35 14	118 32	4.1	60.1	54.4		72.0	69.9	69.6	71.8	67.5	66.0	76.0	80.0	80.0	82.0	87.2		100.0	101.0	
					64.3	30.0		139.3	124.9	120.1	135.3	106.8	112.0	173.9	208.3	184.9	207.6	259.6		304.3	345.5	
July 31																						
154	04:10:21.7	35 17	118 33	4.2	32.5	25.7			42.4	41.9	44.0	36.3	39.3	46.0	51.3	50.0	52.5	59.3	69.0	71.0	69.5	
					67.1	25.3			130.6	126.0	140.9	104.7	108.5	179.1	199.5	189.4	202.7	265.0	336.9	359.5	345.4	
155	12:09:00.0	35 19	118 36	5.8	20.9	13.8			30.5	30.2	32.1	25.6	27.0	36.2	39.3	36.0	41.1	47.1	56.7	59.0	57.6	
					68.2	22.2			136.5	132.0	147.6	106.7	107.3	186.0	192.7	196.6	198.9	271.9	346.1	352.5	349.5	
156	17:19:08.2	35 17	118 35	4.5+	10.9	12.0		31.5	28.9	28.5	30.6	25.4	26.0	35.2	38.3	36.6	40.9	45.8	55.3	58.6	56.1	
					65.0	25.9		139.4	131.5	126.9	142.4	107.2	110.0	181.0	197.8	191.9	203.1	266.8	338.5	357.2	340.4	
157	19:05:14.0	35 19	118 30	4.0	20.9	18.7		39.9	36.0	35.6	37.9	31.3	32.2	41.8	46.0	43.0	46.7	52.8	62.0	65.7	62.6	
					74.0	21.5		147.5	133.1	127.7	142.0	98.9	103.1	179.4	199.0	188.2	196.5	265.4	337.7	360.7	340.1	
158	19:53:14.0	35 20	118 55	4.5	43.3	21.1		54.5	57.6	57.6	60.2	55.3	54.0	64.7	60.9	67.0	66.3	75.6	85.0	89.0	86.7	
					58.8	41.5		122.9	140.1	146.0	164.0	131.1	123.9	205.1	177.7	220.0	204.3	290.3	360.0	330.9	376.0	
Aug. 1																						
159	03:16:11.0	35 17	118 33	4.5+		15.5		33.7	32.9	32.2	34.2	20.1	29.0	38.8	41.5	39.8	42.8	48.7	59.3	62.2	59.4	
						25.3		141.7	130.6	126.0	140.9	104.7	100.5	179.1	199.5	189.4	202.7	265.0	336.9	359.5	345.4	
160	10:35:55.8	35 20	118 32	4.0		59.5		80.1	76.5	76.4	78.4	72.7	72.8	82.8	86.1	84.7	87.1	93.2	103.5	105.7	103.8	
						19.6		140.4	133.6	130.5	145.0	100.3	102.9	182.8	195.7	191.7	197.1	266.8	340.9	357.1	342.6	
161	13:04:30.0	34 54	118 57	5.1		42.8		43.8	47.7	46.8	51.1	34.5	35.9	50.9	61.8	60.2	70.1	66.8	75.1	77.8	83.3	
						70.3		88.8	109.8	111.1	132.3	159.5	163.8	176.2	215.8	200.8	251.4	250.4	324.2	363.5	394.9	
162	21:35:22.4	35 19	118 30	4.0	34.1	26.2		47.4	43.6	43.1	45.2	30.1	39.8	50.9		51.4	53.8	61.3		73.1		
					74.1	21.5		147.5	133.1	127.7	142.0	98.9	103.1	179.4		188.2	196.5	265.4		360.7		
Aug. 2																						
163	05:39:15.1	35 06	118 42	3.8	21.0	22.8		34.1	33.4	33.2	35.9	35.7	37.3	41.7		43.8	50.8	52.3	61.5	65.1		
					43.1	40.5		118.2	118.2	113.6	131.5	127.8	132.9	172.8		189.6	224.9	257.8	327.5	303.1		
164	19:09:19.8	35 22	118 35	3.9+	29.7	22.1		43.1	41.8	41.5	53.3	36.2	36.1	46.3		47.8	50.1	58.8?	69.4			
					73.2	17.8		145.7	140.4	135.8	150.5	102.3	102.1	188.3		197.5	194.0	274.3	340.4			
Aug. 3																						
165	01:51:50.2	35 23	118 27	4.1	69.2	57.3		81.5	78.2	77.9	79.7	70.8	72.3	84.2		85.5	86.8	94.7	104.7			
					81.8	15.2		155.8	139.4	133.3	146.8	91.8	94.4	183.8		189.5	190.7	268.8	341.8			
Aug. 4																						
166	05:34:59.8	35 05	118 35	4+	68.7	67.8		17.4	17.9	17.5	20.2	19.1	20.4	24.8		27.8	33.9	35.7	44.8			
					49.8	47.7		125.7	110.4	106.8	123.8	120.9	129.8	162.7		179.5	225.1	249.5	320.8			
167	19:47:22.4	35 04	118 59	3.8				37.9	42.5	42.6	45.4	40.4	47.8	50.7		53.8	56.3		66.9			
								76.4	126.2	126.3	146.8	150.7	150.4	189.7		210.7	234.4		340.3			
Aug. 5																						
168	00:50:10.4	35 20	118 44	4.4	19.8			31.7	33.4	33.1	35.7	29.1	28.5	40.3		41.8	40.3					
					63.5			133.5	141.2	137.7	154.3	116.1	113.8	193.9		208.2	200.1					
Aug. 6																						
169	03:46:23.4	35 19	118 30	4.3			32.2	47.5	44.8	44.4	46.1	39.8	41.1	51.5		52.8	54.5		71.3			
							53.1	147.5	133.1	127.7	142.8	98.8	103.1	179.4		188.2	196.5		337.7			
170	22:40:13.7	35 20	118 55	3.8		20.3	20.2	34.2	37.2	37.3	39.5	35.2	34.7	44.9		47.2	48.1		66.3			
						41.5	41.2	122.9	140.1	146.0	164.0	131.1	123.9	205.1		220.0	204.3		360.0			
Aug. 7																						
171	16:31:51.2	35 02	119 03	4.9		02.9	03.2	09.1	11.4	11.8	15.0	15.9	16.5	20.0			20.5		30.8			
						71.6	70.4	89.5	120.1	127.9	148.7	156.7	157.0	192.3			239.7		341.4			
172	19:19:07.0	35 20	118 55	4.2		44.1	43.8	27.8	30.4	30.2	32.8	20.8	27.8	37.8		46.8	39.4					
						41.5	41.2	122.9	140.1	146.0	164.0	131.1	123.9	205.1		220.0	204.3					
Aug. 8																						
173	05:17:17.0	35 20	118 34	4-		22.1	23.3	40.3	38.8	38.6	39.8		35.9	46.1		47.8	47.4	57.8	65.5			
						20.8	40.1	144.2	136.8	132.1	146.5		104.4	184.4		189.3	197.4	276.4	342.4			

No.	Time	Lat. N	Long.	*	Mag.		Ch	Hv	*	Sd	P	MW	D	CL	H	K	BB	T	PT	Bt	N	BC
Aug. 9																						
174	10:07:32.1	35 20	118 28		4.2			35.0	41.1	50.4	53.6	53.1	55.2		59.8	59.8	61.0	63.0	75.8	79.7		
								20.1	57.8	151.0	134.3	120.6	143.3		100.0	179.2	187.1	196.4	265.2	337.8		
Aug. 10																						
175	06:01:16.0	35 19½	118 30½		4.0			21.7		42.1	40.6	40.7	42.7	35.7	35.5	47.4	48.8	49.2	57.5	67.5		
								22.2		140.9	136.5	132.0	147.8	108.7	107.3	108.0	198.8	198.9	271.9	343.8		
176	12:23:16.8	35 19	118 30		4.8			19.7		41.9	38.0	37.9	39.8	33.1	34.1	44.0	45.3	48.3	55.1	65.0		
								21.5		147.5	133.1	127.7	142.8	98.9	103.1	179.4	188.2	198.5	265.4	337.7		
177	19:44:23.8	35 00	119 00		4.1			33.1		37.9	43.2	43.0	48.4	40.3	47.5	51.9	48.1	61.8	63.5	70.8		
								71.7		70.1	121.3	122.8	142.8	158.5	157.2	188.4	209.2	241.9	269.2	333.7		
Aug. 11																						
178	13:21:48.8	35 19	118 30		4.4			31.8		73.4	72.1	70.1	72.9	65.2	68.1	78.2	78.8	88.2	87.2			
								21.5		147.5	133.1	127.7	142.8	98.9	103.1	179.4	188.2	198.5	265.4			
Aug. 13																						
179	04:29:37.8	35 19	118 30		4.8+			42.7		63.1	68.8	68.8	68.3	55.7	58.4	68.7	68.8	78.9	77.8	88.8		
								21.5		147.5	133.1	127.7	142.8	98.9	103.1	179.4	188.2	198.5	265.4	337.7		
180	17:39:25.1	35 09	118 41		4.7			32.3		44.7	44.4	44.8	48.7		48.7	52.4	54.8	59.8	63.3	72.7		
								42.7		122.9	120.6	117.6	135.8		127.4	174.7	191.2	219.1	261.8	331.2		
181	21:25:48.3	35 18	118 48		4.1			32.1		72.8	69.9	69.8	71.4	68.8	68.8	78.3	78.2	88.8	88.8	97.8		
								20.4		135.1	135.3	130.8	147.9	112.5	112.4	187.2	199.1	202.8	272.9	344.1		
Aug. 14						Sm																
182	07:28:21.8	35 08	118 31		4.1	31.9		20.8		43.2	39.07	39.3	41.8	40.4	42.1	47.7	52.4	58.4				
						63.9		44.8		133.9	113.8	109.2	125.8	112.7	122.8	164.2	177.3	218.9				
183	11:41:48.1	35 04	118 53		4.2	58.8		55.8		82.3	85.1	85.4	88.8	89.5	78.1	73.1	78.1	81.7	83.3	92.8		
						78.9		59.4		103.8	121.8	128.3	148.8	148.3	145.8	183.1	201.8	232.8	288.8	334.8		
Aug. 16																						
184	05:57:23.7	35 08	118 31		3.9			27.3		44.8	42.8	41.8	44.2	41.8	43.7	49.3	51.8	58.8		69.8		
								41.8		133.9	113.8	109.2	125.8	112.7	122.8	164.2	177.3	218.9		321.2		
Aug. 17																						
185	06:14:03.7	35 03	118 57		4.8			15.8		19.3	23.3	23.8	28.8	27.3	28.7	31.8	34.5	48.8		49.2		
								84.4		97.8	122.9	122.9	143.1	149.2	149.9	188.7	207.1	235.1		337.8		
186	09:09:06.9	35 01	118 59		4.1		18.8	17.7		22.8	26.4	26.9	29.9	31.2	32.8	35.3	38.3	43.8		52.4		
							23.2	89.2		92.4	121.8	122.2	142.9	154.8	154.8	188.3	208.5	239.7		338.1		
187	11:10:26.8	35 01	118 59		3.9-		30.4	37.4		41.4	40.5	46.4	49.4	50.7	52.7	54.8	57.5	63.8		72.2		
							23.2	89.2		92.4	121.8	122.2	142.9	154.8	154.8	188.3	208.5	239.7		338.1		
188	21:04:41.8	35 04	118 53		4.3		48.8	51.8		58.1	60.6	60.9	63.1	64.8	65.8	68.8	71.5	78.3				
							30.9	59.4		103.8	121.8	128.3	148.8	148.3	145.8	183.1	201.8	232.8				
Aug. 18																						
189	04:48:18.4	35 02	119 03		4.7		15.1	22.1±		24.3	30.3	30.8	33.9	34.9	35.5	38.7	41.9	47.1				
							25.2	71.8		89.5	128.1	127.9	148.7	158.7	157.8	192.3	214.9	239.7				
190	07:16:42.8	35 02	118 51		3.9+		47.8	53.1±		59.7	61.2	61.3	64.8	65.8	68.3	69.3	72.8	79.9				
							29.1	81.8		102.9	116.2	115.5	135.2	143.1	148.3	177.9	199.6	234.8				
Aug. 19																						
191	09:01:31.8	35 17	118 35		3.8			41.8		54.4	52.4	52.2		48.8	49.3	59.4	60.6	63.2				
								65.8		139.4	131.5	126.9		107.2	118.8	181.8	191.9	203.1				
192	19:12:28.3	35 03	119 14		4.5			31.8		39.2	49.8	49.1	52.3	53.4	54.6	57.7	61.1	64.2				
								33.8		88.8	139.6	141.5	163.8	171.2	166.8	208.8	231.8	243.3				
Aug. 20						MD																
193	08:47:47.1	34 53	119 02			59.8				59.9	65.2	65.3	66.8	72.1	74.8	74.4	77.7	88.3				
						76.8				77.4	113.6	115.6	137.4	150.2	169.5	182.8	207.8	255.2				
Aug. 22						CC																
194	22:41:23.8	35 20	118 55		5.8	29.8	33.8		30.3	43.8	47.1	47.5	49.4	45.3	44.8	54.5	56.8	58.2			75.9	77.3
						29.3	58.8		41.2	122.9	148.1	146.8	164.8	131.1	123.9	205.1	220.8	208.3			370.9	370.6
Aug. 23																						
195	06:03:03.2	35 00	118 44		4.3		08.8		14.7	20.5	20.3	20.4	24.8	25.1	26.7	28.8	31.8	40.4				
							33.1		78.3	109.2	107.7	106.8	125.1	137.3	144.1	167.4	187.1	238.7				
Aug. 24																						
196	23:11:48.3	34 59	118 54		3.7				01.1	03.8	06.8	07.2	10.1	11.9	13.8	15.4	19.2	25.7				
									79.7	95.9	114.1	114.3	134.7	150.2	153.5	178.8	200.2	241.3				
Aug. 25																						
197	06:20:26.1	35 06	118 58		4.7				37.4	42.8	46.2	46.7	49.2	49.8	50.8	54.4	57.5	61.8		74.8	78.2	79.8
									87.5	100.1	128.3	127.6	148.8	147.8	148.5	190.8	211.1	238.4		342.2	379.7	387.4
Aug. 26																						
198	20:56:40.7	35 05	118 25		4.4					62.8	57.6	57.3	59.7	58.5	61.2		67.5	75.5		86.8	87.7	89.7
										138.8	106.1	104.4	115.6	110.2	143.8		188.7	223.7		311.7	331.8	339.9
Aug. 28																						
199	07:48:41.5	35 21	118 32		3 3/4				49.1	88.8	63.1	62.7	64.8	57.3	57.9	69.2	71.8	72.1		89.6		
									48.8	147.7	137.4	132.2	148.7	99.4	101.3	184.2	192.8	195.2		342.5		
Aug. 30																						
200	04:56:88.8	35 19	118 30		4 3/4		12.1	03.2		24.1	21.4	21.8	23.8	15.6	17.2	27.9	28.8	38.5		48.3	37.2	48.5
							74.8	21.5		147.5	133.1	127.7	152.8	98.9	103.1	179.4	188.2	198.5		337.7	333.6	348.1
201	04:59:55.8	35 19	118 30		4.8		67.8	58.8		79.8	76.4	76.2	77.9	78.9	72.8	83.8	88.8	88.4		103.4		
							74.8	21.5		147.5	133.1	127.7	152.8	98.9	103.1	179.4	188.2	198.5		337.7		
Sept. 1																						
202	10:38:59.8	35 19	118 57		4.1			06.8		19.5	23.8	22.9	25.4	21.1	20.6	29.8	32.7	32.8		49.7		
								45.8		119.6	147.9	146.1	164.6	134.8	127.4	205.9	221.5	206.9		360.3		
Sept. 2																						
203	09:06:15.3	35 06	118 50		3.8					31.3	35.6	35.7	38.1	38.7	39.4	43.2	45.7	50.7		62.5		
										100.1	128.3	127.6	148.8	147.6	146.5	190.8	211.1	238.4		342.2		
204	12:41:32.5	35 08	118 42		4.6		38.4			52.8	51.3	51.8	53.5	52.9	54.7	58.4	88.6	87.4		78.4	81.8	82.9
							45.9			120.5	119.5	117.6	134.5	125.5	129.7	175.4	191.5	221.3		330.5	356.3	363.8
205	16:38:08.7	35 18	118 32		4.8		19.8			32.8	29.5	29.2	31.2	25.1	26.2	36.8	37.4	48.2	45.2	56.8		
							69.9			144.8	132.8	128.9	141.8	102.3	106.1	179.7	189.4	208.7	265.5	337.7		
206	20:45:56.4	34 58	119 00		4.7		59.8	69.8		70.4	75.5	76.8	79.8	81.4	83.5	84.1	87.7	94.6	94.8	102.7	109.8	111.1
							17.6	74.6		87.7	118.4	119.4	148.5	158.5	168.2	184.3	207.9	245.4	266.7	332.8	387.5	394.6
Sept. 4						PC															PR	CCR
207	13:45:43.8	35 12½	118 37½		2±	48.3	53.3	49.5	52.7		64.7	63.8	66.1	62.3		64.8		77.3			48.4	45.5
						27.4	56.7	35.8	58.8		124.7	120.9	137.2	115.1		177.8		211.9			28.2	4.6
208	13:51:30.7	35 20	118 32			40.1	48.5	40.3	45.8	62.8	57.3	57.3	59.3	53.3	53.7	63.8	65.2	68.3		74.5		39.2	38.7
						21.6	72.7	19.8	49.4	146.4	135.6	130.5	145.8	100.3	102.9	182.6	191.7	197.1		340.9		14.3	11.7

No.	Time	Lat. N	Long. W	Mag.	PC	Ch	Hv	w	SB	P	MM	D	CL	H	K	BB	T	Pr	Bt	N	BC	PK	UCK
Sept. 4																							
208a	13:59:09.8	35 20	118 32		13.3	21.0	13.5	17.0		31.2	30.4	32.3	20.3	20.0			41.0		57.9			12.2	11.0
					21.0	72.7	19.0	49.4		135.6	130.5	145.0	100.3	102.9			197.1		340.9			14.3	11.7
209	15:05:03.2	35 22	118 35		06.3	15.5	06.0	10.7		27.3	26.7	28.4	20.5		34.9		35.2					08.0	05.0
					15.0	73.2	17.0	49.9		140.4	135.6	150.5	102.3		168.3		194.0					10.5	13.4
210	15:14:57.9	35 19	118 30	3 1/4	02.1	10.0	01.0	00.4	22.8	19.1	18.6	21.3	14.3	15.3	25.0	27.0	29.5		45.9			00.4	00.1
					25.1	74.0	21.5	53.1	147.5	133.1	127.7	142.0	98.9	103.1	179.4	188.2	190.5		337.7			12.1	12.5
211	16:00:49.5	35 19	118 30	4.4	53.5	01.1		50.4	74.3	70.4	70.3	72.3	65.5	66.9	76.7	76.0	81.0	87.0	97.0	90.4	97.0		91.5
					25.1	74.0		53.1	147.5	133.1	127.7	142.0	98.9	103.1	179.4	188.2	190.5	205.4	337.7	333.0	340.1		12.5
Sept. 5																							
212	04:40:43.1	35 21	118 50		45.3	53.3	40.5	49.1		67.4	66.1	69.4	62.2		74.8		75.2					49.7	40.9
					14.2	01.5	31.0	38.8		146.4	143.0	161.0	123.4		201.8		200.4					41.4	23.3
213	05:16:03.0	35 19½	118 36½		05.7	15.4	00.1	10.4		26.2	27.0	27.7	19.7		34.4	35.9	34.7					00.2	04.7
					17.0	80.2	10.0	46.8		136.5	132.0	147.0	100.7		180.0	190.0	190.9					21.3	0.0
214	06:17:10.0	35 34	118 58		14.0		10.6	12.9					30.7										
					23.0		40.5	15.5					131.0										
215	06:20:11.1	35 16	118 33.5		14.7	23.5	14.5	19.3			32.4		27.6									14.1	12.9
					22.2	80.5	20.3	52.4			127.7		104.3									17.0	7.4
215a	07:03:23.1	35 16	118 34		26.7	34.5	20.6	21.1		46.1	43.6	47.2	40.1		52.5	55.0	55.5	81.7				20.0	24.0
					24.4	65.0	24.1	54.2		120.2	124.6	140.0	107.0		176.6	189.6	204.6	204.5				20.2	4.3
Sept. 12																							
216	10:35:25.1	35 00	119 03	4.5		20.4	37.0		38.7	44.8	45.3	49.1	50.1	51.3	53.7	57.0	61.3				79.8		
						21.3	71.0		85.4	125.6	129.1	149.9	160.0	155.6	193.5	213.3	243.1				397.8		
Sept. 14																							
217	20:43:23.5	35 13	118 40	4.1			29.4	32.7	45.7	43.7	43.5	45.7	42.3	43.8	50.6	52.7	56.9		71.2				
							32.0	55.9	126.0	126.5	121.6	140.2	117.6	120.2	166.2	193.6	211.6		330.4				
Sept. 15																							
218	04:40:13.3	35 19	118 30	4.9-			10.0	21.9	38.2	34.4	34.4	35.9	29.2	30.3	40.0	42.1	44.5		81.2	80.1	81.8		
							10.4	53.1	147.5	133.1	127.7	142.0	98.9	103.1	179.4	188.2	190.5		337.7	333.0	340.1		
Sept. 16																							
219	14:23:53.0	35 19½	118 30½	3.4		05.4	55.9	00.3	77.5	77.1	76.0	78.1	69.9	71.2	82.5	80.4	84.8						
						80.2	10.8	40.0	140.9	136.5	132.0	147.0	106.7	107.3	186.0	190.0	190.9						
220	14:24:11.1	35 22	118 35	3.6		22.7	12.0	10.2	34.7			33.2				44.9							
						73.2	13.0	43.9	145.7			150.5				197.5							
221	14:24:53.5	35 19½	118 30½	4.0+		65.9	56.2	01.2	77.9	77.7	76.3		70.9				85.7						
						80.2	10.0	40.0	140.9	136.5	132.0		106.7				190.9						
222	15:21:07.0	35 22	118 35	4.3+		18.9	09.2	14.7	30.5	29.0	28.9	30.0	23.7	24.0	35.1	37.2	38.2						
						73.2	13.0	43.9	145.7	140.4	135.6	150.5	102.3	102.1	188.3	197.5	194.0						
223	15:30:50.7	35 22	118 35	3½±		82.2	52.4	57.0			72.1	74.2	66.7	67.0	79.0	82.8	81.2						
						73.2	13.0	43.9			135.6	150.5	102.3	102.1	188.3	197.5	194.0						
224	19:37:47.3	35 20	118 34	3.2		60.1	49.6	54.0	70.5	69.2	68.3	71.0	63.5	64.0	76.0	79.2							
						71.0	10.8	40.1	144.2	136.4	132.1	148.5	102.9	104.4	184.4	189.3							
Sept. 20																							
225	06:13:51.9	35 19	118 30	3.6-		03.3	54.0	00.7	70.0	72.5	71.9	74.1	68.1	69.1	79.3	80.4	83.4		99.1				
						74.0	10.4	53.1	147.5	133.1	127.7	142.0	98.9	103.1	179.4	188.2	198.5		337.7				
Sept. 22																							
226	13:15:10.3	35 21	118 37	3.9			12.7	10.0	32.0	32.1	32.1	34.3	27.1	27.4	38.0	40.3	41.2		56.3				
							10.0	43.9	142.3	139.4	134.9	150.3	105.9	105.3	188.7	196.0	196.3		346.4				
Sept. 25																							
227	10:21:35.5	35 03	118 54	4.1-		40.2	45.2	47.0	52.4		54.9	55.3		59.1	59.0	63.3	66.0	72.1	74.1	81.0			
						20.7	80.1	72.3	150.0		120.3	119.8		149.9	147.4	181.9	203.2	234.2	200.4	334.1			
Sept. 26																							
228	03:51:50.0	35 08	118 40	3.9+		58.7	58.3	60.0	67.0		69.0	69.2		72.0	72.8	77.4	79.9	85.2					
						42.5	44.3	63.3	115.8		122.2	119.9		130.4	132.9	180.8	196.8	222.5					
229	20:21:20.0	35 00	118 37	4.0+		27.0	20.0	30.7	40.9		38.2	38.0	40.7	39.7	41.0	45.3		55.5	50.2	65.0			
						40.5	43.2	89.7	124.3		113.2	109.8	128.9	122.0	129.3	167.8		223.7	252.8	323.1			
Oct. 2																							
230	23:10:20.6	35 24	118 38	4.2		32.2	22.5	20.0	44.6		43.8	43.1		37.5	37.0	50.0	51.5	50.5	60.6	71.3			
						74.1	13.1	38.3	145.1		145.1	140.0		104.0	101.0	194.0	203.3	191.1	200.0	351.9			
Oct. 6																							
231	07:51:06.6	35 09	118 40	3.6+		13.0	12.0		27.2		25.9	25.3	20.0	20.0	27.5	33.4	35.5	41.3		53.3			
						49.3	39.1		124.0		120.1	116.0	134.1	122.0	120.0	174.7	189.9	218.9		330.3			
Oct. 13																							
232	22:20:35.1	35 23	118 51	4.0+		45.5		41.0	50.1		56.6	56.5	61.2	54.7	54.0	66.0	67.1	66.3		85.9			
						83.6		41.5	131.0		150.4	140.5	164.0	123.5	115.0	205.1	218.0	197.3		301.1			
Oct. 16																							
233	12:22:07.3	34 57	118 57	4.3		10.0	19.0	20.1	21.0		25.6	25.8	26.9	32.3	34.4	34.8	38.3	45.9					
						15.7	70.0	83.8	90.0		114.1	114.0	135.8	156.0	159.1	179.4	202.7	240.0					
						Ch	Hx	Ag	W		SB	P	MM	D	CL	H	R	BB	T	Pr	Bt			
Oct. 20																							
234	18:14:43.2	35 19	118 30	4.3		55.0		01.1			67.3	64.3	63.9	60.0	59.6	60.4	70.1	72.0	74.2	81.0			
						74.0		113.2			147.5	133.1	127.7	142.0	98.9	103.1	179.4	188.2	190.5	205.4			
Oct. 21																							
235	11:44:10.7	35 04	118 59	3.0+		21.3	27.5	28.9			32.4	37.2	37.5	39.8	40.2	41.0	45.3	48.5	53.0	57.0			
						20.8	82.0	75.2			96.4	126.2	126.3	140.0	150.9	150.4	169.7	210.7	234.4	273.1			
Oct. 22																							
236	20:03:20.3	35 20	118 55	3.9		37.4	33.4	40.7	34.7		47.8	51.7	52.3		40.5	48.0	59.1	61.2		70.5			
						50.8	39.1	75.3	41.2		122.9	118.1	146.0		131.1	123.9	205.1	220.0		290.3			
Oct. 23																							
237	05:33:33.7	35 35	118 30	3.8		49.3	34.7	52.0	38.5		60.6	59.1	58.8		40.9	40.9	65.0	65.8		77.0			
						97.8	11.0	110.5	33.7		171.0	162.0	156.0		85.8	78.1	204.2	208.1		290.0			
Oct. 28																							
238	20:52:50.4	35 22	118 30	3.8		82.9	52.7	00.4	50.0		75.1	72.4	72.0	73.8	65.3	66.0	78.5	79.8	81.0	89.3	99.3		
						77.6	12.9	111.7	48.4		151.3	138.5	133.0	148.9	95.9	98.7	184.0	191.7	193.0	269.9	342.5		
Oct. 31																							
239	15:04:00.1	35 27	118 44	3.9+		10.7	02.0	12.8			22.0	24.5	23.8	20.2	17.8	18.6	31.2	32.2	28.8	42.3			
						75.0	19.0	72.9			143.4	153.3	149.3	165.2	110.7	103.1	203.9	211.0	187.5	289.8			
Nov. 7																							
240	07:15:27.5	35 17	118 43½	3.6		30.2	32.1	41.7			47.4	49.2	48.5	51.1	46.4	46.4	56.5	56.3	59.5				
						56.0	20.4	92.8			130.1	135.7	132.5	148.8	116.1	117.0	189.2	202.4	205.4				

No.	Time	Lat. N	Long. W	Mag.		Ch	Kx	Kg	N	SB	P	MM	D	CL	H	R	BB	T	Pr	Bt	N	BC
Nov. 7																						
241	08:55:35.0	35 00	119 05	4.6		39.4	47.7	40.0		48.1	54.8	55.0	58.0	60.7	62.0	63.8	67.2	72.1				
						22.3	73.0	70.4		84.0	126.3	127.6	148.8	162.0	161.8	192.6	210.2	244.1				
Nov. 9																						
242	18:41:02.0	35 34	118 25	3.5+			04.0	21.6	08.8	30.7	27.1	26.0	27.9	14.6	14.1	31.5	34.0	29.0	43.1				
							13.7	123.5	41.4	172.1	158.9	152.4	164.0	79.2	75.3	190.9	201.5	170.2	284.6				
Nov. 11							Mm															
243	17:22:07.8	35 09	119 03	4.2			14.1±		10.3	23.6	29.0	29.4	31.3	31.8	32.7	37.1	39.6	43.7	48.0				
							43.1		62.7	99.4	137.2	137.1	157.3	151.2	147.2	200.2	220.4	227.3	284.0				
244	16:12:25.2	34 57	119 01	4.1			25.3±		39.2	38.7	44.1	44.5	47.2	50.4	52.5	53.1	56.0	64.0	64.2		78.7		
							53.4		84.7	85.1	118.0	119.3	140.6	160.6	162.0	184.4	200.5	247.4	266.7		387.7		
Nov. 12																						
245	04:16:30.7	34 56	119 00	3.9+					44.6	44.6	49.7	48.9	52.7	55.9	58.2	58.4	61.9	69.2	69.7				
									62.6	87.7	118.4	119.4	140.5	150.5	160.2	184.3	207.9	245.4	266.7				
Nov. 13					Sa																	
246	07:00:50.6	35 14	118 30		07.1	00.4	50.1	73.0	03.3	79.1	76.7	70.2	78.0	74.3	75.7	83.2	84.9	89.9				
					57.5	00.3	7.1	104.8	50.3	134.6	126.7	122.5	130.4	111.6	115.5	177.6	189.9	208.9				
247	12:04:39.2	35 00	119 00		41.7	43.9	40.1	50.2		55.4	59.9	59.9	63.3	64.7		70.3		75.0				
					20.5	32.4	41.0	72.4		98.1	130.1	130.0	150.2	150.1		193.2		231.5				
Nov. 14																						
248	23:34:01.4	35 03	118 57	4.0		05.1	00.0	13.5	12.8	16.5	21.1	21.6	24.4	25.7	27.3	29.0	32.9	37.9	40.3				
						27.4	41.3	79.0	72.7	97.6	122.9	122.9	143.1	149.2	149.9	186.7	207.1	235.1	269.7				
Nov. 27						FT																
249	15:30:51.1	34 58	118 57	4.0		44.0				55.8	59.5	59.6	63.2	65.6	67.0	68.2	71.5	79.7				
						11.5				91.2	115.5	116.2	137.0	154.9	157.5	180.0	203.5	244.3				
Nov. 28																						
250	10:22:29.3	35 03	118 57	3.0			37.1			44.7	49.1	49.6	51.7	53.1	55.0	57.9	60.7	66.1				
							41.3			97.6	122.9	122.9	143.1	149.2	149.9	186.7	207.1	235.1				
Dec. 1																						
251	05:26:10.3	35 00	118 50	4.4		12.4	16.9			26.4	28.3	28.3	30.9	33.3	34.5	37.0	39.2	47.9	47.1	56.1	61.3	63.0
						15.1	38.7			101.6	112.3	111.6	131.7	144.2	140.0	174.4	195.3	230.2	250.1	325.5	370.1	378.9
Dec. 5																						
252	04:01:09.0	35 03	119 18	3 3/4		14.3	18.7	19.4		22.7	30.4	30.7	32.9	35.1	37.0	38.7	42.0	47.0	48.0	57.1		
						29.8	55.0	83.0		85.5	133.9	135.2	156.4	164.0	161.0	200.1	223.3	240.5	282.6	348.4		
253	05:02:20.2	35 04	118 59	3.0		32.5	35.2	40.3		44.0	48.0	46.3	51.3	51.8	53.0	56.7	59.7	63.8	67.3	76.1		
						22.9	42.5	75.2		96.4	126.2	120.3	140.6	150.9	150.4	189.7	210.7	234.4	273.1	340.3		
Dec. 18																						
254	20:40:19.6	35 21	118 50	3.8+		27.8		32.1	25.4	40.7	43.6	42.7	44.6	40.0	39.4	49.7	51.9	51.1	60.5			
						53.2		82.8	50.8	129.1	146.4	143.6	160.9	123.4	117.4	201.0	214.0	200.4	286.6			
Dec. 21																						
255	08:30:02.4	35 05	118 45	3.6+			07.1	17.3	12.9	21.4	21.3	21.2	23.9	23.3	25.7	29.4	31.6	38.5	40.1				
							26.9	94.0	69.0	113.4	116.4	114.5	133.0	132.8	136.0	174.0	192.7	227.0	259.6				
Dec. 25																						
256	05:56:33.4	35 20	118 26	4.1		43.0	35.7	52.1	41.1	58.2	55.0	54.5	50.1	40.5	49.7		62.5	64.0	72.3			
						64.5	13.0	110.2	57.8	151.0	134.3	128.6	143.3	95.3	100.0		107.1	190.4	205.2			
Dec. 26																						
257	18:09:30.3	35 03	118 54	3.9		42.0	44.9	51.2	48.8	54.5	57.8	58.1	60.4	61.4	62.5		66.2	74.3	75.8			
						19.0	38.5	83.0	72.2	100.6	120.3	119.8	140.2	145.7	147.4		204.1	234.2	266.4			
Jan. 10, 1953																						
258	22:17:35.4	35 14	118 36	4.0		45.5	40.1	50.1		60.8	58.0	57.7	60.1	56.0		65.0	67.2	71.0	75.8			
						48.2	7.1	104.8		134.0	126.7	122.5	130.4	111.6		177.0	189.9	208.9	283.2			
Jan. 20																						
259	08:13:22.2	35 19	118 30	4.0		32.2			30.9	47.0	43.9	43.1	45.2	30.1	30.9	50.2	51.5	53.0	61.2			
						61.0			53.1	147.5	133.1	127.7	142.0	90.9	103.1	179.4	188.2	198.5	265.4			
Feb. 19																						
260	08:12:06.4	35 16	118 30	4.4		15.7	07.5	24.1	14.7	31.3	27.4	26.9	28.5	22.7	24.0	33.9	35.1	30.2	45.0	58.7		54.8
						61.0	10.2	113.2	54.2	146.3	131.3	126.0	140.4	99.7	104.7	177.9	187.0	200.4	283.8	330.1		340.0
Mar. 17																						
261	16:15:16.7	35 14	118 32	4.0		24.9				39.2	36.6		38.0	34.1	35.3	42.9	44.4	48.0	54.5			
						51.8				139.3	124.9		135.3	100.8	112.0	173.9	184.9	207.0	259.6			
Mar. 23																						
262	17:06:30.0	34 59	118 34	4.0		37.9			48.3	52.1	55.5		59.5	60.6	61.4	64.0	67.1	73.0	75.1	83.4	87.0	
						12.2			79.7	95.9	114.1		134.7	150.2	153.5	178.0	200.2	241.3	261.6	328.3	378.5	
Apr. 29																						
263	12:47:45.3	35 00	118 44	4.7		48.7		01.3	50.2	63.4	62.5		65.1	67.4	69.1	70.5	73.7	82.2	81.3	90.5	95.0	
						20.4		99.1	70.3	109.2	107.7		129.1	137.3	144.1	167.4	187.1	230.7	251.0	320.3	381.3	
May 1																						
264	00:48:21.0	35 07	118 27	4.1		28.2		40.5	33.0	43.8	39.4		41.0	38.9	41.3	46.9	49.0	55.9	57.7	67.3		
						48.0		120.2	73.9	137.9	110.4		120.3	109.6	121.4	159.0	171.2	222.0	244.8	310.0		
May 23																						
265	07:52:54.0	35 03	119 08	4.2		59.7		05.4	07.5	68.4	76.4		78.0	81.0	82.4	85.4		91.9	95.6	103.2	109.7	
						29.0		83.0	77.0	85.5	133.9		150.4	164.0	161.0	200.1		240.5	282.0	348.4	390.4	
May 25																						
266	03:24:00.8	35 00	119 01	4.0		04.3		13.1	13.4	14.9	20.2		23.5	20.0	27.3	29.5		37.7		40.0	55.2	55.4
						17.9		75.0	79.1	89.1	122.2		144.0	157.6	150.1	187.7		242.3		330.0	388.4	394.9